The plasma membrane Ca^{2+} pump PMCA4b regulates intracellular Ca^{2+} homeostasis and migratory and metastatic activity of BRAF mutant melanoma cells

PhD Dissertation

Luca Hegedűs

Eötvös Loránd University, Faculty of Science

Doctorate School in Biology

Molecular Cell and Neurobiology PhD Program

Supervisor:

Dr. Ágnes Enyedi PhD, DSc

Head of the PhD program:

Dr. Gábor Juhász PhD, DSc

Head of the Doctorate School in Biology:

Prof. Anna Erdei PhD, MTA member

Budapest, 2017

Table of content

1. Acknowledgements

During my PhD studies I was fortunate to work together with many people who helped my work and whom I could learn from. First of all, I would like to thank my supervisor

Ágnes Enyedi with whom I already started to work with during my bachelor studies. She taught me scientific thinking from planning a project to the critical analysis of the results. Her enthusiasm towards science encouraged and helped me through all the difficulties. I am thankful for her open mindedness for new projects and collaborations that made possible for me to continue our work while living in other countries.

I would like to thank all the members of the Ca^{2+} signal laboratory, Krisztina Lór, Rita Padányi, Karolina Varga and Katalin Pászty who were always there to help me and supported me with their advices. I am particularly grateful for our laboratory technician Krisztina Lór who taught me a variety of methodologies and her precise and skillful assistance was indispensable for the preparation of my thesis. I thank all the members of the former Membrane Biology Research Group led by Balázs Sarkadi in the National Blood Center for their helpful advices.

It has been a privilege to be part of the collaborative network between the Medical University of Vienna and the Semmelweis University. I am grateful to Enikö Kállay for her support and for her generosity to embrace me and my project. She always encouraged me and provided strong support during my stay in her laboratory and beyond. I am thankful to Michael Grusch for the inspiring discussions and for hosting me in his laboratory.

I wish to acknowledge the help provided by Balázs Döme, Szilvia Török, Judit Molnár, Matthias Wolf, Tamás Garay and Eszter Molnár.

Finally, I would like to thank my family, especially my husband, Balázs Hegedüs. I am grateful for his support both at home and at work. Special thanks to my parents who tirelessly supported and helped me in my entire life and I am grateful to my children for their love and their resilience.

2. Introduction

2.1 The maintenance of the Ca^{2+} homeostasis

Ca^{2+} is an essential component of living organisms. In vertebrates calcium salts are the building blocks of the bones and teeth while ionized serum calcium is a first messenger in the blood, which by acting through the calcium-sensing receptor regulates diverse physiological processes as bone remodeling or intestinal water absorption [1]. Furthermore, calcium is an important second messenger within the cells where it takes part in the regulation of vital processes from proliferation to cell death [2]. Intracellular Ca^{2+} signals show high spatiotemporal versatility and this way they are capable to regulate distinct intracellular processes [3]. While in synapses Ca^{2+} signal triggers exocytosis in milliseconds, its signaling effect can also last for hours driving cell division or apoptosis. The intracellular Ca^{2+} level is regulated by a cell type specific toolkit. The composition of the toolkit changes adaptively depending on the fate of the cell being that either differentiation or cell death. This remodeling of the Ca^{2+} handling system makes possible for the cell to cope with different circumstances, but its abnormal changes contribute to the formation of several diseases such as Alzheimer disease or cancer.

In resting state the intracellular Ca^{2+} concentration is between 100-200 nM, while in the outer space it is around 1 mM. Most of the cytosolic Ca^{2+} is bound to membrane surfaces or to calcium-binding proteins. The maintenance of the low intracellular Ca^{2+} concentration – that requires a lot of energy - is necessary to avoid the formation of calcium hydroxide phosphates in the cytosol. The steep Ca^{2+} gradient contributes to the strong electrochemical gradient across the plasma membrane that also drives Ca^{2+} uptake [4].

Ca^{2+} works as a second messenger through the formation of calcium transients. Berridge et al. divides the processes, which create Ca^{2+} signals, into two groups; the “ON processes” contribute to the increase, while the “OFF processes” to the decrease of the intracellular Ca^{2+} concentration [5]. Ca^{2+} can enter the cytosol through plasma membrane channels from outside of the cell or from intracellular stores, and then it is actively removed by Ca^{2+} pumps and/or exchangers, and is also buffered by Ca^{2+} binding

proteins/acidic lipids. Given that there are many different isoforms generated from each of these proteins of the Ca^{2+} signaling toolkit, the characteristics of the Ca^{2+} signal can be vastly versatile from small single spikes to high frequency oscillations. Depending on the spatiotemporal features of the Ca^{2+} signal distinct Ca^{2+} - dependent effectors become activated influencing basic cellular processes like proliferation, cell migration, exocytosis or apoptosis (Figure 1.).

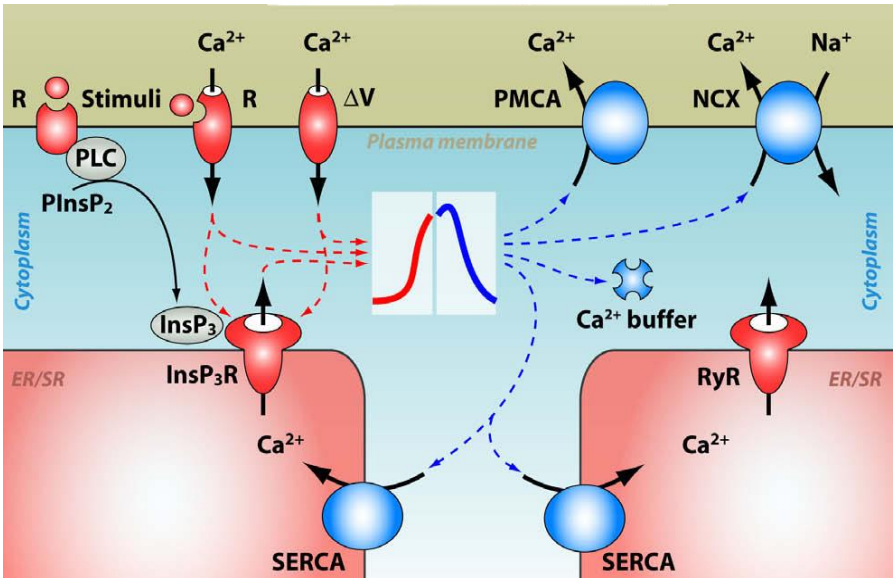

Figure 1. The Ca^{2+} signal is generated by the concerted actions of the "on" and "off" reactions. The Ca^{2+} molecules can enter the cytosol from the extracellular space or they can be released from the internal stores through Ca^{2+} channels. The excess Ca^{2+} is removed by Ca^{2+} pumps, exchangers and buffers [6].

2.1.1 Ca^{2+} increase reactions

2.1.1.1. Ca^{2+} release from the internal stores

Ca^{2+} is stored in distinct compartments within the cells, primarily in the endoplasmic reticulum / sarcoplasmic reticulum (ER/SR) and in the mitochondria. After stimulus Ca^{2+} is quickly released from the ER through the activation of membrane receptors IP_3Rs (inositol 1,4,5-trisphosphate receptor) [7], and from the SR by ryanodine receptors (RYR) [8]. IP_3Rs are receptor channel molecules, which are activated by the second messenger IP_3 and by Ca^{2+} itself. IP_3 is generated from inositol 4,5-bisphosphate (PIP_2) by phospholipase C (PLC), which is coupled to several cell surface receptors, such as G-protein-coupled receptors (GPCRs) or

receptor tyrosine kinase-linked receptors (RTKRs). Ryanodine receptors are mostly found in excitable cells. They are directly activated by L-type Ca^{2+} channels in the striated muscle, while in other cell types their opening is initiated by the increasing cytoplasmic Ca^{2+} concentration. This phenomenon is called Ca^{2+} induced Ca^{2+} release (CICR). IP_3Rs are also activated by Ca^{2+} until its concentration reaches ~ 300 nM in the cytosol, which in turn inhibits Ca^{2+} release through the receptor [6].

The mitochondria are also sensitive to the rise of the cytosolic Ca^{2+} concentration that takes up Ca^{2+} by the mitochondrial calcium uniporter (MCU). Elevated Ca^{2+} concentration within the mitochondria induces ATP production through the activation of the Ca^{2+} sensitive dehydrogenases, which provides energy for the regulation of the Ca^{2+} transients and the following cell responses. An elevated Ca^{2+} concentration in the mitochondria also induces increased production of reactive oxygen species (ROS). During the decay phase of intracellular Ca^{2+} signal Ca^{2+} is removed from the mitochondria by Na^+/Ca^{2+} and H^+/ Ca^{2+} exchangers. In case of a Ca^{2+} overload the mitochondrial permeability transition pores (MTP) open through which cytochrome-c is released that in turn triggers apoptosome formation and ultimately apoptosis in the cell [9].

Calcium is also stored in the Golgi apparatus and a Ca^{2+} efflux – independent of the ER Ca^{2+} store – was shown through the Golgi IP_3Rs. However, the exact mechanism of the Golgi Ca^{2+} release process is still unclear. Calcium ions are also stored in the cytoplasm attached to Ca^{2+}-binding proteins such as calretinin and parvalbumins [10]. The high amount of Ca^{2+} stored in the ER and the mitochondria are also bound to other Ca^{2+}-binding proteins within the organelles, for example to calreticulin in the ER, calsequestrin in the SER.

2.1.1.2. Plasma membrane Ca^{2+} channels

Ca^{2+} influx from the outer space is driven by the electrochemical gradient between the two sides of the plasma membrane. There are many different types of plasma membrane Ca^{2+} channels that can be divided into three groups based on their gating characteristics [5]. Voltage gated Ca^{2+} channels are found in excitable cells and their activation requires only milliseconds, initiating cellular responses such as synaptic vesicle fusion or muscle contraction. Another group of channels are gated by the binding of a specific ligand. The receptor-operated channels bind a ligand from the external space, while second messenger-operated channels react to ligands from the internal space. An example for the former is the

glutamate binding NMDA (N-methyl-D-aspartate) receptors [11], for the latter the arachidonic acid sensitive Ca^{2+} channels [12]. The third large group of channels is activated by the depletion of the internal Ca^{2+} stores, these are the store operated Ca^{2+} channels (SOCs).

Store operated Ca^{2+} entry (SOCE) is noticeable in almost all non-excitable cell types, and it often controls Ca^{2+} mediated processes in excitable cells, as well. SOCE is generated primarily by two families of proteins [13]. STIM proteins (stromal interacting molecule) localize to the ER membrane having a Ca^{2+}-binding EF-hand domain on their ER lumen facing N-terminus. When the Ca^{2+} concentration in the lumen of the ER decreases, the Ca^{2+} ions dissociate from this domain and after oligomerization the STIM molecules relocate to ER-plasma membrane junctions. Here they activate the pore formation of the Orai protein family (Orai1-3) by direct binding allowing Ca^{2+} entry across the plasma membrane from the extracellular space. [13]. As a result, after the decrease of the ER lumen Ca^{2+} level, the so-called calcium release activated calcium (CRAC) current is measurable through the plasma membrane.

In non-excitable cells Ca^{2+} store depletion most often is a consequence of IP_3R activation. IP_3 is produced after cell surface receptor stimulation by many different stimuli, such as hormones, growth factors or ATP. SOCE is an example when the main sources of Ca^{2+} - internal and external - are combined and contribute to the rise of the Ca^{2+} signals [14].

2.1.2 Ca^{2+} decrease reactions

After Ca^{2+} level increase, the intracellular Ca^{2+} concentration needs to be lowered to its basal level by the concerted action of the Na^{+}/Ca^{2+} exchangers (NCX), the plasma membrane Ca^{2+} ATPases (PMCA), the sarco/endoplasmic reticulum Ca^{2+} ATPases (SERCA) and the mitochondrial uniporters. NCX becomes activated by micromolar Ca^{2+} concentration, however, it can remove quickly high amount of Ca^{2+} from the cytosol by virtue of its high transport capacity. It transports one Ca^{2+} ion at the expense of three sodium ions entering the cytoplasm using the transmembrane sodium gradient. It is mostly found in excitable cells, especially in cardiac and skeletal muscle and in the nervous system [15].

PMCA and SERCA pumps are low capacity but high affinity transporters being able to restore the very low 100 nM resting cytosolic Ca^{2+} concentration. They use the energy of ATP molecules to pump Ca^{2+} ions against their concentration gradient towards the outer space or into the ER lumen. Another Ca^{2+} pump, the secretory-pathway Ca^{2+} ATPase (SPCA) transports

Ca^{2+} into the Golgi compartments with high affinity. It does not only contribute to the uptake of excess Ca^{2+} from the cytosol, but it is also able to transport Mn^{2+} ions. Both Ca^{2+} and Mn^{2+} molecules are necessary for the basic function of the secretory pathway such as protein synthesis, folding or trafficking. Mn^{2+} is also a cofactor in number of enzymes and its removal from the cytosol by SPCA prevents its accumulation to toxic levels [16].

Mitochondrial uniporters (MCUs) use the mitochondrial membrane potential as an energy source for ion transport. The uniporter is active when Ca^{2+} concentration is high. This can happen when the Ca^{2+} level in the entire cytosol is strongly increased, or only locally when the ER and mitochondria are in close proximity and Ca^{2+} released by the IP3R or RYR directly activate mitochondrial Ca^{2+} uptake [17]. Fine tuning of intracellular Ca^{2+} signals is accomplished by the regulation of expression and activity of the numerous isoforms and splice variants of this Ca^{2+} toolkit.

2.2. Ca^{2+} transport ATPases

In mammals three types of Ca^{2+} ATPase are known: PMCAs, SPCAs and SERCAs. All of them belong to the P-type ATPases as during their enzymatic cycle a phosphorylated aspartate intermediate is generated. They use ATP to translocate ions against their electrochemical gradient and they all can be inhibited by the transition state analogue orthovanadate. P-type ATPases have 10 transmembrane domains including strongly conserved regions in the cytoplasmic side between the second and third, and the fourth and fifth domains [18].

2.2.1. Sarco/endoplasmic reticulum Ca^{2+}- transport ATPase (SERCA)

There are three SERCA proteins (SERCA1-3) coded by 3 different genes (ATP2A1-3). Their main role is to refill the Ca^{2+} stores and restore the basic Ca^{2+} concentration of the cytosol after transients. They pump 2 Ca^{2+} ions into the ER/SR by hydrolyzing one ATP molecule [19]. Among the Ca^{2+} transport ATPases only the SERCA1 protein was successfully crystalized [20]. Based on its crystal structure SERCA proteins have four large domains: the M-domain (membrane domain), which contains the 10 transmembrane helices, and the cytosolic A (actuator)-, N (nucleotide binding)- and P (phosphorylation)-domains. ATP binds to the N-domain, while the phosphorylated aspartate residue is located in the P-domain. The A-domain coordinates the movement of the N- and P- domains during the catalytic cycle [21].

Detailed information about the SERCA structure helped to build the models describing PMCA structure and function [22].

SERCA1 is most abundant in the skeletal muscle, giving almost 50% of membranes proteins of muscle cells, and being accountable for around 40% of their metabolic rate. SERCA1 has two isoforms generated by the alternative splicing of its exon22. SERCA1b is present during neonatal development, while SERCA1a is expressed in adults [23, 24]. SERCA2 has four known isoforms among which SERCA2b has a housekeeping function and it is expressed in a lower amount but ubiquitously. SERCA2a, c and d are all expressed in the heart. SERCA2a isoform is most abundant in the cardiac muscle but also present in other muscle types and neuronal cells [25]. SERCA3 is the most recently identified and the least known member of the family. It differs from the other two SERCA pumps by having a five-fold lower affinity toward Ca^{2+}. Its expression is widespread but it is found always together with the housekeeping form SERCA2b which makes possible to fine tune the ER Ca^{2+} uptake. The expression of SERCA3 is known to be altered in several cancer types [26]. It is abundantly expressed in normal colon, breast and bronchial epithelium however its expression is lost during the carcinogenesis of these tissues [27-29]. Treatment of colon, breast or lung cancer cell lines with histone deacetylase inhibitors was shown to induce SERCA3 expression together with differentiation. These data suggest that SERCA3 is an important regulator of differentiation and its loss contributes to malignant transformation.

2.2.2. Plasma membrane Ca^{2+}- transport ATPase (PMCA)

There are four plasma membrane Ca^{2+} ATPases (PMCA1-4) coded by four different genes (ATP2B1-4) which all localize on different chromosomes. PMCAs become activated by the increase of the cytosolic Ca^{2+} concentration and their main role to pump excess Ca^{2+} out from the cytosol. They use one ATP to transport one Ca^{2+} [30]. Nevertheless, there is a great functional diversity among these pumps which is further increased by the generation of over 20 splice variants through alternative splicing at two splice sites (Figure 2) [31]. Their general structure consists of 10 transmembrane helices and three intracellular domains.

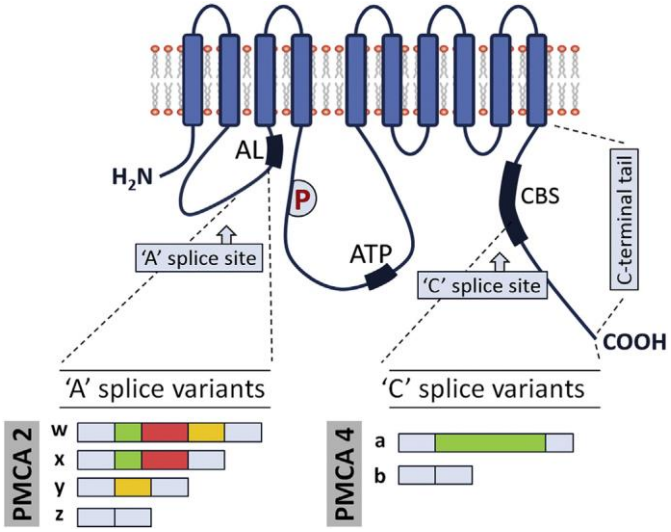

Figure 2. Schematic model of plasma membrane Ca^{2+} ATPase [32]. The PMCA has ten transmembrane helices (on the top), a small intracellular loop including splice site ´A´ and an acidic lipid binding region (AL). In the large intracellular loop there is the ATP binding site (ATP) and the catalytic phosphorylation site (P).The calmodulin binding sequence (CBS) and the ´C´splice site are found in the C-terminal tail. Below the splice variants of PMCA4 at splice cite ´C´ and the splice variants of PMCA2 at splice cite ´A´ are shown.

Splice site A and the acidic lipid binding region (AL) are found in the small intracellular loop, which according to the SERCA structure forms the A domain. The ATP binding region and the catalytic phosphorylation site are located in the large intracellular loop forming the N and P domains, respectively. The C-terminal tail contains the calmodulin binding site (CBS), which overlaps with splice site C. In the resting state the C-terminal tail strongly interacts with the catalytic domains and serves as an autoinhibitor [32]. Splicing at site C affects the interaction of the C-terminal tail both with Ca^{2+}-calmodulin (Ca^{2+}-CaM) and the core regions and determines the basal activity of the pump. In general PMCAs with an ´a´ insert have a higher basal activity and lower CaM affinity than the ´b´splice variant without the insert. Since the strength of the interaction also depends on the sequence composition of the catalytic region large differences can be found among the same splice variants of the different isoforms. For instance, PMCA4b has a lower basal activity and hence a stronger activation by Ca^{2+}-CaM than PMCA2b [31]. Alternative splicing at the C-terminal region also affects the regulation of the pump by other means such as phosphorylation by protein kinases and interaction with other proteins. The splice site A variants differ in their intracellular targeting; for example the PMCA2 proteins with a ´w´ insert are targeted to the apical membrane in polarized

epithelial cells, while the ´x´variants have basolateral localization [33]. Amino acid sequence differences also influence the interaction with acidic phospholipids in the AL region close to splice site ´A´. Because of all these differences a toolkit of PMCA proteins is generated in which each member differs in its activation kinetics, interaction partners and regulation.
The functional diversity is coupled with distinct developmental, tissue and cell type specific distribution (Table 1) [31, 34].

Isoform	Alternative splice variants	Major sites of expression	Gene knockout phenotype (mouse)
PMCA1	x/a x/b x/c x/d x/e	Brain Ubiquitous, lung, kidney Skeletal muscle, heart Skeletal muscle Brain	Embryonic lethal (homozygotes); altered smooth muscle Ca^{2+} regulation (heterozygotes)
PMCA2	w/a x/a z/a w/b x/b z/b	Brain, cochlear outer hair cells Brain Brain Brain, lactating mammary epithelial cells Brain, spinal cord Brain	Profoundly deaf, severe ataxia, reduced milk Ca^{2+}, motor neuron loss (homozygotes)
PMCA3	x/a z/a x/b z/b	Brain, spinal cord Brain, pancreatic beta cells Brain, Skeletal muscle Brain	Not determined
PMCA4	x/a z/a x/b z/b x/d z/d x/e z/e	Smooth muscle, bladder, heart Smooth muscle, heart Ubiquitous, heart, kidney Heart Heart Heart Brain, bladder Brain, bladder	Male infertility due to sperm motility defect (homozygotes)

Table 1: Human PMCA isoforms and splice variants (Based on [31, 34].)

PMCA1x/b is considered as the housekeeping isoform and appears the earliest during mouse embryonal development. Homozygous deletion of the ATP2B1 gene in mice causes embryonic death [35]. However the other splice variants of PMCA1 protein are only expressed in specific cell types mostly in the brain and in striated muscle. PMCA4x/b is also ubiquitously expressed, while other PMCA4 variants are mostly found in the heart and in smooth muscle. Loss of both copies of the ATP2B4 gene causes complete male infertility in mice [35]. PMCA2 and PMCA3 are mostly expressed in excitable cells, and so they abundantly found in the brain and in skeletal muscles. Some of them are present in very specialized cell types, like PMCA2w/a in auditory and vestibular hair cells [36] while

PMCA2w/b in the lactating mammary glands. The phenotype of ATP2B2-/- mice is ataxia, profound deafness [37] and reduced Ca^{2+} content in milk [38]. Furthermore, often multiple PMCA isoforms are present simultaneously in a cell having different expression level and subcellular localization. For example in cochlear hair cells in the inner ear PMCA2w/a is specifically targeted to the apical stereocilia while PMCA1x/b resides in the basolateral membrane [39].

2.2.2.1. Regulators of PMCA activity

The primary regulator of PMCA activity is the Ca^{2+}- calmodulin complex. When the intracellular Ca^{2+}concentration rises, each CaM molecule binds 4 Ca^{2+} ions and Ca^{2+}-CaM complexes are formed. The binding of Ca^{2+}-CaM to the C-terminal region of the PMCA induces a conformational change in the protein and thus the connection between the inhibitory region and the catalytic domains is relieved and the pump becomes active [40]. The kinetics of the binding of Ca^{2+}-CaM to the most common PMCA isoforms was heavily investigated. It was found that PMCA4b binds the Ca^{2+}-CaM complex slowly and also dissociates it slowly, only after a couple of minutes. However, PMCA4a, which has another splice variant in its CaM binding sequence, binds Ca^{2+}-CaM quickly but then dissociates it faster [41], resulting in an overall lower affinity (relatively high K_d) for the Ca^{2+}-CaM complex than the other splice form. The PMCA2 and PMCA3 pumps, which are common in excitable cells, both have fast activation and slow inactivation kinetics, resulting in tight Ca^{2+}-CaM binding (low K_d) [42]. Pumps with a slow inactivation rate have a longer memory of the earlier Ca^{2+} spike, which means that if subsequent signals come quickly the pumps are still active and can act promptly.

Acidic phospholipids are also important regulators of PMCA proteins. PIP_2 (phosphatidylinositol-4,5- bisphosphate) is an important signaling molecule and a known regulator of different pumps and channels. PIP_2 can be hydrolyzed by the Ca^{2+}- dependent PLC into diacyglycerol (DAG) and IP_3, of which the latter induces Ca^{2+} release from the internal stores [43]. Previously, two acidic lipid binding regions were identified, one close to splice site ´A´ and another in the CBS region within the C-terminal tail. Recently, with homology modelling of PMCA4b a third PIP_2 binding area was described, within the stalk region of the pump. This region formed by positively charged residues creates several binding pockets for the inositol ring of the PIP_2 molecule. It was demonstrated that by

binding PIP_2 molecules PMCA4b can influence the amount of available PIP_2 for intracellular signaling. Furthermore, it can directly decrease PLC activation providing a second layer of protection by pumping out Ca^{2+} from the vicinity of the bound PIP_2 molecules [44].

The activity of PMCA proteins is also dependent on their abundance in the plasma membrane. It was shown that PMCA4b mostly resides in the intracellular compartments in sub-confluent cell cultures, while at confluency it translocates to the plasma membrane. A di-leucine sorting signal was identified in the C-terminal tail of the pump (^{1167}LLL) that regulates its internalization to early endosomes after loss of cell-cell contact. Alternation of this motif to three alanines increased the plasma membrane localization of PMCA4b in sub-confluent cells and changed the trafficking of PMCA4b after internalization [45].

Phosphorylation can also change the activity of PMCAs. Several phosphorylation sites for protein kinases A and C were described in the C-terminal tail of these pumps. The effect of phosphorylation is isoform dependent as it can both increase and decrease the activity of the pumps [46, 47].

There are cleavage sites for both calpain and caspase-3 proteases in the C-terminal tail of PMCA. Proteolytic cleavage of this region releases the autoinhibition of the pump [48]. During apoptosis caspase-3 activity removes the complete inhibitory region and the pump becomes fully active [49]. This might help to avoid excessive Ca^{2+} overload and consequently necrotic death of the cells [50].

2.2.2.2. Interactions with scaffold proteins

Several protein partners of PMCAs have been identified. On the one hand these protein-protein interactions can influence the activity of the pump, on the other hand they can target PMCAs into specific membrane microdomains or signaling platforms. One of the most important interaction sites is the PDZ-binding sequence at the C-terminus of each b-splice variant. PDZ proteins have scaffolding and anchoring roles creating platforms for protein-protein interactions or linking proteins to the cytoskeleton. PMCA1b, 2b and 3b carry an identical PDZ-binding sequence (-ETSL). PMCA2b was shown to interact with the scaffold protein Na^+/H^+ exchanger regulatory factor 2 (NHERF2) [51]. It was demonstrated that in polarized MDCK cells “w” A-splice variant PMCA2w/b localizes to the apical membrane and this is stabilized by NHERF2-binding that anchors the pump to the actin cytoskeleton [52]. The PDZ-binding sequence of PMCA4b is different in one amino acid residue (-ETSV), and it

interacts with different PDZ proteins. Co-expression of membrane-associated guanylate kinase (MAGUK) scaffold family member PSD-95 (post synaptic density protein) and PMCA4b in COS-7 cells resulted in the redistribution of the pump into clusters which were fenced by the actin cytoskeleton and hindered the lateral mobility of the protein [53, 54].

2.2.2.3. Interactions with signaling molecules

PMCAs by interacting with other proteins are also able to regulate downstream signaling events. The protein partners come into contact with different regions of the pump. Through its PDZ-domain PMCA4b interacts with the neural nitric oxide synthase (nNOS) molecule. PMCA4b was shown to decrease nNOS activity and as a consequence also β-adrenergic stimulation of cardiomyocytes in mice [55]. Interestingly, this effect is not related to the pump's Ca^{2+} extruding capacity, in this respect PMCA has a structural role by tethering nNOS into a special membrane compartment of the cardiac cell [56].

Interactions with the N-terminal segment of the pump were also described. For example a regulatory protein 14-3-3ε can bind to this region and inhibit the activity of PMCA4 [57].

Several proteins were found to interact with the large intracellular loop as well. Tumor suppressor Ras effector protein, RASSF1 was found to directly interact with PMCA4b in a yeast two hybrid screen system. Co-expression of the two proteins inhibited the activation of the ERK pathway in the cells after activation with epidermal growth factor (EGF) [58].

Also association of PMCA and endothelial nitric oxide synthase (eNOS) was demonstrated through the catalytic loop which led to the inhibition of eNOS activity and NO production in endothelial cells [59].

There is ample evidence in the literature that PMCA can regulate the activity of the calcineurin (CaN) / NFAT (nuclear factor of activated T-cell) pathway. Calcineurin is a Ca^{2+}/CaM dependent serine/threonine protein phosphatase which can activate the NFAT transcription factor family [60]. It was shown that both PMCA4 and PMCA2 directly interact with calcineurin through their catalytic core region which results in a reduced NFAT activation. It was hypothesized that this effect is achieved by keeping the bound calcineurin in a low Ca^{2+} environment [61, 62]. Furthermore, in osteoclasts an autoregulatory loop was described between PMCA1 and 4 and NFATc1, where NFATc1 directly binds to the promoter region of these PMCAs and induces their expression while PMCA activity reduces cytosolic Ca^{2+} oscillations, hence NFAT activation [63]. Additionally, in endothelial cells PMCA4b was

described to decrease NFAT activation after vascular endothelial growth factor (VEGF) induction. PMCA4 also reduced endothelial tube formation of mouse lung endothelial cells both in vitro and in vivo [64].

An interaction of PMCA and a scaffold protein POST (Partner of STIM) in T-cells was also described. POST was discovered as a binding partner of the ER Ca^{2+} sensor molecule STIM1. It is also able to bind to other proteins including SERCAs, PMCAs and Na^{+}/K^{+}-ATPases thus creating multimolecular complexes. Upon interaction with the PMCA POST lowers the activity of the pump and in this way it helps to maintain the elevated intracellular Ca^{2+} concentration upon T-cell stimulation [65].

All these findings revealed that PMCA proteins are important members of the intracellular signaling network and besides removing excess Ca^{2+} from the cytosol they are able to influence specific signaling pathways.

2.3 Alternations of Ca^{2+} transport in cancer

During the malignant transformation cells acquire the features of cancer cells. These features are called as the hallmarks of cancer [66], which are the sustained proliferative signaling, avoidance of cell death, resistance against anti-proliferative signaling, replicative immortality, stimulation of angiogenesis, invasive capacity and ability to form metastasis, altered energy metabolism and avoidance of the immune response. Ca^{2+} plays an important role in the regulation of many of these processes in healthy cells, and alterations of several Ca^{2+} handling proteins were described in cancer cells. These alterations can modify not only the spatial and temporal features of the intracellular Ca^{2+} changes but also the steady state Ca^{2+} level of the subcellular compartments resulting in both cases in an altered activation of downstream signaling pathways [67].

2.3.1. The role of Ca^{2+} in tumor cell survival

Ca^{2+} plays an important role in the regulation of cell cycle in healthy cells. Early in the G1 phase, elevation of cytosolic Ca^{2+} concentration is required for the initiation of the cell cycle through the activation of transcription factors c-fos, c-jun, myc and NFAT. These transcription factors regulate the expression of cell cycler regulator cyclin dependent kinases (CDK2 and 4) and cyclins (D and E). During the G1/S transition phase Ca^{2+} is required for the

phosphorylation step of the retinoblastoma checkpoint protein that causes its inactivation. Furthermore, during the G2/M transition Ca^{2+} oscillations regulate centrosome separation through CaMKII (Ca^{2+}/calmodulin-dependent protein kinase II) activity [68].

In cancer cells the activity of several Ca^{2+}-dependent transcription factors is sustained initiating constant growth. The reason for the sustained growth activation can be the increased Ca^{2+} inflow to the cell [69]. For example in prostate cancer cells transient receptor potential cation channels TRPC6 and TRPV6 have been shown to induce the activation of the NFAT signaling pathway and TRPV6 was identified as a prognosticator for tumor progression [70]. Members of SOCE were found to enhance cell growth in several types of cancer such as breast, prostate, colorectal and cervical cancer [71]. For example, Orai3 channel was reported to be overexpressed in breast, lung and prostate cancer. In MCF-7 breast cancer cells, Orai3 was found to increase cell cycle progression through the induction of proto-oncogene c-myc [72]. In prostate cancer cells, Orai3 and Orai1 form heterotetramers that can be activated by arachidonic acid (AA) independently from store depletion. This, on the one hand, induces the calcineurin-NFAT pathway, which ultimately activates cyclin D1 and proliferation. On the other hand, it contributes to the avoidance of apoptosis by decreasing the ratio of the homomeric Orai1 channels, which are necessary for apoptosis induction through SOCE [73].

It has been known for a long time that Ca^{2+} plays an important role in the regulation of cell death. There are several different forms of cell death including apoptosis, autophagy and necrosis. Ca^{2+} overload in the mitochondria and Ca^{2+} depletion of the ER both can trigger apoptosis, while excessive cytoplasmic Ca^{2+} overload can induce necrosis [74]. During autophagy, a process with particular importance in both cancer cell death and resistance, Ca^{2+} was shown to regulate autophagosome formation and it can activate the death-associated protein kinase (DAPK), one of the major regulatory protein of autophagy [75]. There is a cross-talk among these processes and they can be present in a given tissue, simultaneously.

Cancer cells are able to avoid cell death through altered regulation of Ca^{2+} handling molecules. For example, the decreased expression and/or activation of plasma membrane Ca^{2+} channels can reduce the chance of a Ca^{2+} overload after apoptotic stimuli. In androgen independent prostate cancer cells, the expression of Orai1 and STIM1 proteins were found to be decreased resulting in decreased SOCE [76]. This was coupled with adaptation to a

reduced Ca^{2+} level in the ER because of the reduced expression of the ER Ca^{2+} binding protein calreticulin and the SERCA2b pump [77].

However, increased expression of Ca^{2+} channels can also lead to apoptosis resistance either by inhibiting pro-apoptotic pathways or by directly refilling ER stores with Ca^{2+} and in this way avoiding ER depletion caused ER stress. For example, in breast cancer cells, Orai3 initiated c-myc activation induces not only proliferation but it also decreases the expression of the pro-apoptotic Bax protein [78]. While in certain astrocytoma cells TRPV1 channels are highly expressed both in the plasma membrane (PM) and in the ER membrane and activation of these channels induces apoptosis by initiating ER stress [79].

Ca^{2+} released from the ER through IP_3R channels can be directly taken up by the mitochondria in their contact sites which can initiate permeability transition pore (PTP) opening and cytochrome-c release. Consequently, resistance can come from the decreased expression or activation of IP_3Rs.This was observed in cisplatin resistance bladder cancer cells where decreased expression of IP_3R1 prevented apoptosis [80]. Furthermore, it was demonstrated that anti-apoptotic protein Bcl-2 can directly interact with IP_3Rs and inhibit their activities [81].

2.3.2 The role of Ca^{2+} in tumor cell migration and metastasis

Ca^{2+} is a key regulator of cell migration in healthy cells. In migrating cells, an increasing Ca^{2+} gradient is generated from the front, where protrusions are developed, towards the rear end of the cell, where the trailing edge is retracted. This makes possible to differentially regulate Ca^{2+}-dependent modulators of the migratory process along the polarized cell [82]. One such modulator is the Ca^{2+}-dependent myosin light chain kinase (MLCK), which by phosphorylating the regulatory light chain of myosin II initiates contraction. Focal adhesions (FA) connect the cytoskeleton of the cell with the extra cellular matrix (ECM). For cell motility, FAs need to be assembled in the front and disassembled in the rear. This is primarily controlled by focal adhesion kinase (FAK) which is a non-receptor tyrosine kinase. FAK activity is regulated directly by local Ca^{2+} changes in the focal adhesion site [83] and also through the calcium/calmodulin-dependent kinase II [84]. Furthermore, the Ca^{2+}-dependent protease calpain 2 also regulates FAK activity by proteolysis [85]. In the leading edge of fibroblasts, stretch-activated TRPM7 channels together with IP_3R channels in the ER

generate local Ca^{2+} flickers, which are necessary for directed migration toward chemoattractants [86].

Meyer et al. investigated in detail the spatial distribution and polarized function of Ca^{2+} regulating molecules in the leader cells of collectively migrating human umbilical vein endothelial cells (HUVECs) [87]. They found that receptor tyrosine kinase signaling was increased in the front of the cells and this led to a similarly polarized activation of PLC and generation of IP_3 and DAG. This activity generated local Ca^{2+} pulses in the front that induced MLCK activity. They showed that the global - toward the rear increasing - Ca^{2+} gradient was also present in these cells. Furthermore, the low global Ca^{2+} concentration in the front was the result of the enhanced Ca^{2+} extrusion capacity of the PMCA proteins, which localized mostly in the front of the cells. It was presented that the localization of the ER Ca^{2+} sensor molecule STIM1 also shifted towards the front, which was coupled with a decreasing Ca^{2+} level in the ER lumen.

Metastasis is the major cause of cancer related death and cell migration is a prerequisite for metastasis. While in cancer cells the same set of Ca^{2+} signaling molecules are present as in normal cells, their activity and expression are often remodeled [82]. Increased Ca^{2+} intake through plasma membrane Ca^{2+} channels was shown to enhance cell migration in several cancer types [69]. For example, in metastatic prostate cancer, increased expression of TRPV2 channel was found when compared to the primary tumor. Elevated expression of TRPV2 increased the motility of the cells and the production of invasion associated enzymes, MMP9 and cathepsin B [88]. SOCE was shown to be necessary for enhanced migration and metastasis of MDA-MB-23 breast cancer cells. Downregulation of Orai1 and STIM1 expression or activity decreased cell migration and metastatic potential, in vivo [89]. In the lung cancer cell line A549 EGF treatment induced the expression of TRPM7 channel. Inhibition of TRPM7 activity and/or expression reduced the migratory potential of the cells [90]. ER Ca^{2+} receptor channel IP_3R3 expression was found to be elevated in glioblastoma cells and inhibition of IP_3R3 by caffeine decreased cell motility both in vitro and in vivo [91].

2.3.3 Remodeling of PMCAs in cancer

Changes in the expression and the activity of PMCA proteins were described in several types of cancer, however, their role in carcinogenesis is isoform dependent. PMCA4b expression was found to be downregulated unanimously in cancer cells from various tumor types.

Strong decrease of PMCA4 expression was found in lymph node metastasis of colorectal cancer when compared to normal tissue and adenomas [92]. Furthermore, differentiation of colon cancer cell lines with short chain fatty acids, trichostatin A or by spontaneous differentiation strongly increased PMCA4b expression of the cells [93]. Similarly, PMCA4b is abundantly expressed in normal breast epithelium but it is present in a very low amount in breast cancer cells. Differentiation of breast cancer cell line MCF-7 with histone deacetylase inhibitors also enhanced the expression of this pump [94]. These results suggest that PMCA4b expression strongly correlates with the degree of differentiation of cells.

In the case of PMCA1, the results are more controversial. In oral cancer cell lines its expression was found strongly downregulated by increased methylation in its promoter region, and its amount was also decreased in primary oral squamous cell carcinomas and in premalignant lesions [95]. PMCA1 protein level was also reduced in SV40-transformed fibroblasts compared to control cells [96] but a moderate increase in its mRNA level was detected in breast cancer cell lines [97]. It was demonstrated that PMCA1 was abundantly present in colon cancer cells and its expression only moderately increased after treatment with differentiating agents [93, 98].

Alterations in PMCA2 protein expression was described in breast cancer cells. In healthy breast tissue, PMCA2 is only expressed during lactation. However increased expression of PMCA2 mRNA was detected in several breast cancer cell lines [99]. It was suggested that the higher abundance of PMCA2 decreased the basal cytosolic Ca^{2+} concentration in these cells that resulted in a decreased susceptibility of the cells for apoptosis. PMCA2 was found to interact with calcineurin-A in the human breast cancer cell line MCF-7 and this interaction decreased the activity of transcription factor NFAT in the cells [62]. Inhibition of the PMCA2/calcineurin interaction induced the expression of the proapoptotic protein Fas Ligand on the cell surface and increased apoptosis of the cells [100].

All these changes of Ca^{2+} handling molecules might not be the driving causes of cancer formation but rather consequences, nevertheless, they help to sustain cancer hallmarks. Better understanding of their function and modulation helps to identify new biomarkers or drug target molecules.

2.3.4. The effect of HDAC inhibitor treatment on PMCAs in cancer cells

In eukaryotes, genomic DNA together with histone proteins is organized into the chromatin. The DNA strand is coiled around the globular nucleosomes formed by histone H3, H4, H2A and H2B proteins that are connected by linker histone H1. During gene expression this structure needs to loosen in order to RNA polymerase II binding [101]. Postsynthetic modification of the DNA and/or posttranslational modification of histone proteins can alter gene expression a phenomenon named epigenetic regulation. These alternations of the chromatin are reversible, changing during development and are affected by environmental factors. In the DNA, cytosines in CpG sequences can be methylated and when CpG islands in promoter regions are methylated that can lead to gene silencing. Remodeling of DNA methylation is often described in cancer cells [102].

Histone proteins can go through various posttranslational modifications, like acetylation, methylation, phosphorylation or ubiquitylation. Histone acetyl transferases (HATs) are able to transfer an acetyl group to lysine residues in histone proteins. These acetylated lysines are specifically recognized by bromodomain containing proteins, such as helicases, methyltransferases, transcription coactivators and HATs themselves. Through the action of these proteins, histone acetylation influences chromatin remodeling and subsequently gene transcription, DNA replication and repair as well [103]. Increased acetylation of a chromatin region enhances DNA transcription there. In contrast histone deacetylases (HDACs) remove the acetyl groups from the lysine amino acids of histones. 18 different HDAC proteins were already described. Class I HDACs (HDAC1, HDAC2, HDAC3 and HDAC8) are found only in the nucleus, while class II HDACs shuttle between the nucleus and the cytoplasm (HDAC4, HDAC5, HDAC7, HDAC9, HDAC6 and HDAC10) and they all use Zn^{2+} as cofactor. Class III HDACs are the SIRT proteins that require NAD^{+} to their function. Since NAD^{+} production is dependent on the cellular nutrient levels, the activity of these HDACs is influenced by the metabolic state of the cells [104]. Beside histones they regulate acetylation of non-histone proteins as well. For example HDAC6 deacetylates α-tubulin through which it regulates cell migration [105].

Since it was found that the expression and/or activities of HDACs are often increased in cancer cells, the antitumor effect of HDAC inhibitors was investigated [106]. Several different types of HDAC inhibitors were developed and it was demonstrated that they can affect

differentiation, apoptosis, motility, metastatic capacity and immunogenicity of cancer cells [107]. Hydroxamates – like trichostatin A (TSA) and suberoylanilide hyroxamic acid (SAHA or vorinostat) - interfere with HDAC activity by chelating the catalytic Zn^{2+}. TSA was shown to induce differentiation or apoptosis in colon, gastric and prostate cancer cells [108, 109] and to enhance the effect of other antitumor drugs [110]. SAHA was approved as drug against cutaneous T cell lymphoma. Short chain fatty acids as butyrate or valproic acid (VPA) also has been shown to decrease tumor cell proliferation and increase cell death [111, 112]. VPA was already a known medication for epilepsy and seizures and its inhibitor effect on HDACs was only subsequently discovered. All the above mentioned HDAC inhibitors target multiple HDACs, lately several isoform selective HDAC inhibitors were developed and their clinical effect is currently investigated [107].

The influence of HDAC inhibition on PMCA expression has been examined in gastric, colon and breast cancer cell lines. It was demonstrated that after treatment with TSA or short chain fatty acids expression of PMCA4b was strongly increased in gastric and colon cancer cells while the abundance of PMCA1 isoform was only moderately elevated [93]. Spontaneous differentiation in post-confluent Caco-2 colon cancer cell cultures also induced PMCA4b expression. Similar results were obtained in breast cancer MCF-7 cells. PMCA4b was present in very low amount in control cells however treatment with valproate or SAHA caused a strong increase in PMCA4b expression. There was a higher amount of PMCA1b detected in the untreated cells, and its expression was only slightly elevated by the treatment [94].

The effect of HDAC inhibitor treatment on melanoma cells was also investigated. On one hand it was found that HDAC inhibitors can induce cell death in melanoma cells by increasing the expression of pro-apoptotic proteins (BIM, BAX) and decreasing the anti-apoptotic ones (Bcl-2). On the other hand this effect was strongly cell line and agent dependent [113, 114]. In BRAF mutant melanoma cells combination treatment with BRAF inhibitor PLX4720 and SAHA increased the number of the apoptotic cells compared to single agent treatment. SAHA also sensitized resistant BRAF mutant cells to PLX4720 treatment induced apoptosis [115]. It was also found that HDAC inhibitor treatment affected the immunogenicity of melanoma cells. Pan-HDAC inhibitor (LHB589) increased the expression of MHC and co-stimulatory molecules [116] while treatment with various class I HDAC inhibitors induced PDL-1 ligand expression on melanoma cells [117]. HDAC inhibitors were tested also in clinical

trials in metastatic melanoma patients however as single agents induced high level of toxicity. Since they were shown to increase immunogenicity and increase apoptosis in BRAF inhibitor resistant cells their applicability in combination therapies is currently investigated [118].

2.4. Metastatic melanoma

Incidence of melanoma is constantly rising worldwide but the white skin population in North-America, Australia and Europe is particularly susceptible for this disease [119]. In the USA, melanoma was one of the three most prevalent cancers among men in 2016 [120]. When melanoma is recognized in a localized stage the 5-year survival rate is 98%, however, among patients with regional metastasis it becomes 63% while with distant metastasis it is only 15% [119]. Surgical removal is the primary therapy for stage 0-II and resectable stage III melanomas. For unresectable stage III and IV cases a variety of targeted therapy, immunotherapy and chemotherapy are administered. Several new therapeutic options emerged in the last decade but the low percentage of long-term survivors shows the need for further research in this area.

2.4.1. Melanoma development

In the healthy skin, melanocytes are localized in the junction of the two layers of the skin, the epidermis and the dermis. The epidermis constitutes the barrier toward the outer environment through stratified keratinocytes, which are constantly renewed. The dermis provides nutrients and mechanical support. The basement membrane is localized between these two layers. The role of melanocytes is to produce melanin and transfer it to keratinocytes to provide protective cap over the nucleus against UV radiation. Melanocytes during development migrate to the skin from the neural crest where they develop several dendrites through which they are in connection with about 36 keratinocytes each. The proliferation capacity of melanocytes is tightly controlled by the surrounding keratinocytes [121].

Congenital nevi are present at birth and more nevi are commonly acquired during childhood. Dysplastic nevus shows histological abnormalities and regarded as a precursor towards cutaneous melanoma. The first malignant stage is the radial growth phase of melanoma

where cells rapidly proliferate and show local invasiveness. The second is the vertical growth phase of melanoma where cells spread already toward the subcutaneous tissue and the chance for metastasis is elevated. The final stage is when metastases are developed [122].
Melanoma cells in contrast to melanocytes do not develop dendrites and loss their contacts with keratinocytes, proliferate rapidly and express melanoma-associated antigens (MAA). This high immunogenicity of melanoma cells led to the discovery of several, not only melanoma specific, tumor associated antigens such as MAGE, and that makes melanomas a promising target of immunotherapy [123].

2.4.2. Mutational landscape and targeted therapies

Several oncogenic mutations were identified in melanoma and most of these can lead to the constant activation of mitogen activated protein kinase (MAPK) pathway. This pathway can be stimulated by external stimuli of epidermal growth factor (EGF), insulin-like growth factor (IGF) or transforming growth factor (TGF) through the receptor tyrosine kinase receptors in the plasma membrane, all of which activate the downstream small GTPase RAS proteins (HRAS, KRAS, NRAS). Ras proteins act on the downstream serine-threonine RAF kinases (ARAF, BRAF, CRAF), which turn on the MEK kinases that in turn activate ERK1 and ERK2. ERK proteins can traffic to the nucleus where they directly activate transcription factors such as ELK-1 inducing growth and survival [119]. Mutations in the NRAS gene were identified in 15% of melanomas [124], while in about 50% of the cases BRAF mutation was found. Among the many described BRAF mutations the V600E is particularly prevalent, where a glutamic acid is changed to a valine [125]. This mutation is found in more than 75% of the cases.
Mutations with lower frequency were identified in other pathways as well. Inactivating mutation of the tumor suppressor protein PTEN is often present that enhances PIP_3 production and in this way the activation of the PI3K/Akt/mTOR pathway. Furthermore, activating mutations in the PI3K/Akt/mTOR pathway were also described.
Since the constituent activation of the MAPK pathway is so frequently the driving force of melanoma cell survival and spread, specific inhibitors were developed against the BRAF and MEK kinases. Before these agents only the chemotherapeutic drug dacarbazine was available for patients with metastatic melanoma resulting in median overall survival around 5 months. Introduction of mutant BRAF (V600E) specific inhibitor vemurafenib and later dabrafenib initiated quick and high response rate (60%) and raised median overall survival to around 13

months. However, there were patients with intrinsic resistance and in most of the cases acquired resistance emerged within 6-8 months [126]. A number of molecular mechanisms have been described for the intrinsic resistance such as PTEN loss [127], cyclin D1 amplification and stromal cells produced hepatocyte growth factor (HGF) stimulation through its receptor CMET. Acquired resistance mechanisms are induced by the BRAF inhibitor treatment. They can be either ERK-dependent like upregulation of the RTK receptors which results in the reactivation of ERK, or ERK-independent like the induction of the PI3K/Akt/mTOR pathway [126].

The other successfully targeted molecules in the MAPK pathways are MEK1 and MEK2. Several highly specific inhibitors were developed like trametinib and comibetinib, and since 2014 the combination therapy of BRAF inhibitor dabrafenib and MEK inhibitor trametinib is approved for unresectable and metastatic BRAF mutant melanomas [128]. MEK inhibitors were also tested in clinical trials with NRAS mutant melanoma patients, however, their efficacy were unfortunately very low; combination of MEK inhibitors with PI3K-AKT or CDK4/6 inhibitors might increase the therapeutic benefit [124].

Mutations of receptor tyrosine kinase C-KIT were also identified with lower frequency (2-5%) in cutaneous melanomas and trials with C-KIT inhibitor imatinib and sunitib were conducted and gave promising results [129].

2.4.3. Immunotherapy to treat melanomas

Most efficiently and least invasively the patient´s own immune system could eradicate cancer cells. However, tumor cells are able to evade or suppress immune response even if they are so immunogenic as most melanoma cells. Immunotherapies like treatment with cytokines (IL-2, IFN-α) or adoptive cell therapy with ex vivo grown antitumor lymphocytes were already used in metastatic melanomas [123], however, the breakthrough was recently achieved with the use of immune checkpoint inhibitors. This method is based on the regulation of T-cell activation. CTLA-4 (cytotoxic T-lymphocyte-associated antigen 4) is a transmembrane receptor and its expression is increased after the activation of T-cells. It can interact with the costimulatory molecules B7 (CD80, CD86) expressed on the surface of the antigen presenting cells (APC) which counteracts with T-cell activation and induces anergy of the cell. Inhibition of this interaction by CTLA-4 specific antibody frees B7 molecules so they can interact with costimulatory receptor CD28 and enhance T-cell activation [130].

PD1 (programmed cell death receptor 1) receptors also conduct negative regulatory signals and are present not only in activated T-cells but also on B-cells and natural killer cells. Natural APCs and also cancer cells can express its ligands PD-L1 and PD-L2 and through this interaction decrease T-cell activity [119].

CTLA-4 inhibitor ipilimumab was approved first in 2011, next PD-1 blockers pembrolizumab and nivolumab were introduced which generated higher response rate (~ 40%) and less toxicity. Currently, combination therapy with ipilimumab and nivolumab raised further the response rate over 50% however, serious adverse effects (AEs) were also more frequent (~ 50%). Based on these results PD1 inhibitor nivolumab was approved as first-line therapy for PD-L1 positive tumors. Combination therapy with ipilimumab is proposed for patients with PD-L1 negative tumors because only for this subgroup of patients it was shown to be superior when compared to monotherapy [130].

Of note, AEs rarely can be severe or lethal even with PD-1 inhibitors, and there are many patient who are intrinsic resistant to immunotherapy or acquire quickly resistance during the treatment. Further predictive biomarkers for sensitivity to immunotherapy still need to be identified.

In the case of BRAFV600 melanomas both targeted therapy and immunotherapy is an option. Phase III clinical trials are ongoing to determine in which sequence it is better to employ them [130, 131].

2.4.4. Ca^{2+} signaling in melanoma

As it was discussed earlier the expression and activity of Ca^{2+} regulatory proteins are often altered in tumor cells. In melanomas, changes in the expression of several Ca^{2+} channels and consequently alternations in Ca^{2+} signaling were described [132].

TRPM1 (transient receptor potential melastatin 1) channels are very important regulators of normal melanogenesis and are abundantly expressed in normal melanocytes and in benign nevi. However, their expression is strongly decreased in primary melanomas and they are absent in metastases. It was found that TRPM1 level negatively correlates with tumor aggressiveness and TRPM1 mRNA level might be used as a predictive marker for future metastases. Its expression was shown to be under the control of transcription factor MITF, which is a known regulator of melanocyte differentiation and it is often downregulated in

melanoma cells. TRPM8, TRPM2 and TRPM7 were all found to be upregulated in melanoma cells where they contributed to increased proliferation and metastatic capacity [133].

SOCE is the most common Ca^{2+} entry mechanism is non-excitable cells. Elevated expression of store operated Ca^{2+} channel Orai1 and stromal interacting molecule 2 (STIM2) was described in both melanoma cell lines and melanoma tissues and silencing of these proteins decreased the metastatic and migratory potential of these cells but increased their proliferation [134]. In another study, Orai1 and STIM1 were found to be upregulated in melanoma cells which was associated with the enhanced activity of the CaMKII/Raf-1/ERK signaling pathway. Furthermore, inhibition of SOCE decreased both melanoma cell proliferation and migration [135]. In both studies, the effect of SOCE on melanoma cells was independent of their BRAF mutational status.

A specific mechanism was described by Sun et al. through which SOCE influence cell migration and metastasis in melanoma cells. They found that STIM1 and Orai1 initiate Ca^{2+}oscillations which regulate invadopodium assembly through phosphotyrosine Src activation and ECM degradation by increasing MMP production [136].

Voltage-gated T-type Ca^{2+} channels were also found to be upregulated in melanoma cells that was shown to enhance proliferation [137]. Clinically used T-type channel blockers caused decreased proliferation and autophagy and induced apoptosis in melanoma cell lines [138].

Since Ca^{2+}has a diverse effect on cell migration, it is an important regulator of melanoma cell motility, as well. A guanine nucleotide exchange factor Epac (exchange protein directly activated by cyclic AMP) increases melanoma cell migration by inducing Ca^{2+}release from the ER and ultimately increasing intracellular Ca^{2+} level. This effects cell motility by increasing actin assembly [139]. It was also presented that cGMP-specific phosphodiesterase PDE5A is downregulated in BRAF mutant melanoma cells that results in cytosolic Ca^{2+}elevation. This led to increased contractility of the cells through enhanced phosphorylation of myosin light chain 2 and to enhanced metastatic potential in lung colonization assay [140].

Elevated expression of Ca^{2+}/calcineurin activated transcription factor NFAT2 and NFAT4 was found in BRAF mutant melanoma cell lines which directly increased cyclooxygenase-2 (COX-2) transcription. COX-2 is a known positive regulator of cancer cell migration and invasion and often associated with poor prognosis [141].

Ryanodine receptor RyR2 and ligand gated Ca^{2+} channel P2X7 were also shown to be upregulated in BRAF mutant melanoma cells. Ryr did not function as a Ca^{2+} channel but it modulated P2X7 function while P2X7 had an antiapoptotic effect after simultaneous stimulation with apoptosis inducer 2-methoxyestradiol (2ME) and its agonist ATP. However, after downregulation of P2X7 expression with siRNA the cells became sensitized to 2ME treatment [142].

It was also suggested that inhibition of SERCA pumps can contribute to the induction of apoptosis in BRAF inhibitor resistant melanoma cells. They found that in BRAF mutant melanoma cells BRAF inhibitor treatment causes an increase in the basal cytosolic Ca^{2+} level which induces ER stress and apoptosis. This effect could be further increased by the addition of SERCA inhibitor thapsigargin even in vemurafenib resistant cells [143].

Nevertheless, the role of plasma membrane Ca^{2+} pumps in melanoma progression has not been investigated until now.

3. Aims

PMCA proteins are key regulators of intracellular Ca^{2+} homeostasis in all cell types. They differ in their kinetic and regulatory features that define their ability to respond to a variety of incoming Ca^{2+} signals. By shaping intracellular Ca^{2+} transients and through interactions with other molecules, PMCA proteins play a role in the regulation of crucial cellular processes such as differentiation, migration or cell death.

In this work we wanted to examine how different PMCA isoforms shape the cytosolic Ca^{2+} signal and investigate if PMCA proteins play a role in Ca^{2+} signaling of metastatic melanoma cells. In order to study this:

1. We analyzed the differential effects of PMCA isoforms PMCA4b, PMCA4a and PMCA2b on the pattern of the SOCE induced Ca^{2+} signal. Therefore, we expressed mCherry-tagged PMCA variants together with the genetically encoded Ca^{2+} indicator GCaMP2 in Hela cells.
2. We studied the influence of PMCA proteins on Ca^{2+} signaling in both BRAF mutant and BRAF wild type melanoma cells. We determined the expression pattern of the PMCA proteins and analyzed the effect of mutant BRAF inhibitor treatment on the PMCA expression, localization and the intracellular Ca^{2+} signal.
3. Since metastatic melanoma cells are highly motile we aimed to analyze the effect of mutant BRAF inhibition on the migratory capacity of melanoma cells.
4. We investigated how PMCA affected the motility of melanoma cells. Therefore, we generated BRAF mutant cell lines overexpressing PMCA4b and tested their migratory characteristics *in vitro,* and their metastatic capacity *in vivo*.
5. Since HDAC inhibitor treatment has been shown to induce PMCA4b expression in breast and colon cancer cells, we treated the melanoma cells with HDAC inhibitors alone or in combination with the mutant BRAF inhibitor. We examined the expression, localization and activity of the PMCA, and determined the migratory activity of the cells in response to the HDAC inhibitor treatments.

4. Materials and methods

4.1 Cell culture

In our experiments we used the HeLa cervix adenocarcinoma cell line and four melanoma lines: the BRAF/NRAS wild type MEWO, the NRAS mutant MJZJ and the two BRAF mutant A375 and A2058 cells. MEWO, A375 and A2058 cell lines were obtained from the American Type Culture Collection, MJZJ was established at the Institute of Cancer Research at the Medical University of Vienna [144]. Cells were grown in Dulbecco's modified Eagel's Medium (DMEM) supplemented with 10% FBS, 100 mg/ml streptomycin, 100 U/ml penicillin at 37^{o}C and 5% CO_2 in a humidified atmosphere.

4.2 Transfection of HeLa cells and generation of stable cell lines

For the Ca^{2+} signal measurements, HeLa cells were transiently co-transfected with one of the mCherry-PMCA4b, mCherry-PMCA4b-LA, mCherry-PMCA4a or mCherry-PMCA2b constructs and the pN1- GCaMP2 plasmid. The mCherry-PMCA constructs were generated as described in [44, 45], the pN1-GCaMP2 plasmid was a gift from Junichi Nakai, RIKEN Brain Science Institute, Saitama, Japan [145]. Cells were seeded in an Imaging Chamber Lab-Tek II (Nalge Nunc International) at a 4-6x10^4 cells/well concentration 24 hours before transfection. Transient transfections were performed with transfection reagent FuGENE HD (Roche Applied Science) according to the manufacturer's protocol. Measurements were carried out 48 hours after transfection.

The sh-HeLa cell line was created by stable transfection with PMCA4 shRNA plasmid (sc-42602-SH) and shRNA plasmid-A (sc-108060) was used as control. Cells were seeded in a six-well plate and before transfections medium was changed to the shRNA Plasmid Transfection Medium (sc-108062). Transfection was carried out with shRNA Plasmid Transfection Reagent according to the manufacture's protocol. To select successfully transfected cells Puromycin dihydrochloride (1µg/ml) (sc-108071) was added to the medium 48 hours after transfection. In every 2-3 days, medium was changed to fresh medium with Puromycin for two weeks. Then cell clones were generated using cloning rings and PMCA4b protein level was analyzed by Western Blotting. Sh-HeLa cell lines with lowest PMCA4b expression were established.

4.3 Transfection of melanoma cells and generation of stable cell lines

For the melanoma studies A375-GFP, A375-GFP-PMCA4b I, A375-GFP-PMCA4b II, MEWO-GFP and MEWO-GFP-PMCA4b cell lines were generated by stable transfection with SB-CAG-GFP-PMCA4b-CAG-Puromycin or SB-CAG-GFP-CAG-Puromycin vectors that include a Sleeping Beauty transposon system. These vectors were created by the modification of SB-CAG-GFP-ABCG2-CAG-Puromycin vector (a generous gift from T. Orban [146]) from which the GFP-ABCG2 insert was cut out with AgeI and BclI enzymes. The GFP-PMCA4b sequence was excised from the pEGFP-PMCA4b plasmid [33] by first opening the vector with ClaI enzyme digestion and then with a partial digestion with AgeI and BamHI. Afterwards GFP-PMCA4b was ligated into the open SB-CAG-CAG-Puromycin vector. Stable transfection with the SB-CAG-GFP-PMCA4b-CAG-Puromycin was performed by first seeding 2-3.5x10^5 MEWO and A375 cells/well on 6-well plates. 24 hours later SB-CAG-GFP-PMCA4b-CAG-Puromycin vector and SB100x transposase plasmid were added to the cells in 1:10 ratio together with Fugene HD transfection reagent (Roche Applied Science). 48 hours later selection of transfected cells started with 1µg/ml puromycin dihydrocloride.

4.4 Treatments of melanoma cells

Mutant BRAF (V600E) inhibitors vemurafenib (PLX4032) and GDC0879, and the MEK kinase inhibitor selumetinib were obtained from Selleck Chemicals (Munich, Germany). All these inhibitors were dissolved in DMSO and kept at -80^{o}C. HDAC inhibitors valproic acid sodium salt and suberoylanilide hyroxamic acid (SAHA) were purchased from Sigma-Aldrich. 200 mM stock solution of valproate was prepared in distilled water while SAHA was dissolved in DMSO at 100 mM concentration. Both were stored at -20 ^{o}C. Cells were seeded 24 hours before treatment either on 6-well plates (1-2x10^5 cells/well) or into imaging chambers (1-2x10^4 cells/well). The appropriate drug was applied in fresh medium the next day and cells were cultured for the appropriate period of time. SAHA was replaced daily in fresh medium. The final DMSO concentration was lower than 0.01% in all experiments.

4.5 Ca^{2+} signal measurements

In order to detect the changes in the intracellular Ca^{2+} concentration, HeLa cells were transfected with the genetically encoded Ca^{2+} indicator GCaMP2 (described above) while

melanoma cells were loaded with the synthetic Fluo-4 green fluorescent Ca^{2+} indicator. Before loading the cells with Fluo-4, they were washed twice with HBSS supplemented with 2 mM $CaCl_2$, 0.9 mM $MgCl_2$ and 20 mM HEPES pH7.4. Then to the same solution 0.5 µM Fluo-4 AM (Molecular Probes, F14201) was added and cells were incubated for 30 min at RT. Following the incubation cells were washed twice with the same solution.

Store operated Ca^{2+} entry was induced in two steps. First the intracellular Ca^{2+} stores were depleted. Cells were washed twice and kept in nominally Ca^{2+} free solution (HBSS supplemented with 100 µM EGTA, 100 µM $CaCl_2$, 0.9 mM $MgCl_2$ and 20 mM HEPES pH 7.4) and they were stimulated first by thapsigargin (2 µM) and after 2 minutes also by ATP (100 µM). Than 3 minutes later store operated Ca^{2+} entry was induced by restoring the external Ca^{2+} concentration to 2 mM. Ca^{2+} signal was also evoked by the A23187 Ca^{2+} ionophore treatment. For this, cells were washed twice and kept in HBSS supplemented with 2 mM $CaCl_2$, 0.9 mM $MgCl_2$ and 20 mM HEPES pH7.4. Thereafter, 2 µM A23187 was added to the solution. We used two different inhibitors, $LaCl_3$ and Caloxin 1c2 to investigate the role of PMCA4b in the regulation of the intracellular Ca^{2+} signal. $LaCl_3$ (1 mM) was administered when the Ca^{2+} signal reached its peak. The PMCA4b-specific inhibitor Caloxin 1c2 (20 µM) was added to the cells 10 minutes before the Ca^{2+} signal was triggered.

Time-lapse images were acquired by Zeiss LSM500 and Olympus IX81 laser scanning confocal microscopes with a 60x (1.4) oil immersion objective. Z-resolution was adjusted to 1 µm and images were taken every 0.3 s/1 s. The relative fluorescence intensity values were calculated as F/F_o (where F_o was the average initial fluorescence). We used Fluoview FV500 (v4.1), ImageJ v1.42q and Prism4 v4.01 (GraphPad Software) software products to analyze the data.

4.6 Protein analysis by Western Blot

For total protein extraction cells were washed twice with PBS and then they were incubated with 6% TCA for 1-24 hours at 4 ^{o}C. The precipitated protein was centrifuged (4000g, 10 min, 4^{o}C) and the pellet was dissolved in a modified Laemmli-type sample buffer (62,5 mM Tris-HCl, pH 6,8, 2% SDS, 10% glycerol, 5 mM EDTA, 100 mM DTT, 125 mg/ml urea és 0,28 mg/ml bromphenolblue). The protein concentration of the samples was determined with a modified Lowry method [147, 148]. 20-30 µg proteins were loaded on 7.5% or 10% acrylamide gels and after electrophoresis samples were transferred to PVDF membranes. After blocking with 5% milk solution, the membranes were incubated with the appropriate

primary antibody. Primary antibodies are listed in Table 9.1. Anti-PMCA4b antibody, JA3 is specific for PMCA4b that recognizes the region between residues 1156-1180 [149]. As secondary antibodies, HRP-conjugated anti-rabbit and anti-mouse (Jackson ImmunoResearch, dilution 1:10000) were applied and Pierce ECL Western Blotting Substrate (Thermo Scientific) and luminography were used for detection. Densitometric analysis was performed by ImageJ software v1.42q.

4.7 Immunofluorescence staining

After washing twice with HBSS (37^{o}C), cells were incubated in 4% paraformaldehyde solution at 37^{o}C for 15 minutes. Then they were washed five times with PBS and to permeabilize the cell membrane, they were kept in ice cold methanol for 5 minutes. Cells were washed again five times with PBS and then they were kept in blocking buffer (PBS containing 2 mg/ml bovine serum albumin, 1% fish gelatin, 0.1% Triton-X 100, 5% goat serum) for 1 hour at RT. Subsequently primary antibody against PMCA4b (JA3, dilution 1:200) was applied in blocking buffer for 1 hour at RT. Next, cells were washed three times with PBS and they were incubated with the secondary antibody Alexa Flour 488-conjugated anti-mouse IgG (Invitrogen) in blocking buffer for 1 hour at RT. Images were acquired by Olympus IX-81 and Zeiss LSM500 laser scanning confocal microscopes with a 60x (1.4) oil immersion objective. Images were analyzed with FluoviewFV500 software v4.1 or ImageJ software v1.42q.

4.8 Quantitative real-time reverse transcription PCR (qPCR)

mRNA was isolated with TRIzol reagent (Life Technologies) from control, vemurafenib-treated and HDAC inhibitor-treated melanoma cells. For reverse transcription the RevertAid Reverse Transcriptase (Thermo Scientific) was used and amplification was performed with the Maxima SYBR Green master mix (Thermo Scientific) on an Applied Biosystems® 7500 Real-Time PCR System. All primer pairs used in the experiments are listed in Table 9.2 [150]. PMCA4b mRNA level was determined with the TaqMan assays Hs00608066_m1 (PMCA4b) and Hs99999905_m1 (GAPDH) (both from Thermo Scientific).

4.9 Proliferation assay

Proliferation was analyzed by BrdU incorporation (colorimetric) assay (Roche Applied Science, Vienna, Austria, 11 647 229 001) according to the manufacturer's protocol. A375-GFP, A375-PMCA4bI and A375-PMCA4bII cells were seeded in triplicates on 96-well plates in $1x10^4$ cells/well concentration. Both control and vemurafenib-treated (48 hours) cells were labeled with 10 μM BrdU for 2 hours at 37°C. Incorporated BrdU level was determined by absorbance measurement at 370 nm (reference: 492 nm) and calculated as A_{370}-A_{492}.

4.10 Viability assay

Viability was tested on vemurafenib and HDAC inhibitor treated A375, A2058 and MEWO cells. First the cells were trypsinized and kept in suspension. Two dyes were mixed into the solution (Solution 13, Chemometec, 910-3013) from which Acridine Orange labeled all cells while DAPI stained only the non-viable cells. The number of cells in both populations was determined by the NucleoCounter NC-3000™ system (Chemometec) by applying 10 μl of each sample on 8-well NC-slide. Viability was calculated as total cells - nonviable cells/total cells.

4.11 Cell cycle analysis

The ratio of vemurafenib and HDAC inhibitor treated A375, A2058 and MEWO cells in each cell cycle phases was analyzed based on their DNA content. First lysis buffer (Solution 10, 910-3010, Chemometec) was mixed with DAPI stain solution (Solution 12, 910-3012, Chemometec) at a final concentration 10 μg/ml DAPI. Then cells were trypsinized and incubated with the lysis buffer at 37°C. After five minutes reaction was stopped with stabilization buffer (Solution 11, 910-3011, Chemometec) and from each sample 10 μl was added into 8-well NC-slide. Cellular fluorescence was measured with a NucleoCounter NC-3000™ system (Chemometec).

4.12 Analysis of cellular morphology

Morphological analysis of individual A375-GFP and A375-GFP-PMCA4b cells was performed on phase contrast images of the cells with the ImageJ 1.47v program´s particle analyzing option. We calculated the following morphological parameters: cellular area, aspect ratio

(defined as (major axis) / (minor axis) of the ellipse which best fits the shape of the cell) and circularity (defined as 4π* (cell area) / (cell perimeter)^2).

4.13 Cell migration assays

Random and directional migration of melanoma cells was assessed with three different methodologies.

4.13.1 Random migration assay using phase contrast videomicroscopy

Migratory capacity of control and vemurafenib treated melanoma cells, as well as the A375-GFP and the A375-GFP-PMCA4b cell lines were analyzed. Cells were plated in the inner 8 wells of 24-well plates (Corning Incorporated, Corning, NY) and remained in the incubator overnight for cell attachment. At the beginning of videomicroscopic measurement, medium was changed to CO_2-independent medium (Gibco-BRL Life Technologies, Carlsbad, CA) supplemented with FCS and 4 mM glutamine. Following the first 24-hour-measurement cell were treated with vemurafenib (0.5 μM) and followed for 72 hours afterwards. Cell migration was recorded by an inverted phase-contrast microscope (World Precision Instruments, Sarasota, FL) placed in a custom-built incubator maintaining 37°C and room ambient gas atmosphere. Images of 3 microscopic fields from each well were acquired every 5 minutes. Cell positions were registered by a custom made cell-tracking program that enables manual labeling of individual cells [151]. Cell motility was calculated as the net displacement of cells between 0-12 and 48-60 hours of recordings with or without treatment.

4.13.2 Random migration assay using fluorescent cell nuclei tracking assay

A375 cells were treated with HDAC inhibitor valproate (4mM) for 48 hours. Before measurement cell nuclei were labeled with 0.1 μM Hoechst 33342 for 1 hour. Images were taken automatically by the ImageXpress Micro XL (Molecular Devices, Sunnyvale, CA USA) high content screening system with a Nikon CFI Super Plan Fluor ELWD ADM 10x objective. During the experiment cells were kept at 37^{o}C in 5% CO_2 humidified atmosphere. For Hoechst (447/60 nm) detection excitation wavelength was 377/50 nm. 4 images were acquired in every 30 minutes for 24 h. Data analysis was done with the Multidimensional

Motion Analysis module of MetaXpress High Content Image Acquisition & Analysis Software Version 5.3. The cell nuclei cut-off was 9–15 µm. 100 µm was adjusted as maximum displacement between two points on the trajectory of individual cells.

4.13.3 Directional cell migration assay

A375 cells were treated with various concentration of valproate for 48 hours and then cells were trypsinized and seeded on a 48-well Boyden chamber (Neuro probe, Gaithersburg, MD) with uncoated Nucleopore membranes (Whatman) at $2x10^4$ cells/well concentration. Pore diameter of the membranes was 8 µm. Both in the upper and the bottom chamber DMEM containing 10% FCS was present and fibronectin (100 µg/ml, Millipore) was applied as a chemoattractant to the bottom chamber [152]. Cells were incubated for 6 hours at 37^oC. Then from the upper side of the membrane the cells were removed by scraping and the filter was treated with methanol to fix the cells on the lower side. After staining the cells with toluidine blue, cells were counted with a light microscope at ×200 magnification. When the PMCA4 specific inhibitor caloxin 1c2 was used, it was added to the medium after seeding on the Boyden chamber at a 20 µM concentration.

4.14 Lung colonization assay

Tail vein injection of A375-GFP, A375-GFP-PMCA4b I and II cells ($4x10^5$cells/0.2 ml serum free DMEM) was performed on 11-week old female SCID mice (10 mice / group) provided by the National Institute of Oncology, Hungary. We sacrificed the mice 6 weeks later. The lung and the tumor tissue in the chest cavity were taken out, fixed in formalin and embedded in paraffin. Hematoxylin-eosin stained sections from the tissue blocks were analyzed with TissueFAXS System (TissueGnostics GmbH, Vienna, Austria) (20x). Using Tissue Quest program the tumor regions were highlighted and their area was quantified. The Guidelines for Animal Experiments were followed during the execution of the protocol and permission was obtained from the Department of Experimental Pharmacology in the National Institute of Oncology, Budapest, Hungary (permission number: 22.1/722/3/2010).

5. Results

5.1 Distinct PMCA isoforms shape intracellular Ca^{2+} transients differently

We wanted to analyze how differences in the kinetic properties of PMCA isoforms affected the patterns of Ca^{2+} transients. In our experiments we used three PMCA isoforms, PMCA4b, PMCA4a and PMCA2b, which strongly differed in their kinetics of activation by Ca^{2+}-CaM and they also had distinct inactivation rates. Previous experiments demonstrated that PMCA4b is activated by the Ca^{2+}-CaM complex very slowly (k_{on}) while the activation of PMCA2b and PMCA4a are much faster [42, 153, 154]. Based on these characteristics, PMCA4b is a "slow" pump, while PMCA2b and PMCA4a are "fast" pumps. Furthermore, PMCA4a has a fast Ca^{2+}-CaM off-rate (k_{off}) which means it becomes quickly inactivated after a Ca^{2+} spike. In contrast, PMCA4b and PMCA2b have a much slower Ca^{2+}-CaM off-rates; they remain active longer, a characteristic called as the "memory" of the pumps [154].

We investigated the patterns of Ca^{2+} transients in response to either the store operated Ca^{2+} entry (SOCE) or after a Ca^{2+} ionophore stimulus. SOCE was induced by the addition of the SERCA pump inhibitor Thapsigargin (2 μM) followed by ATP (100 μM) in a nominally Ca^{2+} free solution. In this way the ER Ca^{2+} pool became depleted and its refill with Ca^{2+} was blocked. Then extracellular Ca^{2+} concentration (2 mM) was restored that resulted in a sharp increase in the intracellular Ca^{2+} concentration by allowing Ca^{2+} to enter the cells through store operated Ca^{2+} channels (SOCs). The SOCE-mediated Ca^{2+} signal lasted for about 10-15 minutes depending on cell type and condition (Figure 3B).

5.1.1 The effect of siRNA knockdown of PMCA4b on the SOCE mediated Ca^{2+} signal

In our experimental model we used HeLa cells, which in a sub-confluent state express PMCA1 and PMCA4b in low levels but with confluency the expression of PMCA4b rises (Figure 3A). In order to investigate the role of PMCA4b in Ca^{2+} signaling, we stably downregulated PMC4b expression in HeLa cells with a PMCA4 specific short hairpin RNA. In this new cell line (sh-PMCA4) even in confluent state the abundance of PMCA4b remained very low (Figure 3A) while the expression of PMCA1 did not change.

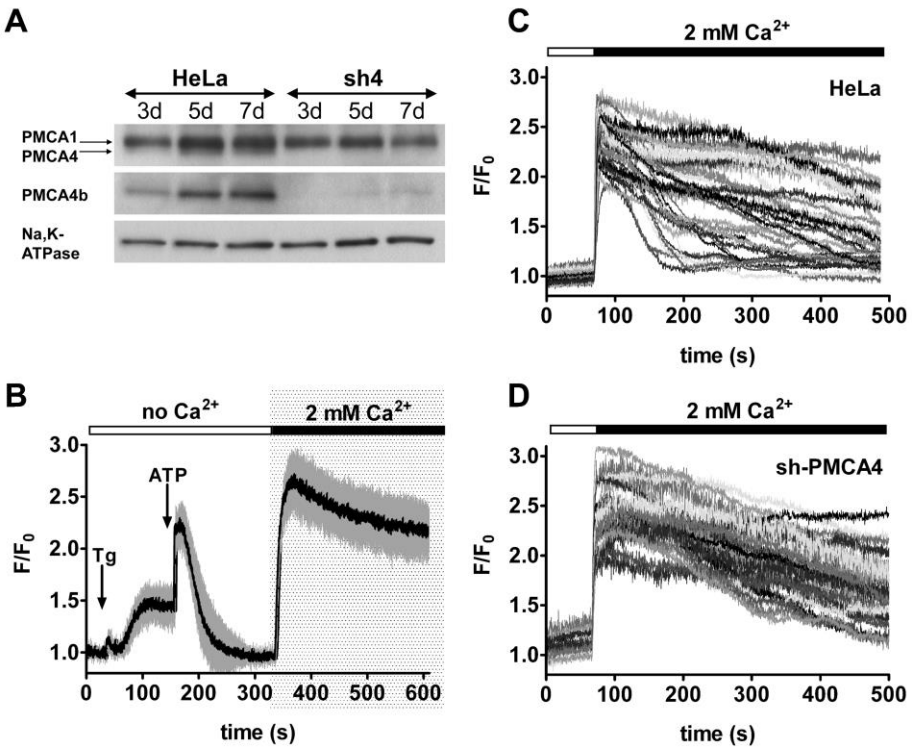

Figure 3. SOCE-mediated Ca^{2+} signal in sh-PMCA4 and control Hela cells. (A) Analysis of PMCA1 and PMCA4 protein levels in 3, 5 or 7 days long grown control HeLa and sh-PMCA4 cells. PMCA1 and PMCA4 protein expression level was analyzed by Western blotting using a pan-PMCA antibody 5F10 and a PMCA4b specific antibody JA3 to detect the two proteins. (B) A representative diagram of a SOCE mediated Ca^{2+} signal in sh-PMCA4 Hela cells. Addition of thapsigargin and ATP empties the ER Ca^{2+}stores in nominally Ca^{2+}-free solution then re-addition of external Ca^{2+} (2 mM) induces SOCE. (C, D) cells were transfected with Ca^{2+}indicator GCAMP2. Ca^{2+} signal was induced with Ca^{2+}readdition in individual control HeLa (C) and sh-PMCA4 (D) cells. Each graph shows over 30 cells.

To detect changes in the intracellular Ca^{2+} concentration cells were transiently transfected with the genetically encoded fluorescent Ca^{2+} indicator GCaMP2. We found that in all sh-PMCA4 cells the decay of the Ca^{2+} transients was slow and nearly all cells responded equally to the incoming Ca^{2+} signal. In contrast, in the control cells the pattern of Ca^{2+} signaling was more diverse; Ca^{2+} clearance was fast in a subpopulation of cells while in the rest of the cells the decay phase was similar to that of the sh-PMCA4b cells indicating that PMCA expression varies quite substantially between cells.

5.1.2 The differential impact of slow and fast pumps with long or short memory on the SOCE mediated Ca^{2+} transients

We generated mCherry-tagged PMCA4b, PMCA2b and PMCA4a constructs and co-transfected HeLa cells with one of the PMCA isoforms and the Ca^{2+} indicator GCaMP2. This way we could follow changes in intracellular Ca^{2+} concentration and visualize PMCA expression in the same cell. In our experiments besides of the wild-type PMCA4b we also used the mutant PMCA4b-LA, in which three leucine residues (Leu1167-1169) were substituted with alanines in the pump´s C-terminal region. Earlier we characterized this mutant [45] and showed that it has an enhanced plasma membrane localization compared to the wild type protein while it retains all other characteristics of the wild type pump. We found that overexpression of PMCA4b (slow pump with memory) strongly altered the shape of the Ca^{2+} transient (Figure 4A).

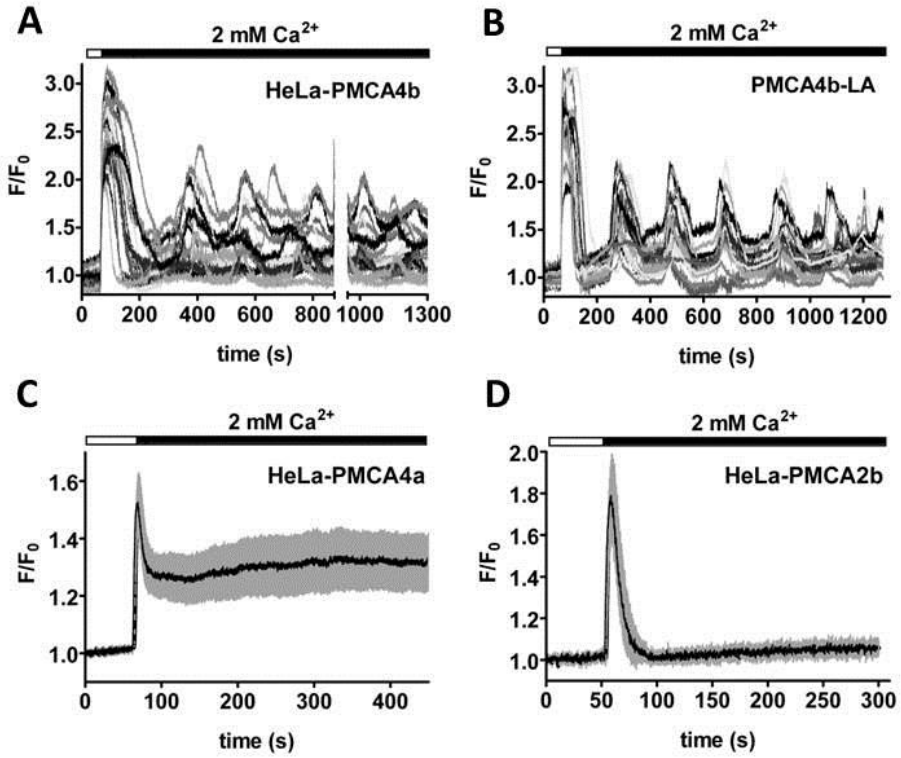

Figure 4. SOCE mediated Ca^{2+} signals in PMCA4b, PMCA4b-LA, PMCA4a and PMCA2b expressing HeLa cells. Cells were co-transfected with mCherry-tagged PMCA constructs and Ca^{2+} indicator GCaMP2. The data in (A, B) shows results from > 15 cells. The graphs in (C) and (D) show the mean values of the Ca^{2+} signals from 20 to 30 cells ± 95% CI.

The first quick rise in the intracellular Ca^{2+} concentration was followed by a much faster decay phase than in the control HeLa or the sh-PMCA4 cells and this was followed by periodic baseline oscillations. Expression of PMCA4b-LA had a similar effect (Figure 4B) except that the baseline oscillations were far more synchronized in these cells presumably due to its higher abundance and more even distribution in the plasma membrane.

Transient expression of PMCA4a (fast pump with no memory) had a very different effect on the Ca^{2+} transient. After a rapid increase, the intracellular Ca^{2+} concentration quickly decreased however it did not return to the baseline but stabilized in a new, increased steady-state level. Furthermore, cells expressing PMCA2b (fast pump with long memory) cleared very quickly the excess Ca^{2+} from the cytosol producing only one short peak.

5.1.3 Influence of PMCA isoforms on Ca^{2+} transients generated independent of SOCE

In order to investigate the effect of different PMCA isoforms on the Ca^{2+} transients initiated by other stimuli, we induced Ca^{2+} transients with the calcium ionophore A23187 in the presence of 2 mM external Ca^{2+}. The ionophore facilitates Ca^{2+} influx into the cells independently from plasma membrane channels. Interestingly, we found that PMCA isoforms influenced the ionophore-mediated intracellular Ca^{2+} transients in a similar manner as SOCE (Figure 5).

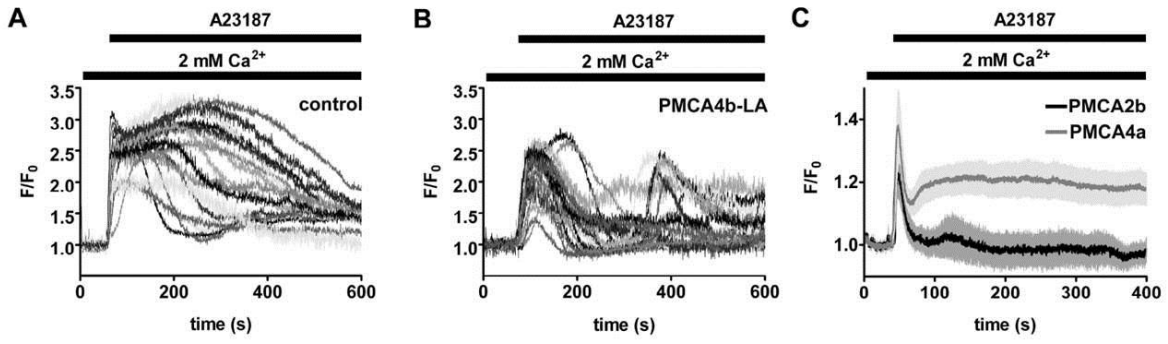

Figure 5. Ca^{2+} transients after ionophore treatment in control, PMCA4b-LA, PMCA2b and PMCA4a expressing HeLa cells. Cells were transfected with Ca^{2+} indicator GCaMP2 and the indicated mCherry-tagged PMCA isoform. Ca^{2+} signal was initiated with A23187 (2 μM). The data in (A, B) are results from > 15 cells. The graphs in (C) and (D) indicate the mean values of the Ca^{2+} signals from 20 to 30 cells ± 95% CI.

In control cells the pattern of the Ca^{2+} signals was diverse (Figure 5A), while in PMCA4b-LA expressing cells after an initial spike baseline oscillation developed (Figure 5B). Expression of fast responding pumps PMCA4a and PMCA2b initiated a quick response to the rise of the cytosolic Ca^{2+} concentration which resulted in a sustained elevation of the Ca^{2+} concentration or a rapid return to the basal level, respectively (Figure 5C).
Our results showed for the first time that PMCA proteins play key role in the regulation of intracellular Ca^{2+} responses and can uniquely shape the incoming Ca^{2+} signal.

5.2 The role of PMCA4b in the regulation of intracellular Ca^{2+} signaling in BRAF mutant melanoma cells

Our results show that alterations in PMCA level and/or type can substantially change the Ca^{2+} signal that may further influence downstream events. Altered expression of PMCA proteins has already been described in several cancer types but not in metastatic melanoma [155]. In our study we used four melanoma cell lines: two BRAF (V600E) mutants (A375, A2058), one NRAS mutant (MZJZ) and one BRAF and NRAS wildtype (MEWO). First we analyzed which PMCA proteins are expressed in these cells and then we investigated the effects of mutant BRAF and MEK inhibitor treatments on PMCA expression and intracellular Ca^{2+} clearance.

5.2.1 BRAF inhibitor treatment increases PMCA4b expression in BRAF mutant melanoma cells

We used two mutant BRAF specific, low molecular weight inhibitors, vemurafenib (PLX4032) and GDC0879, which block the BRAF-MEK-ERK pathway selectively in BRAF (V600E) mutant cells. Cells were treated with 0.5 μM Vemurafenib and 0.5 μM GDC0879 for 72 hours and the expression of PMCA proteins was analyzed by Western blotting (Figure 6, 7).

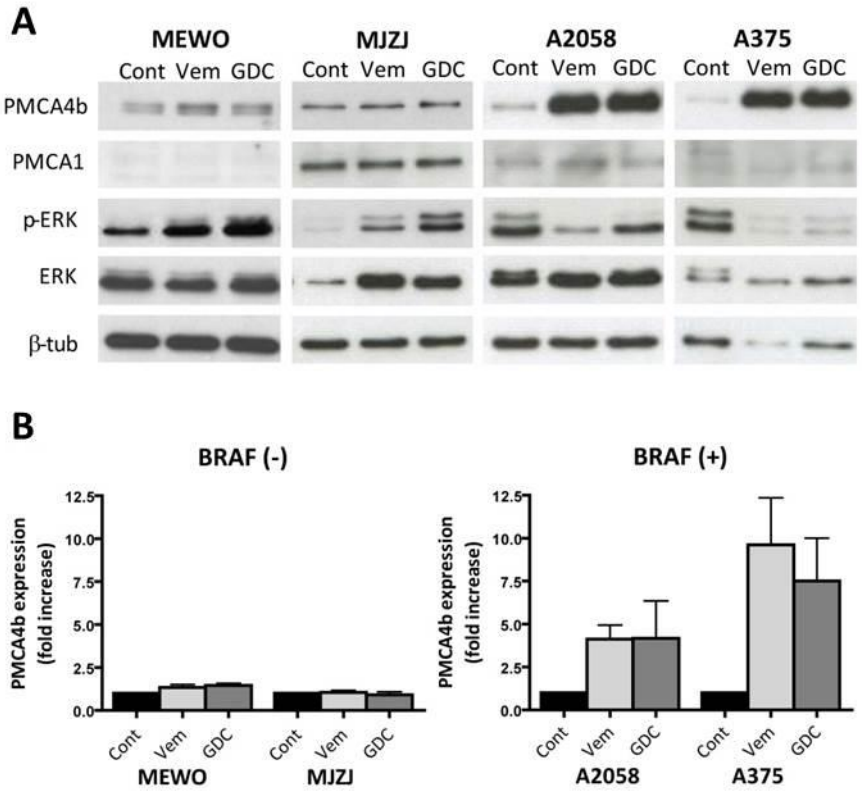

Figure 6. Expression of PMCA4b is increased by BRAF inhibitor treatment selectively in melanoma cells with BRAF mutation. (A)Two BRAF wild type (MEWO, MJZJ) and two BRAF mutant (A2058, A375) cell lines were treated with mutant BRAF specific inhibitor vemurafenib (0.5 μM) and GDC0879 (0.5 μM) for 72 hours. Protein expression levels were determined by Western blot analysis. (B) After densitometric analysis PMCA4b protein levels were normalized to β-tubulin expression and represented as fold increase over the untreated controls. Bars indicate means ± SE from three independent measurements.

We investigated the expression of PMCA proteins with isoform specific antibodies and found that two PMCA isoforms, PMCA1 and PMCA4b were present in these cell lines (Figure 6A) while PMCA2 and PMCA3 were not detected (Figure 7). We found that BRAF inhibitor treatment strongly increased the expression of PMCA4b selectively in BRAF mutant cells while it did not affect the expression of PMCA1 in any of these cells (Figure 6B). Hence in further experiments we concentrated on the changes of the PMCA4b protein.

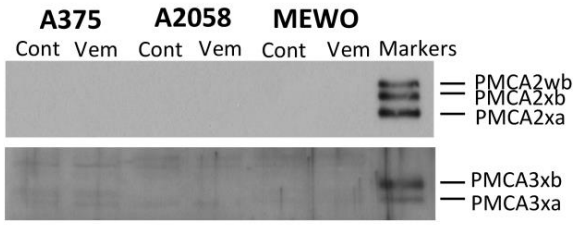

Figure 7. Expression of different isoforms of PMCA3 and PMCA2 proteins were analyzed in control and vemurafenib treated MEWO, A375 and A2058 cells by Western blot. As markers we applied cell lysates from COS cells overexpressing the indicated PMCA isoforms.

We examined the time course of PMCA4b expression at both the mRNA and protein levels in A375 cells.

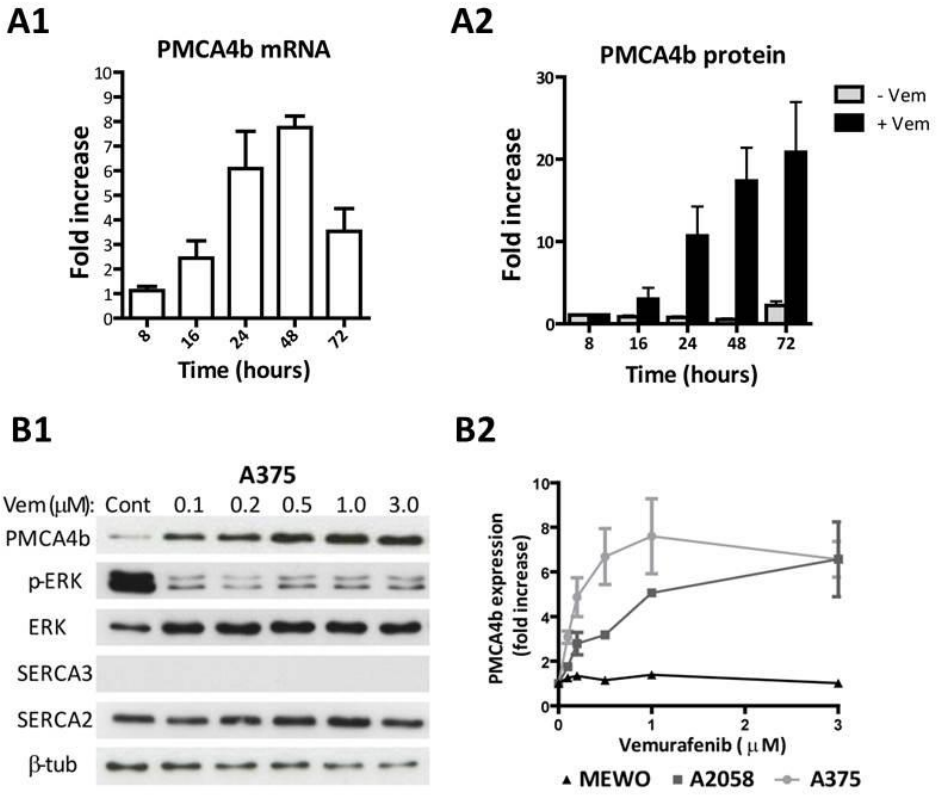

Figure 8. (A1) Changes in PMCA4b mRNA and (A2) protein expression after vemurafenib treatment (0.5 μM) at different time points in A375 cells. (B1) A375 cells were treated with increasing amount of vemurafenib for 72 hours and expression of PMCA4b, SERCA2 and SERCA3, pERK and ERK was analyzed by western blots. (B2) Densitometric analysis of western blots of PMCA4b expression after concentration dependent treatment with vemurafenib in A375, MEWO and A2058 cells. Data are shown as fold increase over the untreated controls. Bars indicate means ± SE from three to five independent measurements.

A substantial increase in PMCA4b expression could be detected between 16 to 48 hours of treatment both at mRNA and protein levels (Figure 8A). After 48 hours PMCA4 mRNA expression declined to a lower level whereas protein abundance increased up to 72 hours and stayed constant at least for an additional 48 hours. Then we tested the effect of increasing concentration of vemurafenib on the abundance of PMCA4b (Figure 8B). We found that 0.5 μM vemurafenib concentration increased PMCA4b protein level almost maximally so we performed all further measurements with this concentration.

We also analyzed the expression of sarco/endoplasmic reticulum Ca^{2+} ATPases, SERCA2 and SERCA3, after BRAF inhibitor treatment, both being important regulators of the intracellular Ca^{2+} homeostasis (Figure 8B2). SERCA3 was not detected in these cells while the expression of SERCA2 was abundant but did not change by the treatment.

We also investigated the effect of vemurafenib treatment on the expression of various Ca^{2+} channels in the two BRAF mutant cell lines A375 and A2058 (Figure 9).

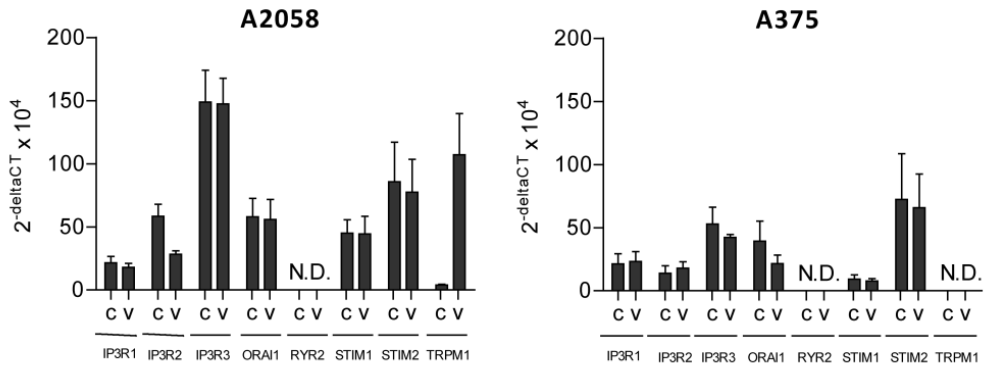

Figure 9. Changes of mRNA expression level of Ca^{2+} channels after vemurafenib treatment (0.5 μM, 72 hours). mRNA level of inositol 1,4,5-triphosphate receptor type 1-3 (IP_3R1, IP_3R2, IP_3R3), Orai calcium release-activated calcium modulator 1 (Orai1), ryanodine receptor 2 (RYR2), stromal interaction molecule 1 and 2 (STIM1, STIM2) and transient receptor potential cation channel subfamily M member 1 (TRPM1) was measured by quantitative real-time PCR analysis. mRNA levels were normalized to glyceraldehyde-3-phosphate dehydrogenase (GAPDH) expression and bars show the means and SEM of two independent measurements implemented in duplicates. N.D., not detectable. C: control, V: vemurafenib.

We found that the mRNA expression of the inositol 1,4,5-trisphosphate receptor type 1-3 (IP_3R1, IP_3R2, IP_3R3), Orai calcium release-activated calcium modulator 1 (Orai1), ryanodine receptor 2 (RYR2) and stromal interaction molecule 1 and 2 (STIM1, STIM2) was not modified by the treatment. Solely in A2058 cells the mRNA level of transient receptor

potential cation channel subfamily M member 1 (TRPM1) was substantially elevated while in A375 cells TRPM1 was not detectable neither before nor after the treatment. These results show that BRAF inhibitor treatment selectively upregulates the expression of the PMCA4b isoform in BRAF mutant melanoma cells.

5.2.2 MEK inhibitor treatment increases PMCA4b expression in both BRAF mutant and NRAS mutant melanoma cells

MEK1 and MEK2 kinases are part of the RAS/RAF/MEK/ERK pathway and since they are activated in both BRAF and NRAS mutant cells MEK inhibitors can be effective in both cell types. We treated one BRAF and NRAS wild type (MEWO), one NRAS mutant (MZJZ) and two BRAF mutant (A375, A2058) cell lines with a MEK1/2 inhibitor selumetinib (0.5 μM AZD6244) for 72 hours and investigated its effect on PMCA4b expression (Figure 10).

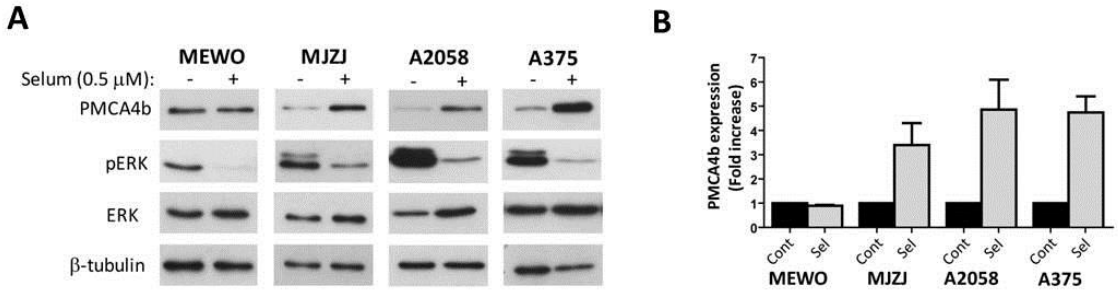

Figure 10. Effect of MEK inhibitor treatment on PMCA4b abundance. BRAF and NRAS wild type (MEWO), NRAS mutant (MZJZ) and BRAF mutant (A375, A2058) cell lines were incubated with MEK1/2 inhibitor selumetinib (0.5 μM) for 72 hours. (A) Protein level of PMCA4b, pERK and ERK was analyzed by western blots. (B) Densitometric analysis of PMCA4b protein levels was performed and data was normalized to β-tubulin expression levels and expressed as fold increase over the untreated controls. Bars indicate means ± SE from three independent measurements.

We found that selumetinib treatment on one hand increased PMCA4b abundance in both BRAF mutant cell lines comparably to BRAF inhibitor treatment, and on the other hand it had a similar effect in the NRAS mutant cells. This indicates that BRAF/MEK signaling plays a role in the regulation of PMCA4b expression.

5.2.3 PMCA4b upregulation is coupled with increased plasma membrane abundance

In order to analyze the intracellular localization of PMCA4b before and after BRAF inhibitor treatment we performed immunofluorescent staining and confocal imaging. One BRAF wild type cell line (MEWO) and two BRAF mutant cell lines (A375, A2058) were treated with 0.5 M vemurafenib for 72 hours (Figure 11).

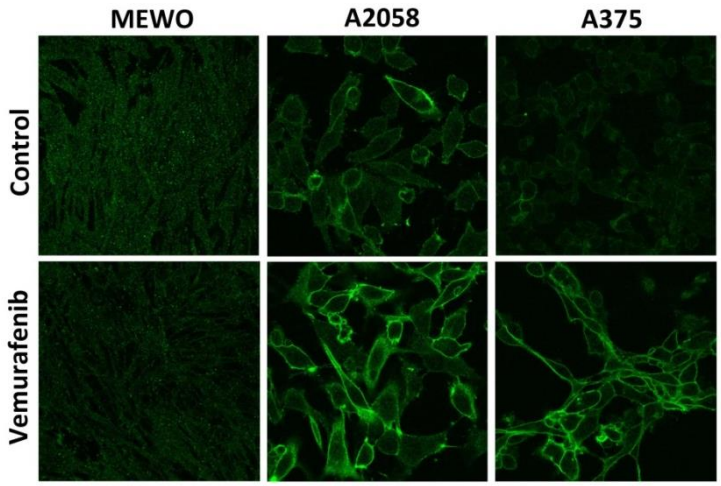

Figure 11. Protein level of PMCA4b in the plasma membrane was analyzed after BRAF inhibitor treatment (0.5 μM vemurafenib, 72 hours). Immunostaining with anti–PMCA4b antibody (JA3) was performed. Images were taken by confocal microscope with a 60X objective.

We found that in the two BRAF mutant cell lines vemurafenib treatment strongly increased PMCA4b abundance in the plasma membrane.

5.2.4 Increased PMCA4b expression results in enhanced Ca^{2+} clearance

To investigate the effect of increased PMCA4b abundance on intracellular Ca^{2+} signaling we initiated intracellular Ca^{2+} signal in both control and vemurafenib treated cells and followed the changes of intracellular Ca^{2+} level in single cells with confocal microscopy. Cells were filled with Ca^{2+} indicator Fluo-4 and then SOCE mediated Ca^{2+} signal was induced in two steps. First external medium was changed to nominally Ca^{2+} free solution and afterwards 2 μM thapsigargin and 100 μM ATP were added to the cells to deplete internal Ca^{2+} stores. Then the external Ca^{2+} concentration was restored to 2 mM and that evoked an intracellular Ca^{2+} increase (Figure 12).

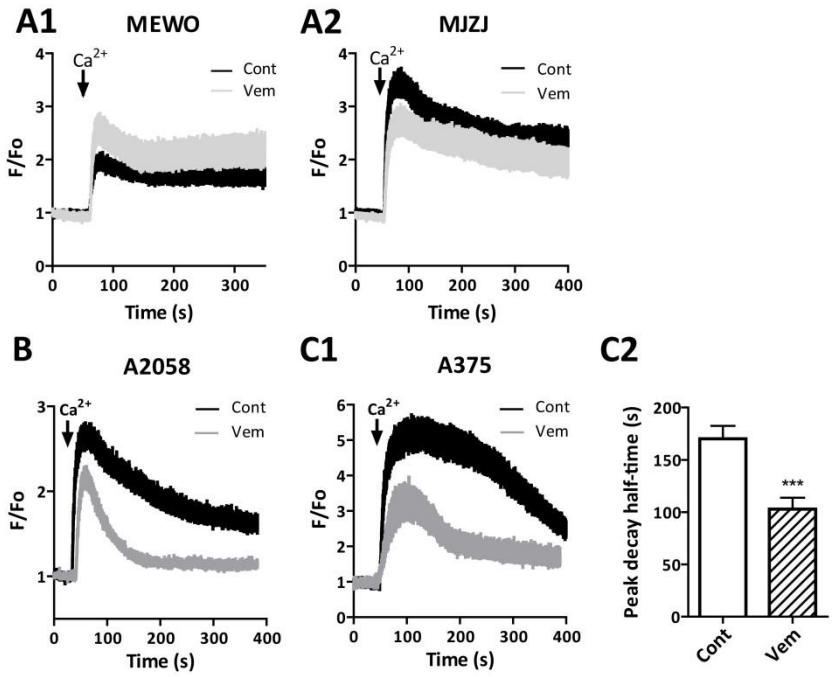

*Figure 12. SOCE mediated Ca^{2+} signal in control and vemurafenib treated melanoma cells. (A1, A2, B, C1) After pretreatment with vemurafenib (0.5 μM, 48 hours) Ca^{2+} stores were depleted with Thapsigargin (2 μM) and ATP (100 μM) in nominally Ca^{2+}-free environment, then extracellular Ca^{2+} concentration was restored (2 mM) which induced intracellular Ca^{2+} increase by allowing Ca^{2+} entry through SOCE channels. Data show the average of normalized fluorescent intensity values (F/F0) of 10-30 cells from three independent measurements. (C2) Half peak decay time of the second phase of the SOCE signal in control and vemurafenib-treated A375 cells was calculated. Bars represent the mean ± SD of individual cells analyzed in two to three independent experiments. Significances compared to control indicated by (***P<0.001); two-tailed unpaired t-test.*

We found that after vemurafenib treatment, intracellular Ca^{2+}clearence was increased in the BRAF mutant cells (Figure 12B, C1) as compared to that of the control cells (Figure 12A1, A2). We also analyzed the changes of the intracellular Ca^{2+}decay after a Ca^{2+} ionophore A23187 stimulus that induced Ca^{2+}uptake independent of the Ca^{2+}entry channels. We found that under these conditions - similarly to that seen in case of SOCE - the peak decay half time was shorter in vemurafenib treated BRAF mutant cells as compared to that of the control cells (Figure 13A, C).

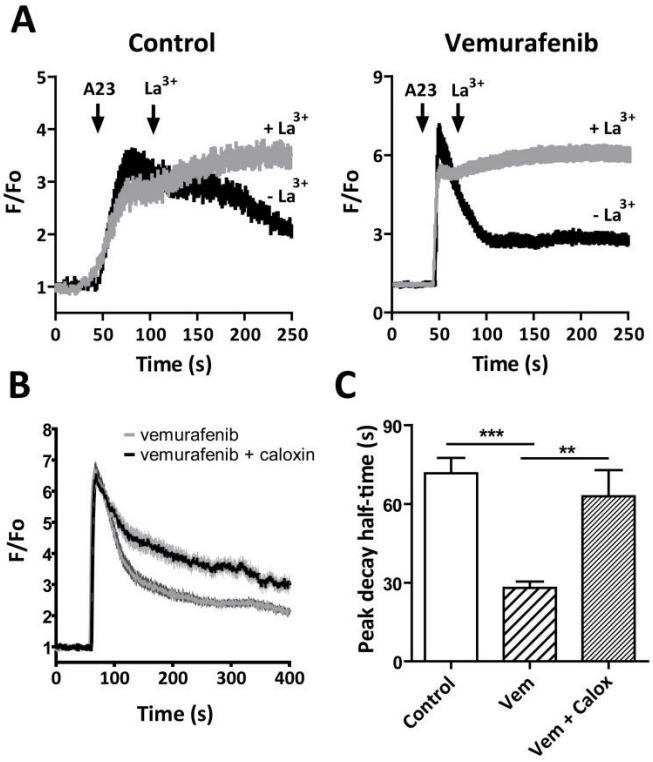

*Figure 13. Ca^{2+}signal in control and vemurafenib treated cells (0.5 μM, 48 hours) after Ca^{2+}ionophore stimulus. (A) A375 cells were treated with Vemurafenib (0.5 μM) for 48 hours then stimulated with A23187 (2 μM) in HBSS supplemented with 2 mM Ca^{2+}. Where indicated lanthanum ($LaCl_3$, 1 mM) was added right after when Ca^{2+} signal reached the peak. (B) Cell were pretreated with caloxin 1c2 for 10 minutes before Ca^{2+} signal was initiated with A23187 in vemurafenib treated cells. (C) Half peak decay time of the Ca^{2+}signal in control and vemurafenib-treated +/- caloxin 1c2 pretreated A375 cells was determined. Data shows the average fluorescent intensity values of 10-15 cells. Bar graphs are mean ± SD of individual cells taken from two to three independent experiments. Significances are denoted by *** (P<0.001), ** (P<0.01); two-tailed unpaired t-test.*

To verify that PMCA4b is primarily responsible for the increased Ca^{2+}decay, we performed the experiments in the presence of PMCA inhibitors lanthanum and a PMCA4-specific inhibitor caloxin1c2. Because lanthanum can also interfere with the function of Ca^{2+}channels, $LaCl_3$ was added right after the Ca^{2+}signal reached its peak. Immediately after addition lanthanum abolished Ca^{2+}clearance and caused a sustained elevation of the cytosolic Ca^{2+} level (Figure 13A). Furthermore, PMCA4 specific inhibitor caloxin1c2 treatment also decreased Ca^{2+} clearance in the cells resulting in a slower decay phase similar to that seen in the control cells (Figure 13B, C). These two experiments show that an increased PMCA4b presence is coupled to an enhanced Ca^{2+} extrusion capacity and consequently faster Ca^{2+} clearance in vemurafenib treated BRAF mutant melanoma cells.

5.3 Elevated PMCA4b expression decreases the migratory capacity of A375 cells

Melanoma cells frequently show increased motility that can be coupled with strong metastatic capacity. Hence we analyzed how BRAF inhibitor treatment influenced the migratory capacity of the BRAF mutant cell lines (A375, A2058) and used the BRAF wild type cells (MEWO) as control. We performed time-lapse video microscopy to follow the movement of individual cells during the 3-day-long treatment period and the net migrated distance was analyzed (Figure 14A).

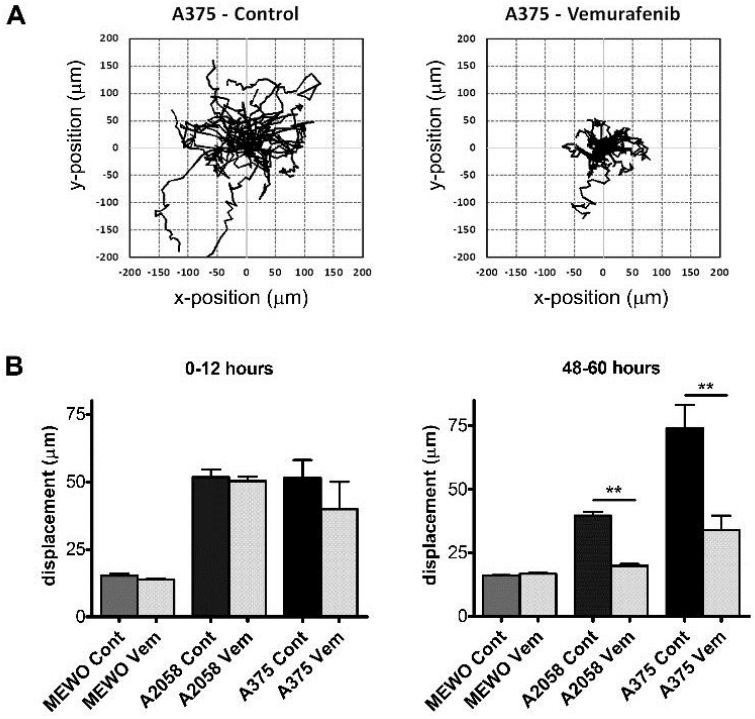

*Figure 14. Vemurafenib treatment strongly decreases the migratory capacity of BRAF mutant melanoma cells. Cells were treated with vemurafenib (0.5 μM, 72 hours) and migration was recorded with time-lapse video microscopy. (A) Migration trajectories of 20 - 24 individual cells of control and vemurafenib treated A375 cells. The starting points of all trajectories were moved to the origin of the graph. (B) Bar graphs represent the mean +/- SEM of the net displacement of single cells during the first twelve hours of the treatment and between 48 – 60 hours. Significance was calculated between control and vemurafenib treated cells as (**P<0.01); two tailed Student's t-test.*

We found that during the first twelve hours of the treatment vemurafenib moderately decreased the migration of A375 cells, while after two days cell migration was strongly

reduced by BRAF inhibition in both BRAF mutant cell lines (Figure 14B). The timing of the inhibitory effect on migration is corresponded with the increase in PMCA4b expression that was most substantial after 48 hours (Figure 8). Migratory capacity of the BRAF wild type MEWO cells was found to be much lower compared to that of the BRAF mutant cells and this was not affected by the treatment, as expected.

In order to investigate the effect of PMCA4b abundance on the migratory capacity of melanoma cells we stably transfected the BRAF mutant A375 and the BRAF wild type MEWO cell lines with GFP alone or with GFP-tagged PMCA4b. From A375 cells we established two PMCA4b expressing cell lines, independently; A375-GFP4b-I and A375-GFP4b-II (Figure 15A). Western blot analysis showed that the expression level of both the endogen and the GFP-tagged PMCA4b were similar in both cells. Protein level of mutant BRAF (V600E) and pERK was not altered by the increased PMCA4b abundance. To verify that the GFP-tagged PMCA4b protein localizes properly, we took confocal images of the cells and found that in both cell types GFP-PMCA4b was present abundantly in the plasma membrane (Figure 15B). We also compared the proliferation rate among the original, the GFP-tagged and the two PMCA4b-expressing A375 cell lines and found that proliferation didn´t differ significantly among them. Treatment with vemurafenib strongly reduced cell division in all cell lines, as expected (Figure 15C).

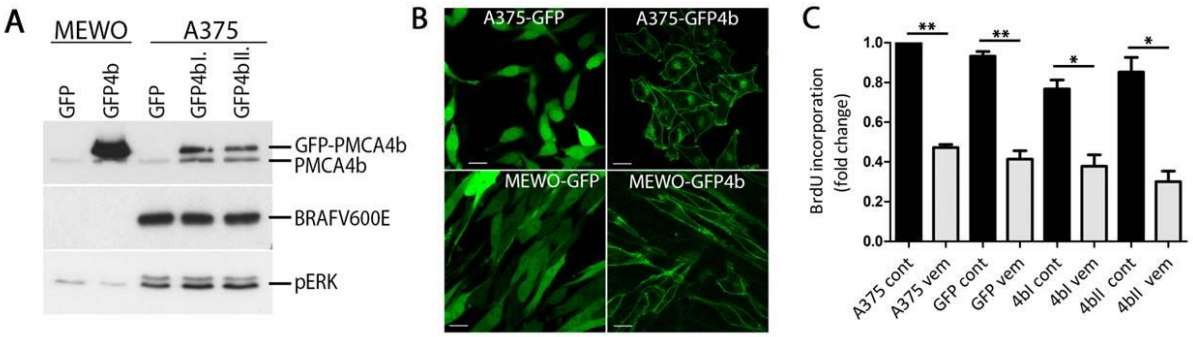

*Figure 15. Generation of stably transfected GFP- and GFP-PMCA4b expressing A375 and MEWO cell lines. (A) Protein expression level of PMCA4b, BRAFV600E and pERK was determined by western blot. (B) Intracellular localization of GFP-PMCA4b was analyzed by confocal imaging (60X objective, scale bar, 20 μm). (C) Proliferation was measured by BrdU incorporation assay. Data indicate the mean +/- SEM of three independent experiments. Significances refer to differences between control and vemurafenib treated cells (*P<0.05; * P<0.01); two tailed Student's t-test.*

However, when we analyzed the migratory capacity of the GFP and the GFP-PMCA4b expressing cells, we found a strong decrease in the motility of both A375-GFP-4b expressing cell lines compared to the control GFP expressing cells (Figure 16). The motility of the MEWO-GFP-4b cells was identical to the control GFP expressing MEWO cells.

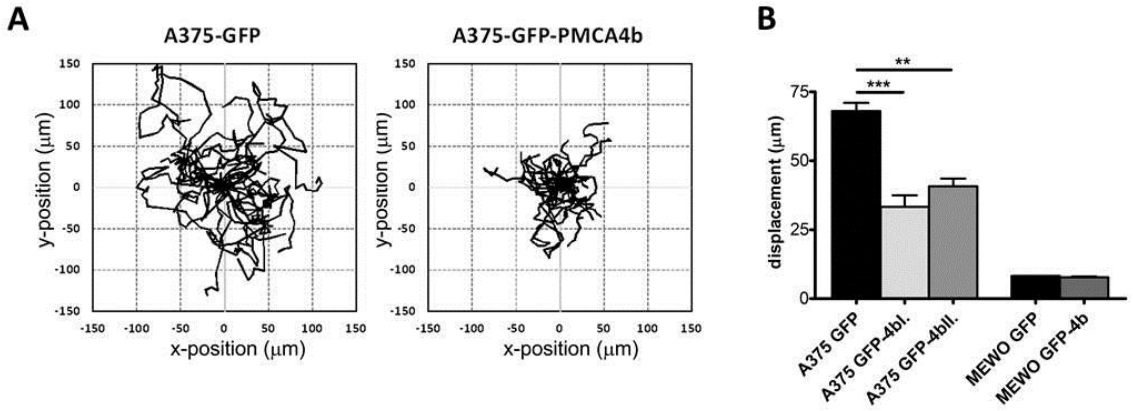

*Figure 16. GFP-PMCA4b expressing A375 cells show decreased migration compared to control. Cell migration was recorded by time-lapse video microscopy for 16 hours. (A) Trajectories show the movement of individual cells. Their initial positions were transferred to the origin of the plot. (B) Net displacement in 12 hours was determined. Significances indicate the differences between GFP-expressing control and GFP-PMCA4b expressing cells (**P<0.01, ***P<0.001); two-tailed unpaired t-test.*

Furthermore, the morphology of the PMCA4b expressing cells was also strongly altered. While the control cells had an elongated shape with more long outgrowths, the PMCA4b overexpressing cells were more epithelial like with a rounded, cobble-stone shape (Figure 17A). We analyzed several morphological parameters of the cells and found that A375-GFP-4b cells show increased circularity and cellular area compared with A375-GFP cells while their aspect ratio (defined as (major axis) / (minor axis)) was decreased (Figure 17B).

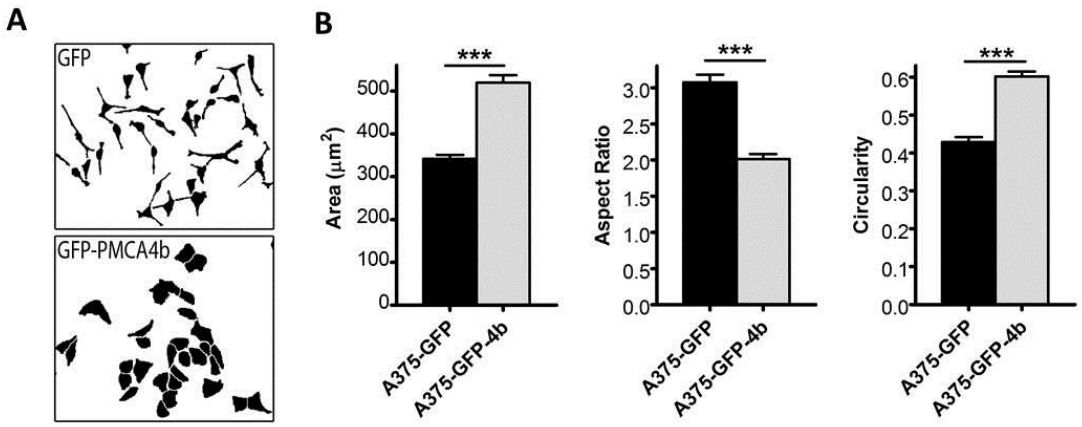

*Figure 17. A375-GFP-PMCA4b cells show altered cellular morphology. (A) Cell masks were generated from phase contrast video microscopy images with ImageJ program to highlight cell shape differences. (B) Quantitative analysis of cellular area, aspect ratio ((major axis) / (minor axis)) and circularity was performed in both GFP expressing (n=249) and GFP-PMCA4b expressing (n=204) cells. Bars demonstrate means ± SEM from 3 independent experiments. Significant differences compared to GFP expressing cells was analyzed (*** (P<0.001); two-tailed unpaired t-test).*

Since PMCA4b overexpression shifted the cellular morphology of the cells toward a more epithelial-like form, we analyzed the mRNA expression of several proteins involved in the epithelial mesenchymal transition process. However, we found no differences in the expression of ZEB-1, Snail and vimentin between the GFP and GFP-PMCA4b expressing cells and E-cadherin was not present in either of these cell lines (Figure 18A).

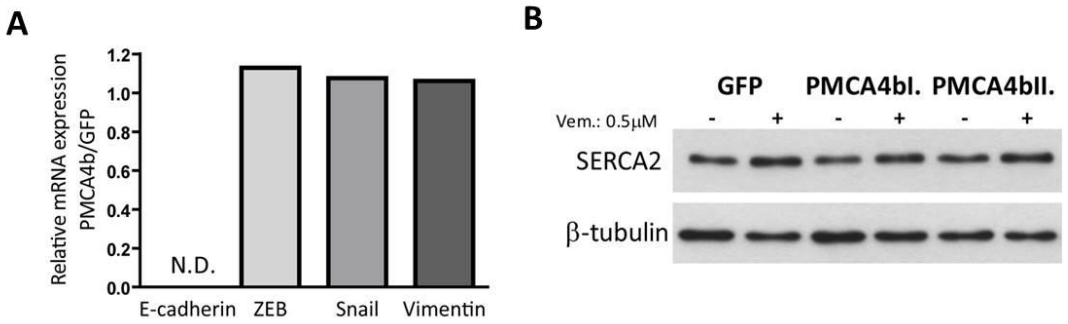

Figure 18. (A) Relative mRNA expression of EMT marker proteins E-cadherin, ZEB-1, Snail and vimentin was determined by quantitative real-time PCR in A375-GFP-PMCA4b and A375-GFP cells. N.D. stands for not detectable. (B) Analysis of SERCA2 protein expression with western blot in vemurafenib treated (48 hours, 0.5 μM) and control A375-GFP-PMCA4b and A375-GFP cell lines.

We also compared the expression of the ER Ca^{2+} pump SERCA2 in the GFP and the two GFP-PMCA4b expressing cell lines and found that it was not modified (Figure 18B).

These results show that overexpression of PMCA4b strongly decreases the migratory capacity of A375 cells and this effect is coupled with an altered cellular morphology. Vemurafenib had a similar effect on the migration of both BRAF mutant melanoma cell lines but BRAF inhibition also decreased the proliferation of the cells while PMCA4b overexpression did not.

5.4 PMCA4b expressing A375 cells have decreased metastatic capacity in vivo

Melanoma patients with metastasis have a particularly grim prognosis. Cell migration is a critical step in metastatic spread therefore, we analyzed the effect of increased PMCA4b presence in A375 cells on their invasive capacity. We performed a lung colonization assay in mice during which $4x10^4$ A375-GFP or A375-GFP-PMCA4b cells/mouse were injected into the animal´s tail vein. After 6 weeks mice were sacrificed and their lung tissues were analyzed. We found that in the control group tumor cells established large tumors in the lung parenchyma and some tumor cells invaded the lung tissue along blood vessels or bronchioles (Figure 19A). While in the two groups of animals injected with PMCA4b expressing cells, only smaller tumors were formed on the surface or in the connective tissue of the lung. Quantification showed that PMCA4b overexpression strongly decreased the number of animals with tumor in their lungs (Figure 19B). Furthermore, the tumor burden - measured as total tumor area in the cross sections of lungs - was also reduced in the PMCA4b expressing group (Figure 19C).

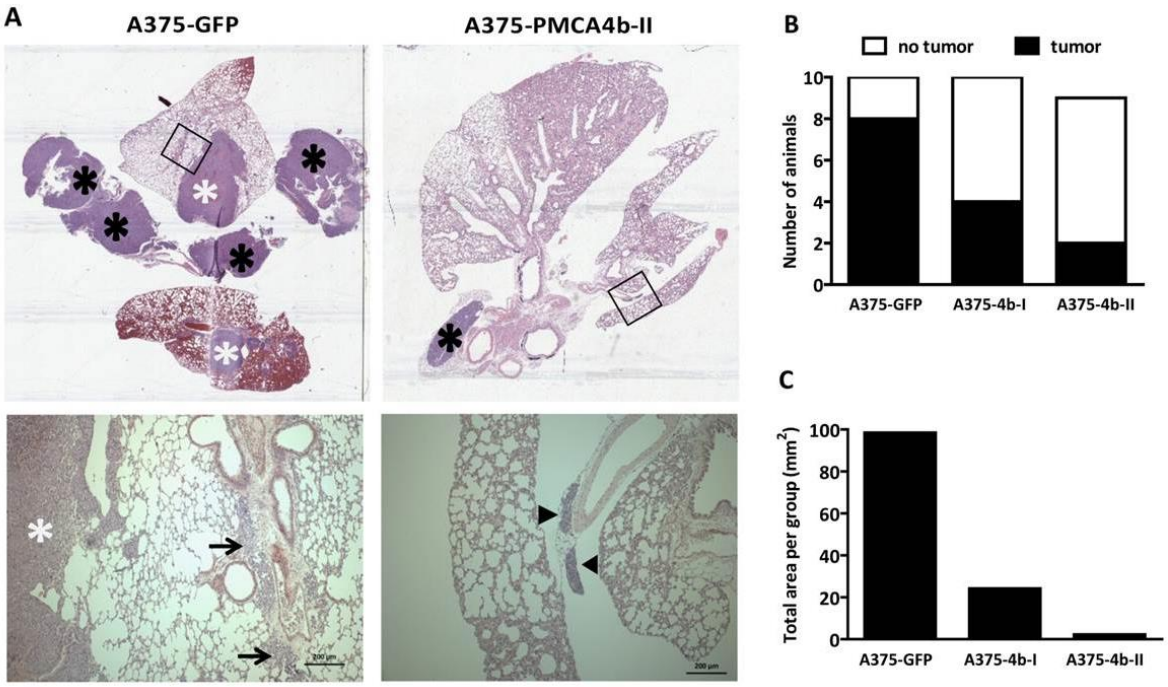

Figure 19. Lung colonization assay in mice to compare the metastatic activity of A375-GFP and A375-GFP-PMCA4b cells. 4x10^4 cells / mouse (n=10) were injected. (A) Tumors could be readily identified with hematoxylin staining in paraffin tissue sections. In the representative images white asterisks mark tumors in the lung parenchyma, black asterisks indicate tumors in the connective tissue. Black frames circumscribe the high-magnification areas of the lower panels. Black arrows point to areas where along blood vessels and bronchiole invasive tumor cells are noticeable. Arrowheads mark interlobular tumors. (B) The number of animals with tumor in the lung was significantly higher in the control group compared with A375-GFP-PMCA4b cells receiving two groups (Chi-square test, P=0.034). (C) Total area of tumors was quantified on hematoxylin-stained tissue sections in each group.

In order to investigate if PMCA4b expression is decreased during the malignant transformation of melanomas, two ONCOMINE data sets with benign nevi and melanoma samples were analyzed (Figure 20). We found that the number of cases with low PMCA4 expression was higher in cutaneous melanomas in both data sets. Furthermore, combination of the data from the two data sets showed that high expression of PMCA4 was present only in 26 melanoma samples out of 69 (38%), while in benign nevi that was the case in 21 samples out of 27 (77%).

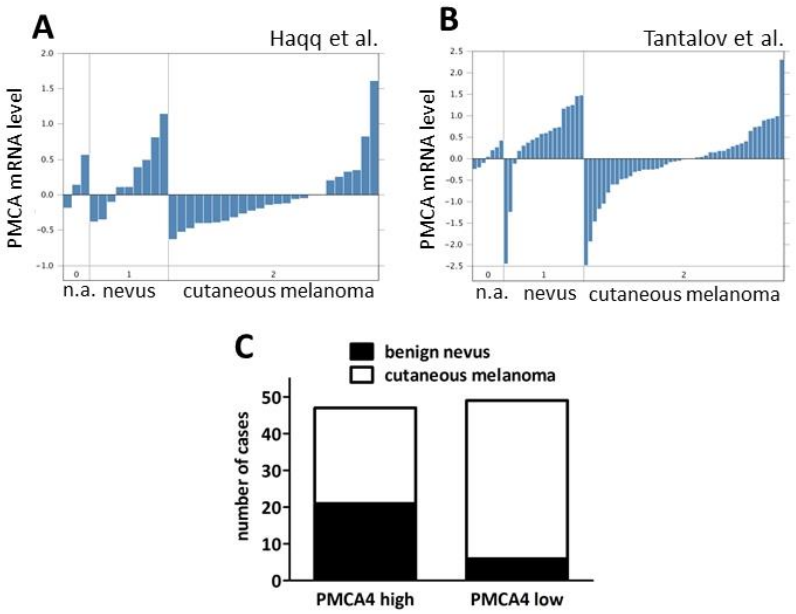

Figure 20. PMCA4b expression in benign nevi and melanoma specimens based on gene expression microarray data from ONCOMINE platform. (A, B) Two independent gene expression microarray dataset were used. (C) The data from the two cohorts were combined which showed that cases with low PMCA4b expression were significantly more in the cutaneous melanoma group than in in the benign nevus group (p=0.0006).

Altogether, our results show that BRAF inhibition selectively upregulates PMCA4b expression in BRAF mutant melanoma cells which results in an increased Ca^{2+} clearance after stimulation. Furthermore, both BRAF inhibition and PMCA4b overexpression decreased the migration capacity of the BRAF mutant A375 cells and PMCA4b overexpression also reduced the cells´ metastatic capacity in vivo. Interestingly, despite its strong anti-migratory effect PMCA4b expression did not alter the proliferation of the cells that is a typical feature of the metastasis suppressor genes.

5.5 The effect of HDAC inhibitor treatment alone and in combination with vemurafenib on PMCA protein expression in melanoma cells

The impact of histone deacetylase treatment on the expression of the PMCA4b has already been investigated in breast and colon cancer cell lines [93, 94]. In these studies both short chain fatty acids such as butyrate and valproic acid and the hydroxamic acid SAHA

(vorinostat) increased the expression. However, the effect of HDAC inhibitor treatment on PMCA expression in melanoma cells was not formerly investigated.

5.5.1 HDAC inhibitor treatment increases the abundance of both the PMCA4b and the PMCA1 isoforms in melanoma cells

First we treated three melanoma cell lines, the BRAF wild type (MEWO) and the two BRAF mutant (A375, A2058) cells, with an increasing concentration of SAHA or valproate, and analyzed the changes in PMCA expression by Western blot (Figure 21). We used two different antibodies against the PMCA proteins, a PMCA4 isoform specific one (JA9) and a pan-PMCA antibody (5F10). The latter recognized two bands in all cell lines from which the lower band corresponded to PMCA4b while the upper band to PMCA1, as determined by the isoform specific antibodies JA9 and NR1, respectively (Figure 21A). We found that PMCA4b expression was strongly elevated in both MEWO and A375 cells while only moderately in A2058 cells in response to the HDAC inhibitor treatments.

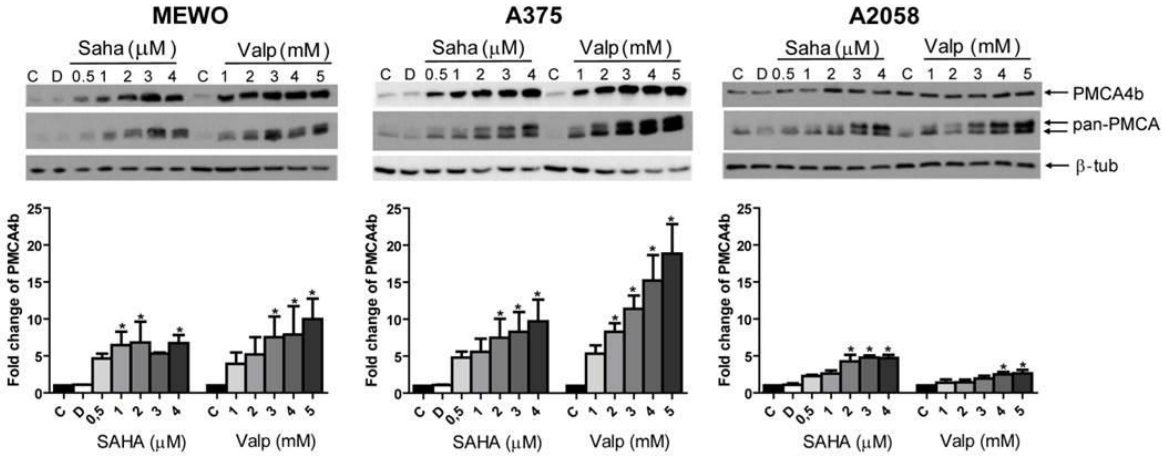

Figure 21. Concentration dependent treatment of melanoma cells with HDAC inhibitor SAHA and valproate. After 48 hours total cell lysates were prepared and analyzed by Western Blotting (30 μg / sample). C: control, D: DMSO. Densitometric analysis of PMCA4b expression was performed than data were normalized to β-tubulin expression level and were presented as fold increase over untreated control. Diagrams show the means ± SE from three independent measurements. Significance was calculated by ANOVA and Dunett`s post hoc tests and asterisks show differences (p < 0.05) from control.*

Surprisingly, beside the increased PMCA4b expression the abundance of PMCA1 was also increased by the treatment of the A375 and A2058 cells. Expression of both isoforms was already elevated after 0.5 μM SAHA and 1 mM valproate treatment (Figure 21B).

Then we analyzed the changes in PMCA expression at different time points of the treatment (Figure 22) and found that PMCA4b level reached saturation after 48 hours in all cell lines. PMCA4b expression also went up in the control samples at later time points as the culture reached confluency in good accordance with earlier findings [45].

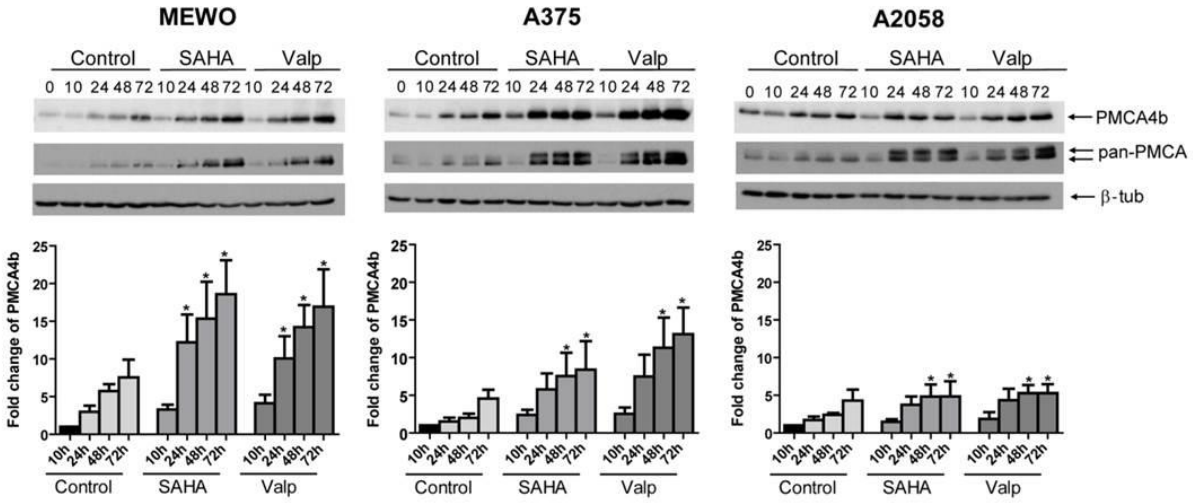

Figure 22. Time dependent change of PMCA proteins during HDAC inhibitor treatment. Cells were treated with 2 μM SAHA or 2 mM valproate for the indicated time points. PMCA protein expression was analyzed with Western Blotting. Densitometric analysis of PMCA4b expression was performed than data were normalized to β-tubulin expression level and were presented as fold increase over untreated control. Diagrams show the means ± SE from three independent experiments. Significance was calculated by ANOVA and Dunett`s post hoc tests and asterisks show differences (p < 0.05) from control.*

Since our experiments showed that BRAF inhibitor treatment induced PMCA4b expression in the BRAF mutant melanoma cell lines, we wanted to test the combined effect of BRAF and HDAC inhibition on the PMCA abundance. Therefore, we treated all three cell lines either with 1 μM SAHA or 2 mM valproate in combination with 0.5 μM vemurafenib (Figure 23). Interestingly, we found no additive effect of the two treatments on PMCA4b expression in these cell lines. In A375 cells BRAF inhibitor treatment had a stronger effect than the HDAC inhibitors, while in A2058 cells all treatment increased PMCA4b expression in a similar extent (Figure 23B). In BRAF wild type MEWO cells only HDAC inhibitors had an effect on PMCA4 abundance, as expected.

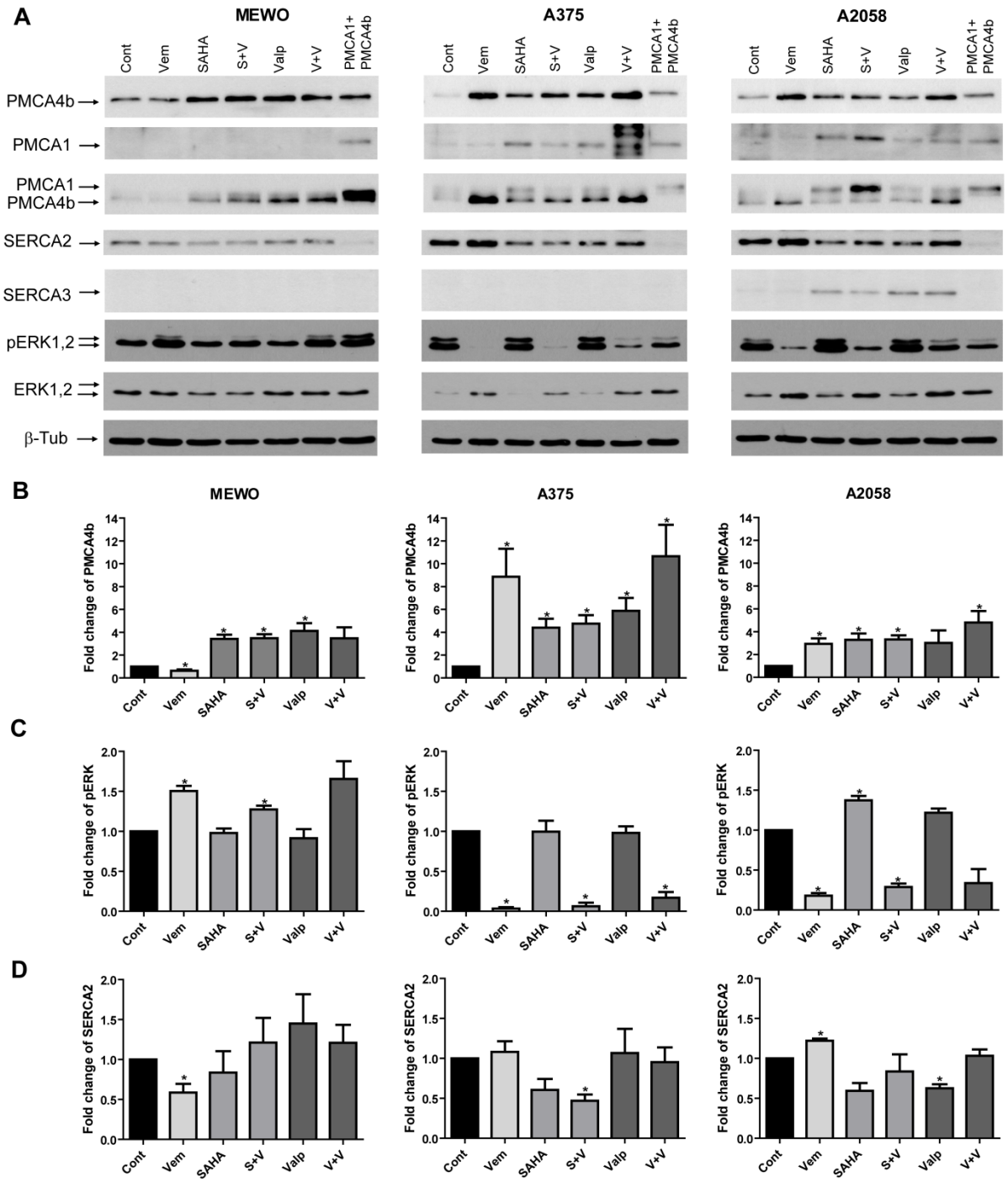

Figure 23. Combination treatment with HDAC inhibitor SAHA or valproate with BRAF inhibitor vemurafenib had no additive effect on PMCA4b protein expression. Treatment was performed with 1 μM SAHA or 2 mM valproate in combination with 0.5 μM vemurafenib for 48 hours. (A) Expressions of proteins were determined with Western Blotting and analyzed with densitometry. PMCA4b and PMCA1 were detected with isoform specific and pan-PMCA antibodies as well. (B, C, D) Data were normalized to β-tubulin expression levels and expressed as fold increase over untreated controls. Diagrams show the means ± SE from three independent experiments. Asterisks represents significant differences compared to control ($p < 0.05$) by two-tailed paired t-test.*

As we have shown earlier, vemurafenib treatment does not influence PMCA1 abundance and combined treatment had no additional effect above HDAC inhibitor treatment alone, as expected. We also analyzed the changes in ERK phosphorylation and found that contrary to vemurafenib treatment HDAC inhibition did not decrease ERK activation but eventually even slightly increased that (Figure 23C). This shows that the effect of HDAC inhibitors on PMCA expression is independent of ERK activation in these cell lines. Furthermore, this effect was also independent from the BRAF mutational status of the cells, since HDAC inhibitors increased PMCA4b expression in both BRAF wild type (MEWO) and BRAF mutant (A375, A2058) cell lines. Additionally, we analyzed the changes in acetylation of the H3 histone protein after HDAC inhibitor and vemurafenib treatment (Figure 24). We found that treatment with the HDAC inhibitors – in contrast to the BRAF inhibitors - increased H3 histone acetylation in all cell lines.

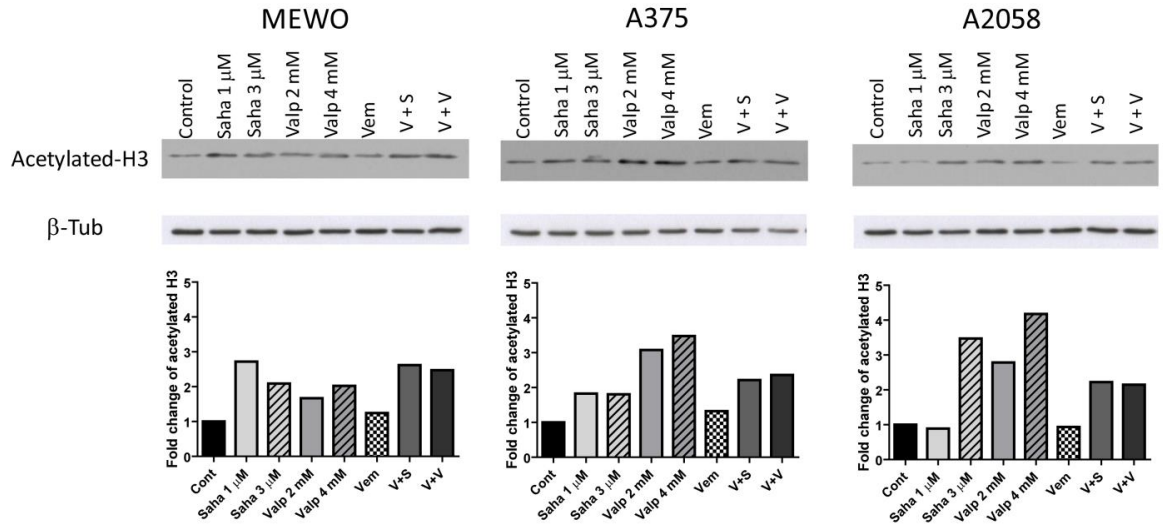

Figure 24. Alternations in H3 histone acetylation following the treatment with HDAC inhibitor SAHA and valproate or BRAF inhibitor vemurafenib for 48 hours. Vem: 0.5 μM vemurafenib, V + S: 0.5 μM vemurafenib and 1 μM SAHA, V + V: 0.5 μM vemurafenib and 2 mM valproate. Acetylated-H3 protein level was determined by Western blot and the data were densitometrically analyzed, normalized to β-tubulin expression levels and expressed as fold change compared to control.

Intracellular Ca^{2+} signals are shaped by the concerted action of Ca^{2+} channels and pumps in the plasma membrane and the ER. It has been shown that treatment with HDAC inhibitors can alter the expression of the Ca^{2+}-signaling molecules [27, 156, 157] hence we analyzed the changes in the expression of SERCA2 and SERCA3 proteins after HDAC inhibitor

treatment alone or in combination with vemurafenib (Figure 24). The housekeeping isoform SERCA2 - which was detected in all three cell lines - was slightly decreased by the treatment in the two BRAF mutant cells (Figure 24D). It has been demonstrated that SERCA3 expression is increased during cancer cell differentiation [27, 156]. We found that HDAC inhibitor treatment evoked SERCA3 expression only in A2058 cells while SERCA3 could not be detected in the other two cell lines with or without treatment. We also investigated the changes in the expression of the Ca^{2+} channels at the mRNA level in response to 2 mM valproate alone or in combination with 0.5 μM vemurafenib (Figure 25).

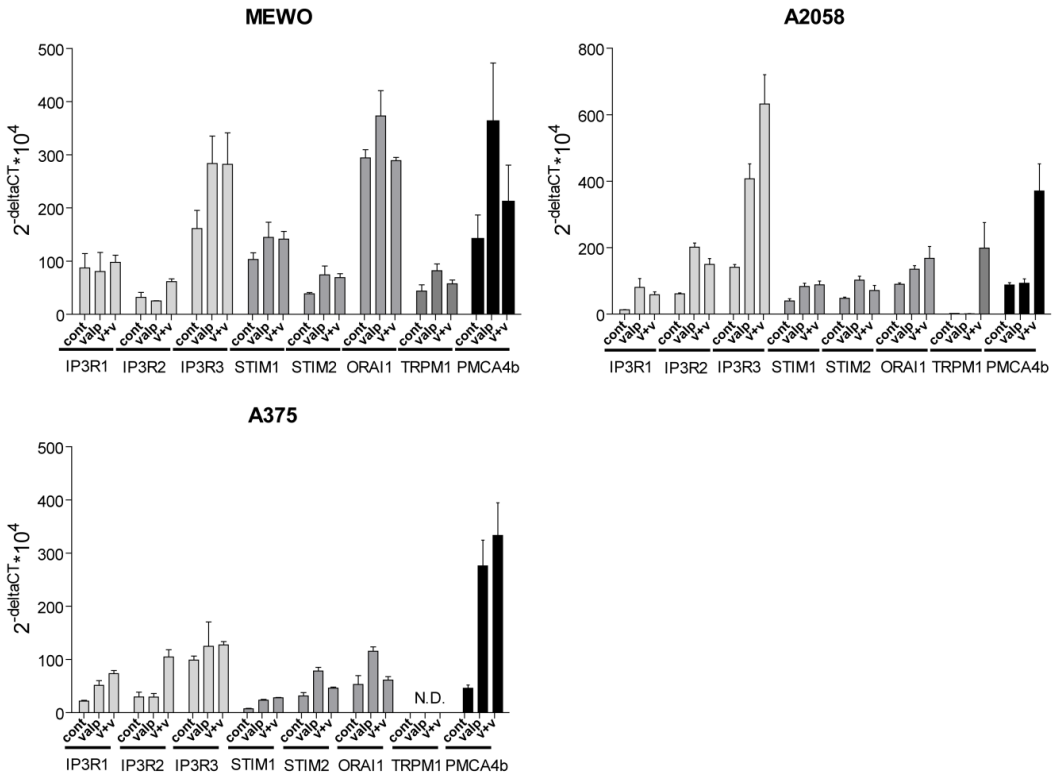

Figure 25. Alternations in the mRNA expression of Ca^{2+} channels and PMCA4b after treatment with valproate alone (2 mM) or in combination with vemurafenib (0.5 μM) for 48 hours. The mRNA level of inositol 1,4,5-triphosphate receptor type 1-3 (IP_3R1, IP_3R2, IP_3R3), stromal interaction molecule 1 and 2 (STIM1, STIM2), Orai calcium release-activated calcium modulator 1 (Orai1), transient receptor potential cation channel subfamily M member 1 (TRPM1) and PMCA4b was determined with quantitative real-time PCR analysis. Data was normalized to the expression level of glyceraldehyde-3-phosphate dehydrogenase (GAPDH). Bars show means ± S.E.M. of three independent measurements done in duplicates. N.D. stands for not detectable.

Importantly, in MEWO and A375 cells the mRNA expression of these channels was not influenced by the treatments. In the A2058 cell line IP_3R3 mRNA level was strongly increased

after valproate treatment while the combination treatment triggered TRPM1 expression. We showed earlier that vemurafenib treatment caused an increase in TRPM1 mRNA level that could be responsible for this latter effect. We also demonstrated that the mRNA level of PMCA4b changed in a similar manner as protein expression after HDAC inhibitor treatment.

5.5.2 HDAC inhibitor treatment increases Ca^{2+} clearance in a PMCA4b dependent manner

Next we studied if the increase in PMCA4b expression affected intracellular Ca^{2+} clearance. In order to study this, we analyzed the intracellular localization of PMCA4b before and after HDAC inhibitor treatment. We found that treatment with either valproate (2 mM) or SAHA (1 μM) induced an increase in the abundance of PMCA4b in the plasma membrane of the cells (Figure 26), indicating that the newly generated pump was functional.

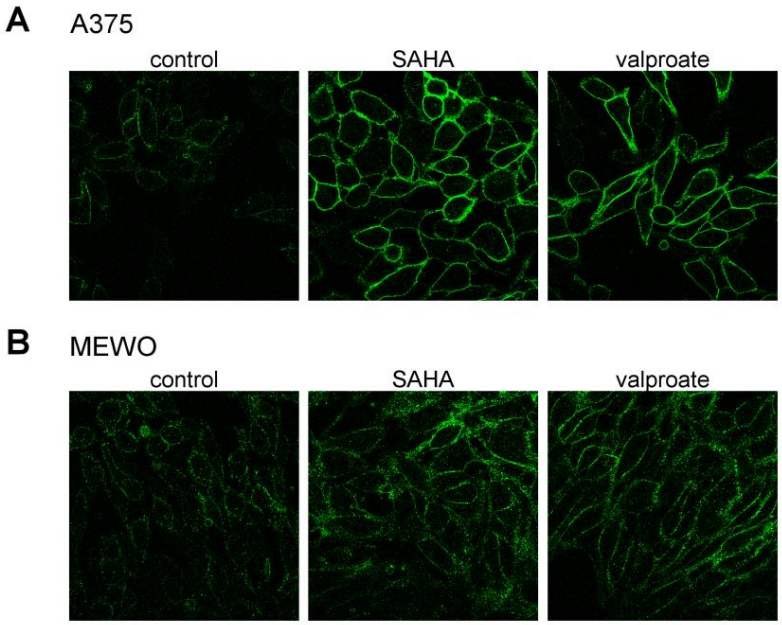

Figure 26. Immunofluorescence staining of PMCA4b in control and HDAC inhibitor treated cells. SAHA (1 μM) and valproate (2 mM) treatment was applied for 48 hours. Immunofluorescence staining was performed with anti-PMCA4b antibody. Confocal microscopy (60x objective) was used for staining analysis.

Then, A375 cells were filled with the Ca^{2+}-sensitive fluorescent indicator Fluo-4 and the intracellular Ca^{2+} signal was measured in both control and HDAC inhibitor treated cells after stimulation with the Ca^{2+} ionophore A23187. We found that in the valproate treated cells the decay of the Ca^{2+} signal was faster than in the control cells (Figure 27A). In order to

investigate the specific role of PMCA4b in the faster decline of the fluorescent signal we repeated the signal measurement after pretreating the cells with the PMCA4-specific inhibitor caloxin 1C2 (20 μM) (Figure 27B, C). Importantly, we found that the inhibitor treatment was able to significantly reverse the increase in Ca^{2+} decay underlining the importance of PMCA4b in shaping the Ca^{2+} signal.

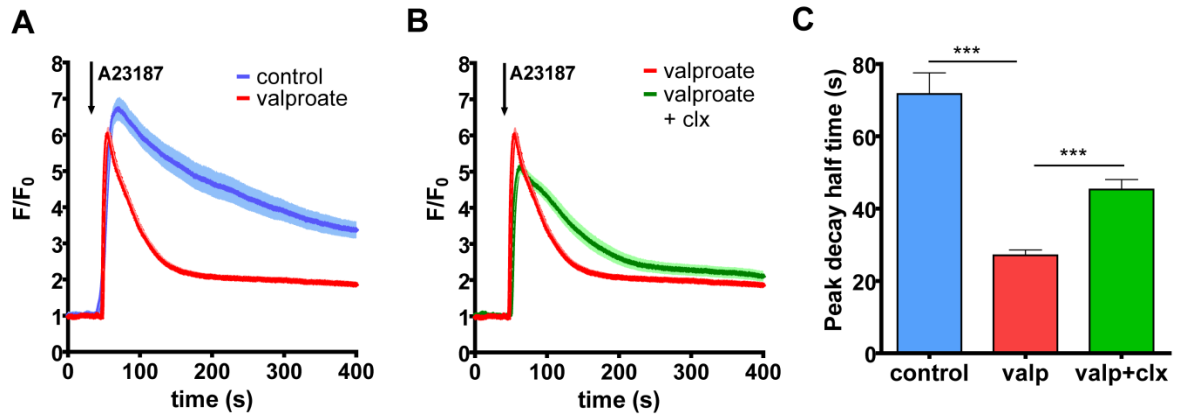

*Figure 27. The effect of HDAC inhibitor treatment on Ca^{2+} clearance is PMCA4 dependent. A375 cells were treated with valproate (2 mM) for 48 hours than they were filled with Ca^{2+}-sensitive fluorescent indicator Fluo-4. (A) Intracellular Ca^{2+} signal was induced with Ca^{2+} ionophore, A23187 (2 μM) in control and valproate treated cells. (B) Valproate treated cells were first pretreated with caloxin 1c2 (20 μM) PMCA4-specific peptide inhibitor for 10 minutes before ionophore stimulation. (C) Analysis of the half-peak decay time in control, valproate treated and valproate and caloxin 1c2 treated A375 cells. Bars represent mean ± SD of individual cells coming from three independent measurements. Significance was calculated between control and valproate-treated cells or valproate and valproate plus caloxin treated cells by two tailed unpaired t-test (*** P<0.001).*

5.5.3 Changes in cell viability and cell cycle progression after HDAC inhibitor treatment in melanoma cells

Since earlier it was found that HDAC inhibitor treatment could influence the viability of cancer cells [107], we analyzed how HDAC inhibitor treatment alone or in combination with vemurafenib influenced cell viability and cell cycle progression in MEWO, A375 and A2058 cells. To calculate viability we measured the number of dead cells and the total number of the cells. While in MEWO and A2058 cells viability was not influenced by any of the treatments, in A375 cells vemurafenib alone and in combination with both HDAC inhibitors had a small, but significant decreasing effect (Figure 28 A1, B1, C1).

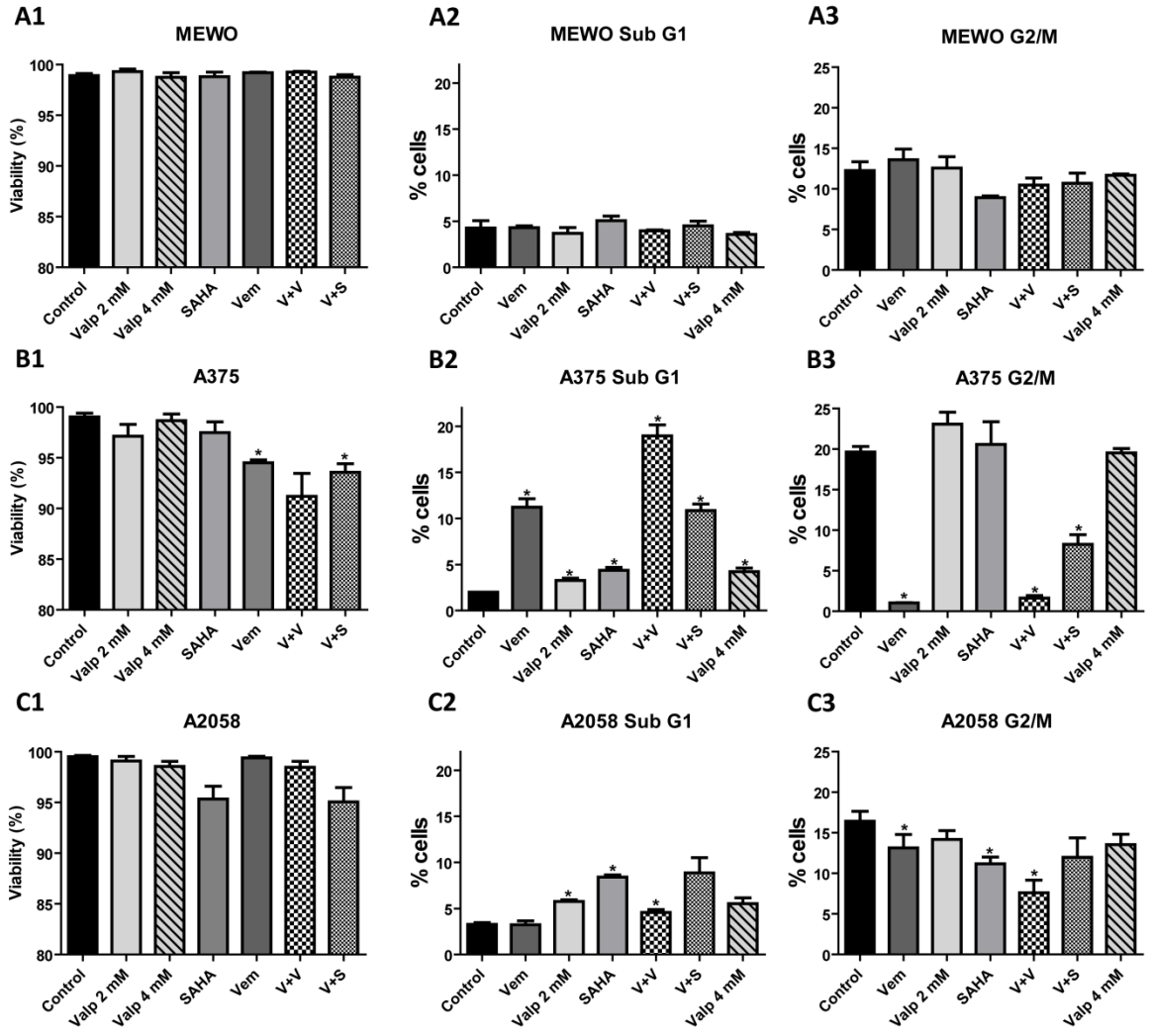

Figure 28. Cell cycle progression and cell viability was assessed after SAHA and valproate treatment alone or in combination with vemurafenib. Experiments were performed for 48 hours. For single treatments vemurafenib (0.5 μM), SAHA (1 μM), valproate (2 or 4 mM) were used, in combination V+S: vemurafenib (0.5 μM) + SAHA (1 μM), V+V: vemurafenib (0.5 μM) + valproate (2 mM) were applied. (A1, B, C1) Viability was calculated as total cells - nonviable cells/total cells. (A, B, C) Ratio of cells in cell cycle phases Sub G1 and G2/M. Data represents the mean of three independent experiments. Significance was calculated compared to control indicated by asterisks ($p < 0.05$); two-tailed paired t-test.*

In order to analyze the impact of the inhibitors on cell cycle progression, we determined the ratio of cells among four cell cycle phases based on their DNA content. Dying cells are in the Sub G1 phase, resting cells in the G0/G1 phase, during DNA synthesis the cells are in the S phase followed by the G2/M phase where cells have two sets of paired chromosomes. We found that all three cell lines were affected differently by the treatment. In MEWO cells

neither proliferation nor cell death were changed by any of the treatments (Figure 28 A2, A3). In A375 cells, in good accordance with our earlier results, cell division was strongly inhibited by vemurafenib, however, it was not influenced by the HDAC inhibitors. In contrast, cell death was increased by all of the treatments and combination of vemurafenib with valproate had an additive effect compared to single treatments (Figure 28 B2, B3). In A2058 cells, cell death was slightly increased by HDAC inhibitor treatment but not by vemurafenib. Proliferation was decreased among the single agents mostly by SAHA, while among combination treatments valproate together with vemurafenib had the strongest effect (Figure 28 B3, C3). Altogether, we found that both the viability and proliferation were only moderately affected by HDAC inhibitor treatments in melanoma cells and this effect was slightly increased by the combination treatments in the BRAF mutant cell lines.

5.5.4 Valproate treatment inhibits both random and directed migration of A375 cells

Earlier we showed that vemurafenib increased PMCA4b expression and decreased cell migration of A375 cells. Moreover, PMCA4b overexpression mimicked the effect of vemurafenib on cell motility. Since valproate treatment increased PMCA4b expression in this cell line in a similar extent as vemurafenib did, we wanted to investigate its effect on the migratory capacity of the cells. First we compared random cell migration between control and valproate treated cells for 24 hours with an automated fluorescence microscope (ImageXpress Micro XL). We found that valproate treatment strongly reduced the velocity of the cells as compared to that of the control cells (Figure 30A). We also tested the effect of valproate treatment on the directed migration of A375 cells with modified Boyden chamber assay, where a fibronectin coat was applied in the lower chamber as chemoattractant. After 48 hours pretreatment with an increasing concentration of valproate, cells were added to the chambers. Following a 6-hour incubation period the number of cells on the lower side of the Boyden chamber membrane was assessed. We found that 1 mM valproate treatment decreased significantly the directional movement of the cells that was further reduced with increasing concentrations of the drug (Figure 30B1).

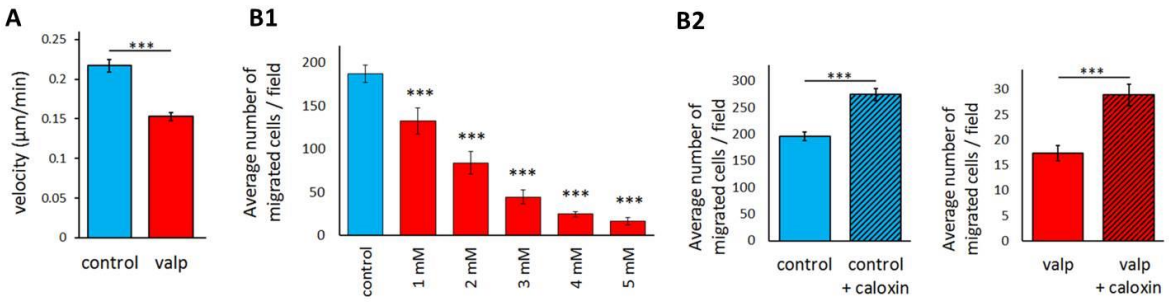

*Figure 30. Both random and directed migration of A375 cells are strongly decreased by valproate treatment. (A) Mean velocity was measured during random migration for 24 hours after 4 mM valproate treatment with an automated fluorescence microscope (ImageXpress Micro XL). Data represents the mean ± SEM of ≥ 100 individual cells from three independent experiments. Significance relative to control is indicated by (*** P<0.001); two-tailed unpaired t-test. (B1) Directed migration was analyzed with modified Boyden chamber assay for 6 hours after treatment with valproate in the indicated concentrations. The number of cells in representative fields on the lower side of the Boyden chamber membrane was counted. (B2) Cells were treated with 4 mM valproate for 48 hours, than caloxin 1c2 (20 nM) was added to the cells before the modified Boyden chamber assay. Data shows the mean of three experiments ± SEM. Significances are indicated by (*** P<0.001); two-tailed unpaired t-test.*

To investigate the specific role of PMCA4b in this effect, we performed the same assay as before but in the presence of the PMCA4b specific inhibitor caloxin 1c2. Interestingly, caloxin treatment increased the directed migration of both control and vaproate treated cells (Figure 30B2) suggesting that PMCA4b played an important role in the regulation of the migration of A375 cells.

6. Discussion

The PMCA (ATP2B1-4) family of proteins shows great diversity counting more than 20 distinct variants. While their biochemical properties and some specific cellular functions have been determined, less was known about their specific role in shaping the Ca^{2+} signal. Therefore, we generated a methodology to test the influence of PMCAs on the Ca^{2+} transients in HeLa cells. Later the same methodology was used to study the role of PMCAs in different kinds of cancer cells, including cell lines of melanoma origin. Recent studies have shown that PMCA4b is downregulated in certain type of cancers. Here we found that inhibition of the BRAF/MEK/ERK pathway in BRAF mutant melanoma cells increased the expression of PMCA4b, and resulted in enhanced Ca^{2+} clearance and decreased cell migration. Similarly, when PMCA expression was induced by HDAC inhibitor treatment independently from the ERK activation, a faster Ca^{2+} clearance rate and reduced migratory capacity was evoked in melanoma cells. Furthermore, specific inhibitors of PMCA4 could partially reverse these effects proving that PMCA4 has a primary role in the regulation of Ca^{2+} signaling and cell migration.

6.1 The effect of PMCA activity on the SOCE induced Ca^{2+} signal

It was suggested earlier that PMCA played an important role in the regulation of the decay phase of the Ca^{2+} signal induced by the store operated or other means of Ca^{2+} entry into the cytosol. After a rise in the intracellular Ca^{2+} level besides the PMCAs also the SERCA proteins, the mitochondria and when present the Na^{+}/Ca^{2+} exchangers can remove Ca^{2+} from the cytosol. The specific effects of each transporter were tested by the use of specific inhibitors. Klishin et al. [158] used calf pulmonary endothelial cells; they depleted the internal Ca^{2+} stores by the addition of thapsigargin in a Ca^{2+} free medium and then Ca^{2+} entry was initiated by increasing the extracellular Ca^{2+} concentration. They found that in these cells PMCA shaped primarily the decay phase of the Ca^{2+} signal while the Na^{+}/Ca^{2+} exchange affected mostly the size of the peak, and mitochondria had no effect.

The role of the PMCA in the regulation of the Ca^{2+} signal decay phase was also demonstrated in immune cells [159]. Interestingly, after activation of Jurkat T-cells with lectin phytohemagglutinin (PHA) a decrease in Ca^{2+} clearance was found. It was shown that both

PMCA and ER Ca^{2+} sensor protein STIM1 translocate to the forming immunological synapse (IS) and STIM1 attenuates PMCA activity by direct binding. Later it was found that another protein partner of STIM1 (POST) was also required to the decreased activity of PMCA in the IS [65]. Upon store depletion POST binds to STIM1 and this complex interacts with PMCA, which results in a decreased Ca^{2+} extrusion capacity of the pump.

It was shown that PMCAs can also influence intracellular Ca^{2+} signaling by controlling the availability of PIP_2. On the one hand, it can decrease PLC activity by removing Ca^{2+} from its vicinity and on the other PMCA can directly bind PIP2 molecules preventing their processing to IP_3. In this way PMCAs regulate Ca^{2+} release from the ER by a mechanism independent of its Ca^{2+} transporting ability [44].

In our experiments we demonstrated that PMCA isoforms due to their distinct kinetic features influence the pattern of the Ca^{2+} signal initiated by SOCE differently. PMCA2b is a fast pump with long memory [154] and its expression resulted in a short Ca^{2+} spike. Because this isoform remains active for about 20 minutes after stimulation - even when Ca^{2+} level decreases - it precludes the formation of another immediate Ca^{2+} signal. Its ability to generate distinct Ca^{2+} spikes is particularly important in the Purkinje neurons in the cerebellum [160, 161]. The activation kinetics of PMCA2 makes it possible to react fast Ca^{2+} signals quickly in the nerves system where it is abundantly present. The length of the Ca^{2+} signal also influences the activation of downstream Ca^{2+} dependent signaling molecules. PMCA2 overexpression was shown to decrease the activation of transcription factor NFAT in HEK cells by decreasing the activity of Ca^{2+}- dependent phosphatase calcineurin [62].

PMCA4a and PMCA4b are the C-terminal splice variants of the same protein but they strongly differ in their kinetic properties and consequently in their tissue distribution. PMCA4a can get activated quickly but then it has a short memory [41]. It is expressed in smooth muscles, in the heart, in the nervous system and it is the only PMCA form that is present in the sperm tail. In sperms a sperm-specific cation channel (CatSper) was described that necessary for sperm hyperactivation [162]. Absence of PMCA4 in mice results in male infertility due to impaired sperm motility [163]. Interestingly, in activated sperm cells the pattern of the Ca^{2+} signal is similar to that observed in PMCA4a expressing Hela cells [164].

PMCA4b is a slow pump with long memory [41, 154] and so it is capable to regulate Ca^{2+} signals in non-excitable cells. We found that in PMCA4b expressing cells, store operated Ca^{2+} entry evoked first a large peak followed by periodic baseline oscillations. In non-excitable

cells, Ca^{2+} oscillations are mostly described as repetitive Ca^{2+} release and uptake from the ER to the cytosol regulated by the IP_3R ER receptor channels and the ER Ca^{2+} pumps SERCA proteins [165]. In our experimental setup, we excluded the effect of the ER by first inducing Ca^{2+} release in zero Ca^{2+} environment and by blocking SERCA activity with thapsigargin. Under these conditions, Ca^{2+} oscillations were produced by the concerted action of SOCE channels and PMCA4b. Ca^{2+} oscillations can greatly vary in their spatial and temporal features and oscillatory signals with distinct frequency and amplitude were shown to initiate different downstream cellular responses [6]. Previously it was demonstrated in human bone marrow-derived mesenchymal stem cells that PMCA can play a role in the regulation of Ca^{2+} oscillations [166]. It was also found that increased presence of PMCA4 resulted in decreased activation of the transcription factor NFAT in both HEK and endothelial cells [61, 64].

Furthermore, a mathematical model was generated by our group that took into account the activation kinetics of the PMCA isoforms and their distinct Ca^{2+} -CaM binding. The mathematical model described well our experimental results. According to the model, the slow activation of PMCA4b was necessary to the formation of Ca^{2+} oscillations. SOCE channels became activated quickly and hence Ca^{2+} concentration increased substantially before PMCA4b was fully active.

6.2 The role of PMCA4b in the regulation of melanoma cell migration

In migrating cells an increasing Ca^{2+} gradient is present from the front towards the rear of the cells [82]. It was found in endothelial cells that there is an increased abundance of PMCA in the front of the cells [87]. It was demonstrated that this increased presence of the PMCA contributed to the maintenance of the low Ca^{2+} level and to the formation of local Ca^{2+} pulses and periodic activation of the MLCK resulting in pulsatile retraction and adhesion in the front. It was also found that ectopic expression of PMCA4 in VEGF treated endothelial cells decreased NFAT activity and migratory capacity of the cells [64]. However the role of PMCAs in cancer cell migration has not been yet investigated.

Melanoma cells often have strong migratory and metastatic capacity and it was demonstrated that increased Ca^{2+} uptake contributes to this phenomena. It was found that SOCE channel OraI1 and its partner STIM2 are strongly expressed in melanoma cells, and in the invasive edge of primary tumors and lymph node metastases [134]. Downregulation of their expression decreased the migratory and metastatic capacity of the cells but enhanced

their proliferation. In another study STIM1 and Orai1 was found to be abundantly present in melanoma cell lines and tissues and their inhibition decreased both the proliferation and migration of the cells [135]. SOCE activation was associated with ERK activation which could be reversed by CaMKII or Raf1 inhibition. Furthermore, STIM1 and ORAI1 induced Ca^{2+} oscillations were shown to initiate invadopodium formation and extracellular matrix degradation [136] through the regulation of Src kinase activity and MT1-MMP release. It was also demonstrated that STIM1 and Orai1 expression was higher in melanoma cell lines than in normal epidermal human melanocytes and their expression was increased in cells derived from metastatic melanoma compared to cells derived from primary melanoma. Downregulation of STIM1 decreased the metastatic capacity of melanoma cells *in vivo* in a lung colonization assay.

Expression of several TRPM channels (TRPM8, TRPM2, TRPM7) was also found to be upregulated in melanoma cells and to have an increasing effect on proliferation [132]. These data suggest that increased Ca^{2+} uptake play a major a role in the strong proliferative and metastatic capacity of melanoma cells.

In our work we found that in BRAF mutant melanoma cells inhibition of the BRAF/MEK/ERK pathway induced PMCA4 expression and that was coupled with enhanced Ca^{2+} clearance and decreased migratory capacity of the cells. The expression of PMCA4b alone was able to strongly reduce the motility and metastatic capacity of A375 melanoma cells *in vivo*. Microarray data showed that PMCA4b expression was lower in melanoma specimens than in benign nevi. Our data are in good accordance with the above described results on Ca^{2+} channels. Ca^{2+} uptake is elevated by synergistic actions of the upregulated Ca^{2+} channels and downregulated Ca^{2+} release mechanisms resulting in increased migratory and metastatic activity of melanoma cells. Since we demonstrated that PMCA activity can influence the SOCE mediated Ca^{2+} signal it is possible that PMCA reduces melanoma cell motility by opposing the Ca^{2+} entry by SOCs, especially because we found no change in the expression of store operated Ca^{2+} channels (Orai1, STIM1 and 2) and inositol 1,4,5-trisphosphate receptors type 1-3 (IP_3R1, IP_3R2, IP_3R3) after BRAF inhibitor treatment, or in the PMCA4b expressing cells.

We demonstrated that increased PMCA4b expression strongly reduced the metastatic capacity of A375 cells. However, we found that it did not influence the proliferation of the

cells. In conclusion, PMCA4b reduces the ability of melanoma cells to metastasize without affecting proliferation fulfilling the definition of metastasis suppressors [167].

6.3 The effect of HDAC inhibitor treatment on PMCA expression and cell migration in melanoma cells

It was found previously that HDAC inhibitor treatment increased the expression of PMCA4 in colon and breast cancer cells. Treatment with short chain fatty acids and trichostatin A evoked a marked increase in the expression of PMCA4b and a moderate elevation of PMCA1b protein level in various gastric and colon cancer cell lines [93]. In MCF-7 breast cancer cells, both short chain fatty acid and SAHA treatments induced a strong upregulation in PMCA4b expression and that was coupled with an enhanced Ca^{2+} clearance from the cells [94]. It was also demonstrated that PMCA4 is present in a substantial amount in the normal breast tissue.

We found a similar pattern of PMCA expression in melanoma cells in response to HDAC inhibitor treatments. Both valproate and SAHA increased the expression of PMCA4b in melanoma cell lines independent of their BRAF mutational status. Interestingly, HDAC inhibitor treatments also induced the expression of PMCA1 in two out of the three melanoma cell lines. We showed that increased PMCA4b abundance resulted in enhanced Ca^{2+} clearance in the A375 cells and their motility was also strongly decreased by valproate treatment. Both effects were partially reverted by the use of PMCA4 specific inhibitor caloxin 1c2 proving that PMCA4b play a primary role in regulation of the intracellular Ca^{2+} signal and cell migration. Importantly, we found no change in the expression of the SOCE channels by the treatments suggesting that they are not responsible for the decreased motility of the HDACi treated cells.

We found that HDACis enhanced the abundance of PMCA1 in the BRAF mutant A375 and A2058 cells but it did not change that of in the BRAF wild type MEWO cell line. Previously, it was shown that the expression of PMCA1 was moderately altered by HDAC inhibitors in colon cancer cells while it was not modified in MCF-7 breast cancer cells [93, 94]. It was demonstrated that PMCA1 expression is regulated by vitamin D in osteoblasts, the small intestine, kidney distal tubules and also in colon cancer cells [168, 169]. Deletion of PMCA1 specifically in the intestinal absorptive cells caused decreased responsiveness to 1, 25-

dihydroxyvitamin D3 and reduced bone mineral density in mice [170]. In melanoma cell lines, the antiproliferative effect of 1, 25(OH)2D3 was shown to be cell line dependent [171], however, lower vitamin D levels in the blood of melanoma patients were associated with advanced melanoma stage [172]. Since Vitamin D can influence HDAC activity [173] it is possible that vitamin D regulate PMCA1 expression through epigenetic mechanisms.

We also tested the effect of HDAC inhibitors alone or in combination with vemurafenib on the viability of melanoma cells. It was found previously that treatment with HDAC inhibitors can induce apoptosis in melanoma cells, however, this effect was strongly cell line and inhibitor dependent [113]. We found that the viability of these cell lines was not substantially altered by any of the treatments. We also analyzed the ratio of the proliferative and apoptotic cells after treatments and found that the changes were cell type specific. Proliferation of A375 cells was strongly reduced by BRAF inhibition but it was not affected by the HDAC inhibitor treatment. The ratio of cells in the SubG1 phase was increased by both treatments and it was further increased by the combination treatment with vemurafenib and valproate. The PTEN mutant A2058 cell line showed a moderate response to vemurafenib treatment but HDAC inhibitor could decrease proliferation and increase cell death significantly in these cells. Similar results were obtained on cell viability by other groups as well [174] and a higher ratio of apoptotic cells was observed only at higher concentration of HDACis [115].

Taken together, our data show that PMCA proteins play an important role in the regulation of the intracellular Ca^{2+} signal. BRAF inhibitor treatment selectively upregulated the expression of the PMCA4b isoform only in BRAF mutant melanoma cells, while HDAC inhibitor treatment increased PMCA4b abundance in all cell lines independent of their BRAF mutational status. Increased PMCA4b expression enhanced intracellular Ca^{2+} clearance and decreased the migratory and metastatic capacity of the highly motile A375 melanoma cells.

7. Summary

Plasma membrane calcium ATPases (PMCA) maintain the resting low intracellular calcium concentration by pumping out excess calcium from the cytosol. There are four different PMCA proteins (PMCA1-4) coded by four genes and through alternative splicing more than 20 isoforms are produced. PMCA isoforms differ in their kinetic properties, tissue distribution and in their intracellular localization. Regarding their activation by Ca^{2+}-calmodulin PMCAs can be categorized as fast or slow pumps. Depending on their inactivation rates PMCAs with short and long lasting activity can be distinguished that is referred as to the memory from earlier Ca^{2+} spikes.

We found that PMCA isoforms due to their distinct kinetic features influence the pattern of the Ca^{2+} signal initiated by SOCE differently and this is in good accordance with their physiological role in specific cell types and tissues. In our measurements, the quickly activating PMCA2b with long memory produced distinct Ca^{2+} spikes just like the spikes in the Purkinje neurons in the cerebellum. PMCA4a is also a fast pump but with a short memory. As a result, after a fast decay the intracellular Ca^{2+} concentration stabilized in a new, increased steady-state level in the PMCA4a expressing cells. Earlier a similar pattern was found also in activated sperm cells. The PMCA4b isoform is primarily present in non-excitable cells, we found that its slower activation rate allows the formation of relatively large Ca^{2+} transients and can initiate periodic baseline oscillations.

Earlier it was demonstrated that expression of PMCA proteins can be altered in colon and breast cancer cells. We found that inhibition of the BRAF/MEK/ERK pathway selectively upregulated the expression of PMCA4b in BRAF mutant melanoma cells and this effect was coupled with enhanced Ca^{2+} clearance in the cells. Expression of PMCA4b in BRAF mutant A375 cells profoundly changed the morphology of the cells, decreased their migratory capacity in vitro and reduced their metastatic capacity in vivo. Furthermore, histone deacetylase inhibitor treatment increased PMCA4b expression in melanoma cells independent from ERK activation and it enhanced the Ca^{2+} clearance and decreased the motility of the cells in a PMCA4b dependent manner. Our data demonstrates for the first time that PMCA4b is an important regulator of the migration of melanoma cells and that PMCA4b is a putative metastasis suppressor protein.

8. Összefoglalás

A plazmamembrán típusú kalcium ATPázok (PMCA) részt vesznek a nyugalmi kalcium koncentráció fenntartásában. A négy PMCA fehérje (PMCA1-4) négy különböző génen kódolt, melyekről alternatív "splicing" során több mint húsz izoforma képződhet. Az izoformák különböznek kinetikai tulajdonságaikban, szöveti megoszlásukban és sejten belüli elhelyezkedésükben.

Úgy találtuk, hogy az egyes PMCA fehérjék eltérő kinetikai tulajdonságainak köszönhetően különbözőképpen befolyásolják a Ca^{2+} szignál mintázatát, ami összhangban áll fiziológiás szerepükkel az egyes sejttípusokban. A Ca^{2+}/kalmodulin komplex által gyorsan aktiválódó, de hosszan aktívan maradó, hosszú memóriájú PMCA2b hatására egyedi Ca^{2+} tüskék alakultak ki kísérleteinkben csak úgy, mint a Purkinje sejtekben, a kisagyban. A PMCA4a variáns szintén gyorsan aktiválódik, azonban az aktivitását gyorsan elveszíti. Ennek következtében a PMCA4a-t kifejező sejtekben a kezdeti gyors csökkenés után egy új, megemelkedett intracelluláris Ca^{2+} szint alakult ki, amihez hasonló mintázatot találtak aktivált spermiumokban is. A PMCA4b elsősorban nem-ingerelhető sejtekben van jelen, amelyekben lassú aktivációja hozzájárul a relatíve nagyobb amplitudójú és hosszabb ideig fenntartott Ca^{2+} jelek és az azt követő periodikus alapszintű oszcilláció kialakulásához.

Korábbi eredmények alapján a PMCA fehérjék kifejeződése megváltozik vastagbél es emlő tumor sejtekben a normál szövethez képest. Kísérleteinkben azt tapasztaltuk, hogy BRAF mutáns melanóma sejtekben a BRAF/MEK/ERK jelátvitel gátlásakor a PMCA4b szintje megemelkedett és ezzel összhangban a sejtet érő stimulust követően a Ca^{2+} eltávolítás sebessége megnőtt. A PMCA4b túltermeltetése BRAF mutáns A375 sejtekben a sejtalak drasztikus változását okozta, valamint *in vitro* a sejtek mozgását, *in vivo* pedig az áttétképzést csökkentette. Úgy találtuk, hogy a PMCA4b fehérje kifejeződése hiszton deacetiláz gátló kezelés hatására is megemelkedett a melanóma sejtekben, de ez a hatás független volt az ERK fehérje aktivációjától. Ugyanakkor ezekre a sejtekre is fokozott Ca^{2+} eltávolítás és csökkent migráció volt a jellemző, PMCA4b függő módon.

Eredményeink azt mutatják, hogy a PMCA4b fontos szerepet játszik a sejtek Ca2+ jelátviteli folyamataiban és feltehetően ezen keresztül a melanóma sejtek mozgásának szabályozásában. Végül érdemes kiemelni, hogy a PMCA4b fehérjét elsőként azonosítottuk, mint lehetséges metasztázis szuppresszort.

9. Tables and abbreviations

9.1 Primary antibodies

Name	Source	Type	Dilution
Anti-PMCA4b (JA3)	[149]	Mouse monoclonal	1:1000
Anti-PMCA1	Affinity BioReagents, PA1-914	Rabbit polyclonal	1:1000
Anti-PMCA2	[175]	Rabbit polyclonal	1:1500
Anti-PMCA3	[175]		
Anti-pan-PMCA (5F10)	[175]	Mouse monoclonal	1:5000
Anti-SERCA2	Sigma-Aldrich, S1439	Mouse monoclonal	1:2500
Anti-SERCA3 (PL/IM430)	[93]	Mouse monoclonal	1:200
Anti-phospho-p44/42MAPK (ERK1/2)	Cell Signaling, CST4370S	Rabbit monoclonal	1:1000
Anti-ERK1/2 (MK1)	Santa Cruz, sc135900	Mouse monoclonal	1:500
Anti-β-tubulin	Abcam, ab6046	Rabbit polyclonal	1:1000
Anti-BRAF-V600E (VE_1)	Spring Bioscience Corp. E19290	Mouse monoclonal	1:500
Anti-acetyl-Histone H3 (Lys 9/Lys 14)	Cell Signaling, 9677	Rabbit polyclonal	1:1000
Anti-Na^+/K^+ ATPase	Enzo Life Sciences BML-SA247-0100	Mouse monoclonal	1:2000

9.2 Primers used for SYBR Green expression analysis

Oligo Name	Sequence (5'-3')
IP3R1 forward	TTG GGC CTG GTT GAT GAT CG
IP3R1 reverse	TTT GGG CAG AGT AGC GGT TC
IP3R2 forward	AGA AGA ATG CCA TGC GTG TG
IP3R2 reverse	ACC CTC GCT TCT CAG TTT CC
IP3R3 forward	CCT AAG AAG TTC CGT GAC TG
IP3R3 reverse	TCC TTG TCC TGC TTA GTC TG
ORAI1 forward	TGG ACG CTG ACC ACG ACT AC
ORAI1 reverse	CCT CGA TGT TGG GCA GGA TG
RYR2 forward	ATG TAT CTG TGC TGC CTG TC
RYR2 reverse	CTT CTG ATC GCT GCT TAG AG
STIM1 forward	GAT GGA CGA TGA TGC CAA TG
STIM1 reverse	GAA GGT GCT GTG TTT CAC TG
STIM2 forward	AAC GAC ACT TCC CAG GAT AG
STIM2 reverse	ACC ACA TCC AAT GCC TTG AG
TRPM1 forward	GTG TCA GCA CAG GTG TTA TC
TRPM1 reverse	TCC TTT CCA ACC AGG TCT TC
E-cadherin forward	CAGAGCCTCTGGATAGAGAACGCA
E-cadherin reverse	GGCATTGTAGGTGTTCACATCATCGTC
SNAIL1 forward	TATGCTGCCTTCCCAGGCTTG
SNAIL1 reverse	ATGTGCATCTTGAGGGCACCC
ZEB1 forward	CCAGTGGTCATGATGAAAATGGAACACC
ZEB1 reverse	CAGACTGCGTCACATGTCTTTGATCTC
Vimentin forward	GGCTCAGATTCAGGAACAGC
Vimentin reverse	CTGAATCTCATCCTGCAGGC
GAPDH forward	AGCTCACTGGCATGGCCTTC
GAPDH reverse	ACGCCTGCTTCACCACCTTC

9.3 Abbreviations

AA: arachidonic acid

AE: adverse effect

APC: antigen presenting cell

ATP: adenosine triphosphate

CaM: calmodulin

CaMKII: Ca^{2+}/calmodulin-dependent protein kinase II

CaN: calcineurin

CBS: calmodulin binding sequence

CDK: cyclin dependent kinase

CICR: Ca^{2+} induced Ca^{2+} release

COX-2: cyclooxygenase-2

CRAC: calcium release activated calcium current

CTLA-4: cytotoxic T-lymphocyte-associated antigen 4

DAG: diacyglycerol

DAPI: 4´,6-diamidino-2-fenilindol

DAPK: death-associated protein kinase

DTT: dithiothreitol

ECM: extracellular matrix

EGF: epidermal growth factor

eNOS: endothelial nitric oxide synthase

Epac: exchange protein directly activated by cyclic AMP

ER: endoplasmic reticulum

ERK: extracellular-signal regulated kinase

FA: focal adhesion

FAK: focal adhesion kinase

GAPDH: glyceraldehyde-3-phosphate dehydrogenase

GCaMP2: GFP-based Ca^{2+} probe

GFP: green fluorescent protein

GPCR: G-protein-coupled receptor

HAT: histone acetyl transferase

HBSS: Hanks´ Balanced Salt Solution

HDAC: histone deacetylase

HGF: hepatocyte growth factor

HUVEC: human umbilical vein endothelial cell

IGF: insulin like growth factor

IP_3: inositol 1,4,5-trisphosphate

IP_3R: inositol 1,4,5-trisphosphate receptor

IS: immunological synapse

MAGE: melanoma-associated antigen

MAGUK: membrane-associated guanylate kinase

MAPK: mitogen activated protein kinase

MCU: mitochondrial calcium uniporter

MEK: MAPK/ERK kinase

MLCK: myosin light chain kinase

MMP: matrix metalloproteinase

mTOR: mechanistic target of rapamycin

NCX: $Na^{+/}Ca^{2+}$ exchanger

NFAT: nuclear factor of activated T-cell

NHERF2: Na^+/H^+ exchanger regulatory factor 2

NMDA: N-methyl-D-aspartate

nNOS: neural nitric oxide synthase

PD1: programmed cell death receptor 1

PD-L1: programmed death-ligand 1

PIP_2: phosphatidylinositol-4,5- bisphosphate

PIP_3: phosphatidylinositol-3,4,5- bisphosphate

PLC: phospholipase C

PMCA: plasma membrane Ca^{2+} ATPases

POST: partner of STIM

PSD-95: post synaptic density protein 95

PTEN: phosphatase and tensin homolog

PTP: permeability transition pore

RAF: rapidly accelerated fibrosarcoma

RAS: rat sarcoma

RASSF1: Ras association domain-containing protein 1

ROS: reactive oxygen species

RTKR: receptor tyrosine kinase-linked receptor

RYR: ryanodine receptor

SAHA: suberoylanilide hyroxamic acid

SERCA: sarco/endoplasmic reticulum Ca^{2+} ATPases

SOC: store operated Ca^{2+} channel

SOCE: store operated Ca^{2+} entry

SPCA: secretory-pathway Ca^{2+} ATPase

SR: sarcoplasmic reticulum

STIM: stromal interacting molecule

TCA: trichloroacetic acid

TGF: transforming growth factor

TRPC: transient receptor potential cation channel subfamily C (“C” for canonical)

TRPM: transient receptor potential cation channel subfamily M (“M” for melastatin)

TRPV: transient receptor potential cation channel subfamily V (“M” for vanilloid)

TSA: trichostatin A

VEGF: vascular endothelial growth factor

10. List of publications

Publications related to the thesis:

1. **Hegedüs L**, Padányi R, Molnár J, Pászty K, Varga K, Kenessey I, Sárközy E, Wolf M, Grusch m, Hegyi Z, Homolya L, Aigner C, Garay T, Hegedüs B, Tímár J, Kállay E, Enyedi A. " Histone Deacetylase Inhibitor Treatment Increases the Expression of the Plasma Membrane Ca^{2+}Pump PMCA4b and Inhibits the Migration of Melanoma Cells Independent of ERK. " *Front. Oncol.*, 24 May 2017, https://doi.org/10.3389/fonc.2017.00095

2. **Hegedűs L**, Garay T, Molnar E, Varga K, Bilecz A, Torok S, Padanyi R , Paszty K , Wolf M, Grusch M, Kallay E, Dome B, Berger W, Hegedus B, Enyedi A." The plasma membrane Ca^{2+} pump PMCA4b inhibits the migratory and metastatic activity of BRAF mutant melanoma cells. " *Int J Cancer.* 2017 Jun 15;140(12):2758-2770. Epub 2016 Nov 17.

3. Pászty K, Caride AJ, Bajzer Ž, Offord CP, Padányi R, **Hegedűs L**, Varga K, Strehler EE, Enyedi A. "Plasma membrane Ca2+-ATPases can shape the pattern of Ca2+ transients induced by store-operated Ca2+ entry. " *Sci Signal.* 2015 Feb;8(364):ra19.

Further publications:

Padányi R, Pászty K, **Hegedűs L**, Varga K, Papp B, Penniston JT, Enyedi Á. "Multifaceted plasma membrane Ca2+ pumps: From structure to intracellular Ca^{2+} handling and cancer. " *Biochim. Biophys. Acta.* 2016 Jun;1863(6 Pt B):1351-63. doi: 10.1016/j.bbamcr.2015.12.011. Epub 2015 Dec 17. Review

Varga K, Pászty K, Padányi R, **Hegedűs L**, Brouland JP, Papp B, Enyedi A. "Histone deacetylase inhibitor- and PMA-induced upregulation of PMCA4b enhances Ca2+ clearance from MCF-7 breast cancer cells. " *Cell Calcium*. 2014 Feb;55(2):78-92.

Penniston JT, Padányi R, Pászty K, Varga K, **Hegedus L**, Enyedi A. "Apart from its known function, the plasma membrane Ca^{2+}ATPase can regulate Ca^{2+} signaling by controlling phosphatidylinositol 4,5-bisphosphate levels. " *J Cell Sci*. 2014 Jan 1;127(Pt 1):72-84.

Apáti Á, Pászty K, **Hegedűs L**, Kolacsek O, Orbán TI, Erdei Z, Szebényi K, Péntek A, Enyedi Á, Sarkadi B. "Characterization of calcium signals in human embryonic stem cells and in their

differentiated offspring by a stably integrated calcium indicator protein." *Cell Signal*. 2013 Apr;25(4):752-9.

Arbabian A, Brouland JP, Apáti A, Pászyt K, **Hegedűs L**, Enyedi Á, Chomienne C, Papp B. "Modulation of endoplasmic reticulum calcium pump expression during lung cancer cell differentiation." *FEBS Journal* 280 (2013) 5408–5418

Antalffy G, Pászty K, Varga K, **Hegedűs L**, Enyedi A, Padányi R. "C-terminal di-leucine motif controls plasma membrane expression of PMCA4b." *Biochim Biophys Acta*. 2013 Dec;1833(12):2561-72.

Antalffy G, Mauer AS, Pászty K, **Hegedus L**, Padányi R, Enyedi A, Strehler EE. (2012). "Plasma membrane calcium pump (PMCA) isoform 4 is targeted to the apical membrane by the w-splice insert from PMCA2." *Cell Calcium*. 51(2):171-178.

Antalffy G, Caride AJ, Pászty K, **Hegedus L**, Padanyi R, Strehler EE, Enyedi A. (2011). "Apical localization of PMCA2w/b is enhanced in terminally polarized MDCK cells." *Biochem Biophys Res Commun.* 410(2):322-327.

Hegedus L, Hyojin C, Xian X, Eliceiri G. (2008). "Additional MDA-MB-231 Breast Cancer Cell Matrix Metalloproteinases Promote Invasiveness." *J Cell Physiol*. 216: 480–485.

Paszty K, Antalffy G, **Hegedus L**, Padanyi R, Penheiter AR, Filoteo AG, Penniston JT , Enyedi A. (2007). "Cleavage of the plasma membrane Ca+ATPase during apoptosis." *Ann N Y Acad Sci.* 1099: 440-450.

11. References

1. Tennakoon, S., A. Aggarwal, and E. Kallay, *The calcium-sensing receptor and the hallmarks of cancer.* Biochim Biophys Acta, 2016. **1863**(6 Pt B): p. 1398-407.
2. Clapham, D.E., *Calcium signaling.* Cell, 2007. **131**(6): p. 1047-58.
3. Berridge, M.J., *Calcium signalling remodelling and disease.* Biochem Soc Trans, 2012. **40**(2): p. 297-309.
4. Berridge, M.J., P. Lipp, and M.D. Bootman, *The versatility and universality of calcium signalling.* Nat Rev Mol Cell Biol, 2000. **1**(1): p. 11-21.
5. Berridge, M.J., M.D. Bootman, and H.L. Roderick, *Calcium signalling: dynamics, homeostasis and remodelling.* Nat Rev Mol Cell Biol, 2003. **4**(7): p. 517-29.
6. Uhlen, P. and N. Fritz, *Biochemistry of calcium oscillations.* Biochem Biophys Res Commun, 2010. **396**(1): p. 28-32.
7. Mikoshiba, K., *IP3 receptor/Ca2+ channel: from discovery to new signaling concepts.* J Neurochem, 2007. **102**(5): p. 1426-46.
8. Santulli, G. and A.R. Marks, *Essential Roles of Intracellular Calcium Release Channels in Muscle, Brain, Metabolism, and Aging.* Curr Mol Pharmacol, 2015. **8**(2): p. 206-22.
9. Santo-Domingo, J. and N. Demaurex, *Calcium uptake mechanisms of mitochondria.* Biochim Biophys Acta, 2010. **1797**(6-7): p. 907-12.
10. Schwaller, B., *Cytosolic Ca2+ buffers.* Cold Spring Harb Perspect Biol, 2010. **2**(11): p. a004051.
11. Perkel, D.J., et al., *The role of Ca2+ entry via synaptically activated NMDA receptors in the induction of long-term potentiation.* Neuron, 1993. **11**(5): p. 817-23.
12. Shuttleworth, T.J., *Arachidonic acid, ARC channels, and Orai proteins.* Cell Calcium, 2009. **45**(6): p. 602-10.
13. Smyth, J.T., et al., *Activation and regulation of store-operated calcium entry.* J Cell Mol Med, 2010. **14**(10): p. 2337-49.
14. Putney, J.W., *Pharmacology of store-operated calcium channels.* Mol Interv, 2010. **10**(4): p. 209-18.
15. Sharma, V. and D.M. O'Halloran, *Recent structural and functional insights into the family of sodium calcium exchangers.* Genesis, 2014. **52**(2): p. 93-109.
16. Van Baelen, K., et al., *The Ca2+/Mn2+ pumps in the Golgi apparatus.* Biochim Biophys Acta, 2004. **1742**(1-3): p. 103-12.
17. Giacomello, M., et al., *Ca2+ hot spots on the mitochondrial surface are generated by Ca2+ mobilization from stores, but not by activation of store-operated Ca2+ channels.* Mol Cell, 2010. **38**(2): p. 280-90.
18. Kuhlbrandt, W., *Biology, structure and mechanism of P-type ATPases.* Nat Rev Mol Cell Biol, 2004. **5**(4): p. 282-95.
19. Wuytack, F., L. Raeymaekers, and L. Missiaen, *Molecular physiology of the SERCA and SPCA pumps.* Cell Calcium, 2002. **32**(5-6): p. 279-305.
20. Toyoshima, C., et al., *Crystal structure of the calcium pump of sarcoplasmic reticulum at 2.6 A resolution.* Nature, 2000. **405**(6787): p. 647-55.
21. Toyoshima, C. and T. Mizutani, *Crystal structure of the calcium pump with a bound ATP analogue.* Nature, 2004. **430**(6999): p. 529-35.
22. Di Leva, F., et al., *The plasma membrane Ca2+ ATPase of animal cells: structure, function and regulation.* Arch Biochem Biophys, 2008. **476**(1): p. 65-74.
23. Brandl, C.J., et al., *Adult forms of the Ca2+ATPase of sarcoplasmic reticulum. Expression in developing skeletal muscle.* J Biol Chem, 1987. **262**(8): p. 3768-74.

24. Lee, K.J., et al., *Stromal interaction molecule 1 (STIM1) regulates sarcoplasmic/endoplasmic reticulum Ca(2)(+)-ATPase 1a (SERCA1a) in skeletal muscle.* Pflugers Arch, 2014. **466**(5): p. 987-1001.
25. Stammers, A.N., et al., *The regulation of sarco(endo)plasmic reticulum calcium-ATPases (SERCA).* Can J Physiol Pharmacol, 2015. **93**(10): p. 843-54.
26. Arbabian, A., et al., *Endoplasmic reticulum calcium pumps and cancer.* Biofactors, 2011. **37**(3): p. 139-49.
27. Arbabian, A., et al., *Modulation of endoplasmic reticulum calcium pump expression during lung cancer cell differentiation.* FEBS J, 2013. **280**(21): p. 5408-18.
28. Papp, B. and J.P. Brouland, *Altered Endoplasmic Reticulum Calcium Pump Expression during Breast Tumorigenesis.* Breast Cancer (Auckl), 2011. **5**: p. 163-74.
29. Brouland, J.P., et al., *The loss of sarco/endoplasmic reticulum calcium transport ATPase 3 expression is an early event during the multistep process of colon carcinogenesis.* Am J Pathol, 2005. **167**(1): p. 233-42.
30. Strehler, E.E., et al., *Plasma-membrane Ca(2+) pumps: structural diversity as the basis for functional versatility.* Biochem Soc Trans, 2007. **35**(Pt 5): p. 919-22.
31. Strehler, E.E., *Plasma membrane calcium ATPases: From generic Ca(2+) sump pumps to versatile systems for fine-tuning cellular Ca(2.).* Biochem Biophys Res Commun, 2015. **460**(1): p. 26-33.
32. Padanyi, R., et al., *Multifaceted plasma membrane Ca(2+) pumps: From structure to intracellular Ca(2+) handling and cancer.* Biochim Biophys Acta, 2016. **1863**(6 Pt B): p. 1351-63.
33. Chicka, M.C. and E.E. Strehler, *Alternative splicing of the first intracellular loop of plasma membrane Ca2+-ATPase isoform 2 alters its membrane targeting.* J Biol Chem, 2003. **278**(20): p. 18464-70.
34. Strehler, E.E., et al., *Plasma membrane Ca2+ ATPases as dynamic regulators of cellular calcium handling.* Ann N Y Acad Sci, 2007. **1099**: p. 226-36.
35. Okunade, G.W., et al., *Targeted ablation of plasma membrane Ca2+-ATPase (PMCA) 1 and 4 indicates a major housekeeping function for PMCA1 and a critical role in hyperactivated sperm motility and male fertility for PMCA4.* J Biol Chem, 2004. **279**(32): p. 33742-50.
36. Hill, J.K., et al., *Splice-site A choice targets plasma-membrane Ca2+-ATPase isoform 2 to hair bundles.* J Neurosci, 2006. **26**(23): p. 6172-80.
37. Kozel, P.J., et al., *Balance and hearing deficits in mice with a null mutation in the gene encoding plasma membrane Ca2+-ATPase isoform 2.* J Biol Chem, 1998. **273**(30): p. 18693-6.
38. Reinhardt, T.A., et al., *Null mutation in the gene encoding plasma membrane Ca2+-ATPase isoform 2 impairs calcium transport into milk.* J Biol Chem, 2004. **279**(41): p. 42369-73.
39. Dumont, R.A., et al., *Plasma membrane Ca2+-ATPase isoform 2a is the PMCA of hair bundles.* J Neurosci, 2001. **21**(14): p. 5066-78.
40. Vorherr, T., et al., *Interaction of calmodulin with the calmodulin binding domain of the plasma membrane Ca2+ pump.* Biochemistry, 1990. **29**(2): p. 355-65.
41. Caride, A.J., et al., *The plasma membrane Ca2+ pump isoform 4a differs from isoform 4b in the mechanism of calmodulin binding and activation kinetics: implications for Ca2+ signaling.* J Biol Chem, 2007. **282**(35): p. 25640-8.
42. Caride, A.J., et al., *Delayed activation of the plasma membrane calcium pump by a sudden increase in Ca2+: fast pumps reside in fast cells.* Cell Calcium, 2001. **30**(1): p. 49-57.
43. Sun, Y., et al., *Phosphatidylinositol 4,5-bisphosphate: targeted production and signaling.* Bioessays, 2013. **35**(6): p. 513-22.
44. Penniston, J.T., et al., *Apart from its known function, the plasma membrane Ca(2)(+)ATPase can regulate Ca(2)(+) signaling by controlling phosphatidylinositol 4,5-bisphosphate levels.* J Cell Sci, 2014. **127**(Pt 1): p. 72-84.
45. Antalffy, G., et al., *A C-terminal di-leucine motif controls plasma membrane expression of PMCA4b.* Biochim Biophys Acta, 2013. **1833**(12): p. 2561-72.

46. Enyedi, A., et al., *Protein kinase C activates the plasma membrane Ca2+ pump isoform 4b by phosphorylation of an inhibitory region downstream of the calmodulin-binding domain.* J Biol Chem, 1996. **271**(50): p. 32461-7.
47. Enyedi, A., et al., *Protein kinase C phosphorylates the "a" forms of plasma membrane Ca2+ pump isoforms 2 and 3 and prevents binding of calmodulin.* J Biol Chem, 1997. **272**(44): p. 27525-8.
48. Padanyi, R., et al., *Intramolecular interactions of the regulatory region with the catalytic core in the plasma membrane calcium pump.* J Biol Chem, 2003. **278**(37): p. 35798-804.
49. Paszty, K., et al., *Plasma membrane Ca2+ATPase isoform 4b is cleaved and activated by caspase-3 during the early phase of apoptosis.* J Biol Chem, 2002. **277**(9): p. 6822-9.
50. Paszty, K., et al., *Cleavage of the plasma membrane Ca+ATPase during apoptosis.* Ann N Y Acad Sci, 2007. **1099**: p. 440-50.
51. DeMarco, S.J., M.C. Chicka, and E.E. Strehler, *Plasma membrane Ca2+ ATPase isoform 2b interacts preferentially with Na+/H+ exchanger regulatory factor 2 in apical plasma membranes.* J Biol Chem, 2002. **277**(12): p. 10506-11.
52. Padanyi, R., et al., *Apical scaffolding protein NHERF2 modulates the localization of alternatively spliced plasma membrane Ca2+ pump 2B variants in polarized epithelial cells.* J Biol Chem, 2010. **285**(41): p. 31704-12.
53. Kim, E., et al., *Plasma membrane Ca2+ ATPase isoform 4b binds to membrane-associated guanylate kinase (MAGUK) proteins via their PDZ (PSD-95/Dlg/ZO-1) domains.* J Biol Chem, 1998. **273**(3): p. 1591-5.
54. Padanyi, R., et al., *PSD-95 mediates membrane clustering of the human plasma membrane Ca2+ pump isoform 4b.* Biochim Biophys Acta, 2009. **1793**(6): p. 1023-32.
55. Holton, M.L., et al., *Plasma membrane calcium ATPase proteins as novel regulators of signal transduction pathways.* World J Biol Chem, 2010. **1**(6): p. 201-8.
56. Mohamed, T.M., et al., *Plasma membrane calcium pump (PMCA4)-neuronal nitric-oxide synthase complex regulates cardiac contractility through modulation of a compartmentalized cyclic nucleotide microdomain.* J Biol Chem, 2011. **286**(48): p. 41520-9.
57. Rimessi, A., et al., *Inhibitory interaction of the 14-3-3{epsilon} protein with isoform 4 of the plasma membrane Ca(2+)-ATPase pump.* J Biol Chem, 2005. **280**(44): p. 37195-203.
58. Armesilla, A.L., et al., *Novel functional interaction between the plasma membrane Ca2+ pump 4b and the proapoptotic tumor suppressor Ras-associated factor 1 (RASSF1).* J Biol Chem, 2004. **279**(30): p. 31318-28.
59. Holton, M., et al., *Endothelial nitric oxide synthase activity is inhibited by the plasma membrane calcium ATPase in human endothelial cells.* Cardiovasc Res, 2010. **87**(3): p. 440-8.
60. Mognol, G.P., et al., *Cell cycle and apoptosis regulation by NFAT transcription factors: new roles for an old player.* Cell Death Dis, 2016. **7**: p. e2199.
61. Buch, M.H., et al., *The sarcolemmal calcium pump inhibits the calcineurin/nuclear factor of activated T-cell pathway via interaction with the calcineurin A catalytic subunit.* J Biol Chem, 2005. **280**(33): p. 29479-87.
62. Holton, M., et al., *The interaction between endogenous calcineurin and the plasma membrane calcium-dependent ATPase is isoform specific in breast cancer cells.* FEBS Lett, 2007. **581**(21): p. 4115-9.
63. Kim, H.J., et al., *Plasma membrane calcium ATPase regulates bone mass by fine-tuning osteoclast differentiation and survival.* J Cell Biol, 2012. **199**(7): p. 1145-58.
64. Baggott, R.R., et al., *Plasma membrane calcium ATPase isoform 4 inhibits vascular endothelial growth factor-mediated angiogenesis through interaction with calcineurin.* Arterioscler Thromb Vasc Biol, 2014. **34**(10): p. 2310-20.
65. Krapivinsky, G., et al., *POST, partner of stromal interaction molecule 1 (STIM1), targets STIM1 to multiple transporters.* Proc Natl Acad Sci U S A, 2011. **108**(48): p. 19234-9.
66. Hanahan, D. and R.A. Weinberg, *Hallmarks of cancer: the next generation.* Cell, 2011. **144**(5): p. 646-74.

67. Prevarskaya, N., et al., *Remodelling of Ca2+ transport in cancer: how it contributes to cancer hallmarks?* Philos Trans R Soc Lond B Biol Sci, 2014. **369**(1638): p. 20130097.
68. Roderick, H.L. and S.J. Cook, *Ca2+ signalling checkpoints in cancer: remodelling Ca2+ for cancer cell proliferation and survival.* Nat Rev Cancer, 2008. **8**(5): p. 361-75.
69. Deliot, N. and B. Constantin, *Plasma membrane calcium channels in cancer: Alterations and consequences for cell proliferation and migration.* Biochim Biophys Acta, 2015. **1848**(10 Pt B): p. 2512-22.
70. Fixemer, T., et al., *Expression of the Ca2+-selective cation channel TRPV6 in human prostate cancer: a novel prognostic marker for tumor progression.* Oncogene, 2003. **22**(49): p. 7858-61.
71. Fiorio Pla, A., K. Kondratska, and N. Prevarskaya, *STIM and ORAI proteins: crucial roles in hallmarks of cancer.* Am J Physiol Cell Physiol, 2016. **310**(7): p. C509-19.
72. Faouzi, M., et al., *ORAI3 silencing alters cell proliferation and cell cycle progression via c-myc pathway in breast cancer cells.* Biochim Biophys Acta, 2013. **1833**(3): p. 752-60.
73. Dubois, C., et al., *Remodeling of channel-forming ORAI proteins determines an oncogenic switch in prostate cancer.* Cancer Cell, 2014. **26**(1): p. 19-32.
74. Zhivotovsky, B. and S. Orrenius, *Calcium and cell death mechanisms: a perspective from the cell death community.* Cell Calcium, 2011. **50**(3): p. 211-21.
75. Bialik, S. and A. Kimchi, *Lethal weapons: DAP-kinase, autophagy and cell death: DAP-kinase regulates autophagy.* Curr Opin Cell Biol, 2010. **22**(2): p. 199-205.
76. Flourakis, M., et al., *Orai1 contributes to the establishment of an apoptosis-resistant phenotype in prostate cancer cells.* Cell Death Dis, 2010. **1**: p. e75.
77. Vanden Abeele, F., et al., *Bcl-2-dependent modulation of Ca(2+) homeostasis and store-operated channels in prostate cancer cells.* Cancer Cell, 2002. **1**(2): p. 169-79.
78. Faouzi, M., et al., *Down-regulation of Orai3 arrests cell-cycle progression and induces apoptosis in breast cancer cells but not in normal breast epithelial cells.* J Cell Physiol, 2011. **226**(2): p. 542-51.
79. Stock, K., et al., *Neural precursor cells induce cell death of high-grade astrocytomas through stimulation of TRPV1.* Nat Med, 2012. **18**(8): p. 1232-8.
80. Tsunoda, T., et al., *Inositol 1,4,5-trisphosphate (IP3) receptor type1 (IP3R1) modulates the acquisition of cisplatin resistance in bladder cancer cell lines.* Oncogene, 2005. **24**(8): p. 1396-402.
81. Wen, J., et al., *Altered expression of stromal interaction molecule (STIM)-calcium release-activated calcium channel protein (ORAI) and inositol 1,4,5-trisphosphate receptors (IP3Rs) in cancer: will they become a new battlefield for oncotherapy?* Chin J Cancer, 2016. **35**: p. 32.
82. Prevarskaya, N., R. Skryma, and Y. Shuba, *Calcium in tumour metastasis: new roles for known actors.* Nat Rev Cancer, 2011. **11**(8): p. 609-18.
83. Giannone, G., et al., *Calcium rises locally trigger focal adhesion disassembly and enhance residency of focal adhesion kinase at focal adhesions.* J Biol Chem, 2004. **279**(27): p. 28715-23.
84. Easley, C.A.t., et al., *CaMK-II promotes focal adhesion turnover and cell motility by inducing tyrosine dephosphorylation of FAK and paxillin.* Cell Motil Cytoskeleton, 2008. **65**(8): p. 662-74.
85. Chan, K.T., D.A. Bennin, and A. Huttenlocher, *Regulation of adhesion dynamics by calpain-mediated proteolysis of focal adhesion kinase (FAK).* J Biol Chem, 2010. **285**(15): p. 11418-26.
86. Wei, C., et al., *Calcium flickers steer cell migration.* Nature, 2009. **457**(7231): p. 901-5.
87. Tsai, F.C., et al., *A polarized Ca2+, diacylglycerol and STIM1 signalling system regulates directed cell migration.* Nat Cell Biol, 2014. **16**(2): p. 133-44.
88. Monet, M., et al., *Role of cationic channel TRPV2 in promoting prostate cancer migration and progression to androgen resistance.* Cancer Res, 2010. **70**(3): p. 1225-35.
89. Yang, S., J.J. Zhang, and X.Y. Huang, *Orai1 and STIM1 are critical for breast tumor cell migration and metastasis.* Cancer Cell, 2009. **15**(2): p. 124-34.

90. Gao, H., et al., *EGF enhances the migration of cancer cells by up-regulation of TRPM7.* Cell Calcium, 2011. **50**(6): p. 559-68.
91. Kang, S.S., et al., *Caffeine-mediated inhibition of calcium release channel inositol 1,4,5-trisphosphate receptor subtype 3 blocks glioblastoma invasion and extends survival.* Cancer Res, 2010. **70**(3): p. 1173-83.
92. Ruschoff, J.H., et al., *Plasma membrane calcium ATPase expression in human colon multistep carcinogenesis.* Cancer Invest, 2012. **30**(4): p. 251-7.
93. Ribiczey, P., et al., *Isoform-specific up-regulation of plasma membrane Ca2+ATPase expression during colon and gastric cancer cell differentiation.* Cell Calcium, 2007. **42**(6): p. 590-605.
94. Varga, K., et al., *Histone deacetylase inhibitor- and PMA-induced upregulation of PMCA4b enhances Ca2+ clearance from MCF-7 breast cancer cells.* Cell Calcium, 2014. **55**(2): p. 78-92.
95. Saito, K., et al., *Plasma membrane Ca2+ ATPase isoform 1 down-regulated in human oral cancer.* Oncol Rep, 2006. **15**(1): p. 49-55.
96. Reisner, P.D., P.C. Brandt, and T.C. Vanaman, *Analysis of plasma membrane Ca(2+)-ATPase expression in control and SV40-transformed human fibroblasts.* Cell Calcium, 1997. **21**(1): p. 53-62.
97. Lee, W.J., et al., *Expression of plasma membrane calcium pump isoform mRNAs in breast cancer cell lines.* Cell Signal, 2002. **14**(12): p. 1015-22.
98. Aung, C.S., et al., *Plasma membrane Ca2+-ATPase expression during colon cancer cell line differentiation.* Biochem Biophys Res Commun, 2007. **355**(4): p. 932-6.
99. Lee, W.J., S.J. Roberts-Thomson, and G.R. Monteith, *Plasma membrane calcium-ATPase 2 and 4 in human breast cancer cell lines.* Biochem Biophys Res Commun, 2005. **337**(3): p. 779-83.
100. Baggott, R.R., et al., *Disruption of the interaction between PMCA2 and calcineurin triggers apoptosis and enhances paclitaxel-induced cytotoxicity in breast cancer cells.* Carcinogenesis, 2012. **33**(12): p. 2362-8.
101. Venkatesh, S. and J.L. Workman, *Histone exchange, chromatin structure and the regulation of transcription.* Nat Rev Mol Cell Biol, 2015. **16**(3): p. 178-89.
102. Jaenisch, R. and A. Bird, *Epigenetic regulation of gene expression: how the genome integrates intrinsic and environmental signals.* Nat Genet, 2003. **33 Suppl**: p. 245-54.
103. Verdin, E. and M. Ott, *50 years of protein acetylation: from gene regulation to epigenetics, metabolism and beyond.* Nat Rev Mol Cell Biol, 2015. **16**(4): p. 258-64.
104. Delcuve, G.P., D.H. Khan, and J.R. Davie, *Roles of histone deacetylases in epigenetic regulation: emerging paradigms from studies with inhibitors.* Clin Epigenetics, 2012. **4**(1): p. 5.
105. Tran, A.D., et al., *HDAC6 deacetylation of tubulin modulates dynamics of cellular adhesions.* J Cell Sci, 2007. **120**(Pt 8): p. 1469-79.
106. Mottamal, M., et al., *Histone deacetylase inhibitors in clinical studies as templates for new anticancer agents.* Molecules, 2015. **20**(3): p. 3898-941.
107. Zhang, H., et al., *Histone deacetylases function as novel potential therapeutic targets for cancer.* Hepatol Res, 2016.
108. Wang, X., et al., *Trichostatin A, a histone deacetylase inhibitor, reverses epithelial-mesenchymal transition in colorectal cancer SW480 and prostate cancer PC3 cells.* Biochem Biophys Res Commun, 2015. **456**(1): p. 320-6.
109. Zou, X.M., et al., *Gastric cancer cell lines induced by trichostatin A.* World J Gastroenterol, 2008. **14**(30): p. 4810-5.
110. Zhang, X., et al., *Effects of histone deacetylase inhibitor trichostatin A combined with cisplatin on apoptosis of A549 cell line.* Thorac Cancer, 2015. **6**(2): p. 202-8.
111. Witt, D., et al., *Valproic acid inhibits the proliferation of cancer cells by re-expressing cyclin D2.* Carcinogenesis, 2013. **34**(5): p. 1115-24.

112. Fung, K.Y., et al., *Butyrate-induced apoptosis in HCT116 colorectal cancer cells includes induction of a cell stress response.* J Proteome Res, 2011. **10**(4): p. 1860-9.
113. Facchetti, F., et al., *Modulation of pro- and anti-apoptotic factors in human melanoma cells exposed to histone deacetylase inhibitors.* Apoptosis, 2004. **9**(5): p. 573-82.
114. Zhang, X.D., et al., *The histone deacetylase inhibitor suberic bishydroxamate regulates the expression of multiple apoptotic mediators and induces mitochondria-dependent apoptosis of melanoma cells.* Mol Cancer Ther, 2004. **3**(4): p. 425-35.
115. Lai, F., et al., *Histone deacetylases (HDACs) as mediators of resistance to apoptosis in melanoma and as targets for combination therapy with selective BRAF inhibitors.* Adv Pharmacol, 2012. **65**: p. 27-43.
116. Woods, D.M., et al., *The antimelanoma activity of the histone deacetylase inhibitor panobinostat (LBH589) is mediated by direct tumor cytotoxicity and increased tumor immunogenicity.* Melanoma Res, 2013. **23**(5): p. 341-8.
117. Woods, D.M., et al., *HDAC Inhibition Upregulates PD-1 Ligands in Melanoma and Augments Immunotherapy with PD-1 Blockade.* Cancer Immunol Res, 2015. **3**(12): p. 1375-85.
118. Hornig, E., et al., *Inhibition of histone deacetylases in melanoma-a perspective from bench to bedside.* Exp Dermatol, 2016. **25**(11): p. 831-838.
119. Niezgoda, A., P. Niezgoda, and R. Czajkowski, *Novel Approaches to Treatment of Advanced Melanoma: A Review on Targeted Therapy and Immunotherapy.* Biomed Res Int, 2015. **2015**: p. 851387.
120. Miller, K.D., et al., *Cancer treatment and survivorship statistics, 2016.* CA Cancer J Clin, 2016. **66**(4): p. 271-89.
121. Hsu, M.Y., F. Meier, and M. Herlyn, *Melanoma development and progression: a conspiracy between tumor and host.* Differentiation, 2002. **70**(9-10): p. 522-36.
122. Herlyn, M., *Human melanoma: development and progression.* Cancer Metastasis Rev, 1990. **9**(2): p. 101-12.
123. Maio, M., *Melanoma as a model tumour for immuno-oncology.* Ann Oncol, 2012. **23 Suppl 8**: p. viii10-4.
124. Johnson, D.B. and I. Puzanov, *Treatment of NRAS-mutant melanoma.* Curr Treat Options Oncol, 2015. **16**(4): p. 15.
125. Polsky, D. and C. Cordon-Cardo, *Oncogenes in melanoma.* Oncogene, 2003. **22**(20): p. 3087-91.
126. Sullivan, R.J. and K.T. Flaherty, *Resistance to BRAF-targeted therapy in melanoma.* Eur J Cancer, 2013. **49**(6): p. 1297-304.
127. Paraiso, K.H., et al., *PTEN loss confers BRAF inhibitor resistance to melanoma cells through the suppression of BIM expression.* Cancer Res, 2011. **71**(7): p. 2750-60.
128. Flaherty, K.T., et al., *Combined BRAF and MEK inhibition in melanoma with BRAF V600 mutations.* N Engl J Med, 2012. **367**(18): p. 1694-703.
129. Guo, J., et al., *Phase II, open-label, single-arm trial of imatinib mesylate in patients with metastatic melanoma harboring c-Kit mutation or amplification.* J Clin Oncol, 2011. **29**(21): p. 2904-9.
130. Franklin, C., et al., *Immunotherapy in melanoma: Recent advances and future directions.* Eur J Surg Oncol, 2016.
131. Gibney, G.T., L.M. Weiner, and M.B. Atkins, *Predictive biomarkers for checkpoint inhibitor-based immunotherapy.* Lancet Oncol, 2016. **17**(12): p. e542-e551.
132. Macia, A., et al., *Calcium channel expression and applicability as targeted therapies in melanoma.* Biomed Res Int, 2015. **2015**: p. 587135.
133. Guo, H., J.A. Carlson, and A. Slominski, *Role of TRPM in melanocytes and melanoma.* Exp Dermatol, 2012. **21**(9): p. 650-4.
134. Stanisz, H., et al., *Inverse regulation of melanoma growth and migration by Orai1/STIM2-dependent calcium entry.* Pigment Cell Melanoma Res, 2014. **27**(3): p. 442-53.

135. Umemura, M., et al., *Store-operated Ca2+ entry (SOCE) regulates melanoma proliferation and cell migration.* PLoS One, 2014. **9**(2): p. e89292.
136. Sun, J., et al., *STIM1- and Orai1-mediated Ca(2+) oscillation orchestrates invadopodium formation and melanoma invasion.* J Cell Biol, 2014. **207**(4): p. 535-48.
137. Das, A., et al., *Functional expression of voltage-gated calcium channels in human melanoma.* Pigment Cell Melanoma Res, 2012. **25**(2): p. 200-12.
138. Das, A., et al., *T-type calcium channel blockers inhibit autophagy and promote apoptosis of malignant melanoma cells.* Pigment Cell Melanoma Res, 2013. **26**(6): p. 874-85.
139. Baljinnyam, E., et al., *Exchange protein directly activated by cyclic AMP increases melanoma cell migration by a Ca2+-dependent mechanism.* Cancer Res, 2010. **70**(13): p. 5607-17.
140. Arozarena, I., et al., *Oncogenic BRAF induces melanoma cell invasion by downregulating the cGMP-specific phosphodiesterase PDE5A.* Cancer Cell, 2011. **19**(1): p. 45-57.
141. Flockhart, R.J., et al., *NFAT signalling is a novel target of oncogenic BRAF in metastatic melanoma.* Br J Cancer, 2009. **101**(8): p. 1448-55.
142. Deli, T., et al., *Functional genomics of calcium channels in human melanoma cells.* Int J Cancer, 2007. **121**(1): p. 55-65.
143. Beck, D., et al., *Vemurafenib potently induces endoplasmic reticulum stress-mediated apoptosis in BRAFV600E melanoma cells.* Sci Signal, 2013. **6**(260): p. ra7.
144. Berger, W., et al., *Intrinsic MDR-1 gene and P-glycoprotein expression in human melanoma cell lines.* Int J Cancer, 1994. **59**(5): p. 717-23.
145. Nakai, J. and M. Ohkura, *Probing calcium ions with biosensors.* Biotechnol Genet Eng Rev, 2003. **20**: p. 3-21.
146. Kolacsek, O., et al., *Reliable transgene-independent method for determining Sleeping Beauty transposon copy numbers.* Mob DNA, 2011. **2**(1): p. 5.
147. Lowry, O.H., et al., *Protein measurement with the Folin phenol reagent.* J Biol Chem, 1951. **193**(1): p. 265-75.
148. Bensadoun, A. and D. Weinstein, *Assay of proteins in the presence of interfering materials.* Anal Biochem, 1976. **70**(1): p. 241-50.
149. Caride, A.J., et al., *Detection of isoform 4 of the plasma membrane calcium pump in human tissues by using isoform-specific monoclonal antibodies.* Biochem J, 1996. **316 (Pt 1)**: p. 353-9.
150. Sakuma, K., M. Aoki, and R. Kannagi, *Transcription factors c-Myc and CDX2 mediate E-selectin ligand expression in colon cancer cells undergoing EGF/bFGF-induced epithelial-mesenchymal transition.* Proc Natl Acad Sci U S A, 2012. **109**(20): p. 7776-81.
151. Garay, T., et al., *Cell migration or cytokinesis and proliferation?--revisiting the "go or grow" hypothesis in cancer cells in vitro.* Exp Cell Res, 2013. **319**(20): p. 3094-103.
152. Albini, A., et al., *A rapid in vitro assay for quantitating the invasive potential of tumor cells.* Cancer Res, 1987. **47**(12): p. 3239-45.
153. Caride, A.J., et al., *The rate of activation by calmodulin of isoform 4 of the plasma membrane Ca(2+) pump is slow and is changed by alternative splicing.* J Biol Chem, 1999. **274**(49): p. 35227-32.
154. Caride, A.J., et al., *The plasma membrane calcium pump displays memory of past calcium spikes. Differences between isoforms 2b and 4b.* J Biol Chem, 2001. **276**(43): p. 39797-804.
155. Curry, M.C., S.J. Roberts-Thomson, and G.R. Monteith, *Plasma membrane calcium ATPases and cancer.* Biofactors, 2011. **37**(3): p. 132-8.
156. Gelebart, P., et al., *Expression of endomembrane calcium pumps in colon and gastric cancer cells. Induction of SERCA3 expression during differentiation.* J Biol Chem, 2002. **277**(29): p. 26310-20.
157. Huang, W., et al., *Inhibition of store-operated Ca2+ entry counteracts the apoptosis of nasopharyngeal carcinoma cells induced by sodium butyrate.* Oncol Lett, 2017. **13**(2): p. 921-929.

158. Klishin, A., M. Sedova, and L.A. Blatter, *Time-dependent modulation of capacitative Ca2+ entry signals by plasma membrane Ca2+ pump in endothelium.* Am J Physiol, 1998. **274**(4 Pt 1): p. C1117-28.
159. Ritchie, M.F., E. Samakai, and J. Soboloff, *STIM1 is required for attenuation of PMCA-mediated Ca2+ clearance during T-cell activation.* EMBO J, 2012. **31**(5): p. 1123-33.
160. Empson, R.M., M.L. Garside, and T. Knopfel, *Plasma membrane Ca2+ ATPase 2 contributes to short-term synapse plasticity at the parallel fiber to Purkinje neuron synapse.* J Neurosci, 2007. **27**(14): p. 3753-8.
161. Empson, R.M., et al., *Reduced expression of the Ca(2+) transporter protein PMCA2 slows Ca(2+) dynamics in mouse cerebellar Purkinje neurones and alters the precision of motor coordination.* J Physiol, 2010. **588**(Pt 6): p. 907-22.
162. Singh, A.P. and S. Rajender, *CatSper channel, sperm function and male fertility.* Reprod Biomed Online, 2015. **30**(1): p. 28-38.
163. Schuh, K., et al., *Plasma membrane Ca2+ ATPase 4 is required for sperm motility and male fertility.* J Biol Chem, 2004. **279**(27): p. 28220-6.
164. Lefievre, L., et al., *2-APB-potentiated channels amplify CatSper-induced Ca(2+) signals in human sperm.* Biochem J, 2012. **448**(2): p. 189-200.
165. Dupont, G. and L. Combettes, *Fine tuning of cytosolic Ca (2+) oscillations.* F1000Res, 2016. **5**.
166. Kawano, S., et al., *Ca(2+) oscillations regulated by Na(+)-Ca(2+) exchanger and plasma membrane Ca(2+) pump induce fluctuations of membrane currents and potentials in human mesenchymal stem cells.* Cell Calcium, 2003. **34**(2): p. 145-56.
167. Rinker-Schaeffer, C.W., et al., *Metastasis suppressor proteins: discovery, molecular mechanisms, and clinical application.* Clin Cancer Res, 2006. **12**(13): p. 3882-9.
168. Ritchie, M.F., Y. Zhou, and J. Soboloff, *Transcriptional mechanisms regulating Ca(2+) homeostasis.* Cell Calcium, 2011. **49**(5): p. 314-21.
169. Ribiczey, P., et al., *Selective upregulation of the expression of plasma membrane calcium ATPase isoforms upon differentiation and 1,25(OH)2D3-vitamin treatment of colon cancer cells.* Biochem Biophys Res Commun, 2015. **464**(1): p. 189-94.
170. Ryan, Z.C., et al., *Deletion of the intestinal plasma membrane calcium pump, isoform 1, Atp2b1, in mice is associated with decreased bone mineral density and impaired responsiveness to 1, 25-dihydroxyvitamin D3.* Biochem Biophys Res Commun, 2015. **467**(1): p. 152-6.
171. Reichrath, J., et al., *In vitro comparison of the vitamin D endocrine system in 1,25(OH)2D3-responsive and -resistant melanoma cells.* Cancer Biol Ther, 2007. **6**(1): p. 48-55.
172. Fang, S., et al., *Association of Vitamin D Levels With Outcome in Patients With Melanoma After Adjustment For C-Reactive Protein.* J Clin Oncol, 2016. **34**(15): p. 1741-7.
173. Fetahu, I.S., J. Hobaus, and E. Kallay, *Vitamin D and the epigenome.* Front Physiol, 2014. **5**: p. 164.
174. Diaz-Nunez, M., et al., *Histone deacetylase inhibitors induce invasion of human melanoma cells in vitro via differential regulation of N-cadherin expression and RhoA activity.* BMC Cancer, 2016. **16**: p. 667.
175. Filoteo, A.G., et al., *Plasma membrane Ca2+ pump in rat brain. Patterns of alternative splices seen by isoform-specific antibodies.* J Biol Chem, 1997. **272**(38): p. 23741-7.

ADATLAP

a doktori értekezés nyilvánosságra hozatalához*

I. A doktori értekezés adatai

A szerző neve: Hegedűs Luca.....

MTMT-azonosító:.....10035810 .....

A doktori értekezés címe és alcíme:... The plasma membrane Ca^{2+} pump PMCA4b regulates intracellular Ca^{2+} homeostasis and migratory and metastatic activity of BRAF mutant melanoma cells

DOI-azonosító[46]:..... 10.15476/ELTE.2017.116 .....

A doktori iskola neve:...Biológia Doktori Iskola.....

A doktori iskolán belüli doktori program neve: Molekuláris Sejt- és Neurobiológia Program

A témavezető neve és tudományos fokozata:...Dr. Enyedi Ágnes, PhD, DSc.....

A témavezető munkahelye: II. Számú Patológiai Intézet, Semmelweis Egyetem...

II. Nyilatkozatok

1. A doktori értekezés szerzőjeként
a) hozzájárulok, hogy a doktori fokozat megszerzését követően a doktori értekezésem és a tézisek nyilvánosságra kerüljenek az ELTE Digitális Intézményi Tudástárban. Felhatalmazom a Természettudományi kar Dékáni Hivatal Doktori, Habilitációs és Nemzetközi Ügyek Csoportjának ügyintézőjét, hogy az értekezést és a téziseket feltöltse az ELTE Digitális Intézményi Tudástárba, és ennek során kitöltse a feltöltéshez szükséges nyilatkozatokat.
b) kérem, hogy a mellékelt kérelemben részletezett szabadalmi, illetőleg oltalmi bejelentés közzétételéig a doktori értekezést ne bocsássák nyilvánosságra az Egyetemi Könyvtárban és az ELTE Digitális Intézményi Tudástárban;
c) kérem, hogy a nemzetbiztonsági okból minősített adatot tartalmazó doktori értekezést a minősítés (*dátum*)-ig tartó időtartama alatt ne bocsássák nyilvánosságra az Egyetemi Könyvtárban és az ELTE Digitális Intézményi Tudástárban;
d) kérem, hogy a mű kiadására vonatkozó mellékelt kiadó szerződésre tekintettel a doktori értekezést a könyv megjelenéséig ne bocsássák nyilvánosságra az Egyetemi Könyvtárban, és az ELTE Digitális Intézményi Tudástárban csak a könyv bibliográfiai adatait tegyék közzé. Ha a könyv a fokozatszerzést követőn egy évig nem jelenik meg, hozzájárulok, hogy a doktori értekezésem és a tézisek nyilvánosságra kerüljenek az Egyetemi Könyvtárban és az ELTE Digitális Intézményi Tudástárban.

2. A doktori értekezés szerzőjeként kijelentem, hogy
a) az ELTE Digitális Intézményi Tudástárba feltöltendő doktori értekezés és a tézisek saját eredeti, önálló szellemi munkám és legjobb tudomásom szerint nem sértem vele senki szerzői jogait;
b) a doktori értekezés és a tézisek nyomtatott változatai és az elektronikus adathordozón benyújtott tartalmak (szöveg és ábrák) mindenben megegyeznek.

3. A doktori értekezés szerzőjeként hozzájárulok a doktori értekezés és a tézisek szövegének plágiumkereső adatbázisba helyezéséhez és plágiumellenőrző vizsgálatok lefuttatásához.

Kelt: 2017.09.19.....

Hegedűs Luca
.....
a doktori értekezés szerzőjének aláírása